Department of Electrical Engineering

Modeling and Experimental Investigation of Lightning Arcs and Overvoltages for Medium Voltage Distribution Lines

Michael Adebayo Omidiora

A!

DOCTORAL DISSERTATIONS

Aalto University publication series
DOCTORAL DISSERTATIONS 70/2011

Modeling and Experimental Investigation of Lightning Arcs and Overvoltages for Medium Voltage Distribution Lines

Michael Adebayo Omidiora

Doctoral dissertation for the degree of Doctor of Science in Technology to be presented with due permission of the School of Electrical Engineering for public examination and debate in Auditorium S1 at the Aalto University School of Electrical Engineering (Espoo, Finland) on the 24th of October 2011 at 13:00.

Aalto University
School of Electrical Engineering
Electrical Engineering Department
Power Systems and High Voltage Engineering

Supervisor
Professor Matti Lehtonen

Preliminary examiners
Professor Akihiro Ametani, Doshisha University, Kyoto, Japan
Professor Stanislaw Grzybowski, Mississippi State University, USA

Opponent
Professor Mustafa Kizilcay, University of Siegen, Germany

Aalto University publication series
DOCTORAL DISSERTATIONS 70/2011

ISBN 978-952-60-4243-5 (pdf)
ISBN 978-952-60-4242-8 (printed)
ISSN-L 1799-4934
ISSN 1799-4942 (pdf)
ISSN 1799-4934 (printed)

Aalto Print
Helsinki 2011

Finland

The dissertation can be read at http://lib.tkk.fi/Diss/

Author
Michael Adebayo Omidiora

Name of the doctoral dissertation
Modeling and Experimental Investigation of Lightning Arcs and Overvoltages for Medium Voltage Distribution Lines

Publisher School of Electrical Engineering

Unit Department of Electrical Engineering

Series Aalto University publication series DOCTORAL DISSERTATIONS 70/2011

Field of research Power Systems and High Voltage Engineering

Manuscript submitted 28 April 2011 **Manuscript revised** 15 August 2011

Date of the defence 24 October 2011 **Language** English

☐ **Monograph** ☒ **Article dissertation (summary + original articles)**

Abstract

In this dissertation, lightning overvoltages in Medium Voltage (MV) lines are thoroughly investigated. The other goal is to propose new protection schemes for the designs. The lines consist of overhead lines, underground cables and covered conductors. These overvoltage problems range from direct and indirect strokes to lightning arcs. All the models and simulations are developed using the Electromagnetic Transient Program (EMTP) and Finite Element Method (FEM), while MATLAB is used for post-processing the results and identification of the model parameters.

Improvement in the surge protection of MV overhead lines is demonstrated with a combination of surge arresters and a shield wire. Using the IEEE 34-node feeder injected with multiple lightning strokes, the feeder is simulated using EMTP. The response of the line is modeled both with and without the surge protection devices. The simulation study extends to the performance of a MV underground cable due to a nearby lightning discharge using FEM. The use of shield wire for limiting the overvoltage stress in the cables is proposed. A numerical analysis and simulations are performed to determine the outage rate of MV covered conductors due to lightning strokes of different characteristics. The optimum distance for surge protective devices on the conductors is also assessed.

An enhancement in the surge analysis of distribution lines with the shielding effect of trees is proposed. An experimental study shows that a tree can intercept a lightning stroke in the vicinity of a distribution line. This study also analyzes experimental results of the shielding effectiveness of a tree and the induced voltages existing between the tree and the distribution line. The study is extended to evaluate the induced voltage on a distribution line for larger clearances using a Rusck model.

This work investigates the lightning arc between an overhead line and a nearby tree under artificial rainfall. A full-scale laboratory experiment confirms that a direct stroke to a tree can cause severe damage to nearby power lines by initiating an arc channel through air to the conductors. A complete model of this phenomenon is developed by combining the existing static and dynamic arc equations. The model is accomplished by the bilateral interaction between the EMTP and Transient Analysis Control System (TACS) field. The experimental results have been reproduced by the computer simulations.

The performance of the arc phenomenon is examined using a typical Finnish distribution network design. Using the modified arc model, the lightning arc performance of the MV/ LV network under the influence of nearby trees and the network characteristics is evaluated.

Keywords Overvoltage, lightning arc, medium voltage distribution lines, tree

ISBN (printed) 978-952-60-4242-8 **ISBN (pdf)** 978-952-60-4243-5

ISSN-L 1799-4934 **ISSN (printed)** 1799-4934 **ISSN (pdf)** 1799-4942

Location of publisher Espoo **Location of printing** Helsinki **Year** 2011

Pages 191 **The dissertation can be read at** http://lib.tkk.fi/Diss/

Acknowledgements

Firstly, I thank Almighty God who has allowed me to reach this height in my academic study.

I am indebted to my supervisor Professor Matti Lehtonen for his guidance, advice and encouragement towards the success of this work. He has been my mentor throughout my academic and research career since I began.

I wish to thank the power systems research group and all the staff in the department for their support. I would like to thank Dr. Petri Hyvönen, Mr. Hannu Kokkola, Mr. Jouni Mäkinen, Mr. Joni Klüss, Mr. Tatu Nieminen and Mr. Veli-Matti Niiranen for their time spent with me in the laboratory. I express my warm gratitude to all people who have worked with me during this study, especially Dr. John Millar, for the conversations we had together during the writing of some of the papers. In addition, I am very grateful to my friends outside the working environment for their support.

I am grateful to the pre-examiners, Professor Akihiro Ametani and Professor Stanislaw Grzybowski, for their valuable comments.

I would like to express my sincere gratitude to the financial bodies that have helped me in realizing this successful work. Without the funding by the ETA Graduate School, the Fortum Foundation and the Research Foundation of Helsinki University of Technology, this study would not have been possible.

I express my warmest gratitude to my parents, Pa Jacob Adefolaji Omidiora and Late Madam Elizabeth Tinuola Omidiora, my brothers, Dr. E. O. Omidiora and Mr. Banwo Ogundipe, and sister, Mrs. Esther Ogundipe, for their support and encouragement throughout my studies. Finally, I owe my thanks to my beloved wife, Abimbola Olayemi, who has been there for me for the smooth completion of this work.

Michael Adebayo Omidiora

Espoo, August 2011.

This work is dedicated to the soul of my mother Mrs Elizabeth Tinuola Omidiora

Dissertation's Publications and Author's Contribution

The main part of this dissertation work is based on the following publications which are referred to as Publication I – VIII:

I M. A. Omidiora and M. Lehtonen "An Approach to the Lightning Overvoltage Protection of Medium Voltage Lines in Severe Lightning Areas", *Current Themes in Engineering Technologies, American Institute of Physics (AIP), USA. Edited by Sio-long A, Mahyar A.A. and Su-Shing C.*, Vol. 1007, pp. 140-151, 2008.

II M. A. Omidiora and M. Lehtonen "Simulation Performance of Lightning Discharges around Medium Voltage Underground Cable", *The 44th International Universities Power Engineering Conference (UPEC2009),* Glasgow, UK. Sept. 1st – 4th, 2009.

III M. A. Omidiora and M. Lehtonen "Protection of Lightning Disturbances on MV Underground Cable", *International Review of Electrical Engineering (I.R.E.E.),* Vol. 5, No. 1, Feb. 2010.

IV M. A. Omidiora and M. Lehtonen "Performance Analysis of Lightning Overvoltage on Medium Voltage Distribution Lines Equipped with Covered Conductors", *2nd International Conference on Adaptive Science & Technology (ICAST 2009)*, Accra, Ghana. Dec. 14th- 16th, 2009.

V M. A. Omidiora and M. Lehtonen "A Comparative Study on the Shielding Effect of Tree, Concrete Building on Direct Lightning Strokes to Medium Voltage Distribution Line", *North American Power Symposium (NAPS2008),* University of Calgary, Canada, Sept. 28th-30th, 2008.

VI M. A. Omidiora and M. Lehtonen "Experimental Performance of Induced Voltage on Power Line due to Lightning Discharge to nearby Tree*", International Symposium on Modern Electric Power Systems (MEPS'10),* Wroclaw, Poland, Sept. 20th- 22nd, 2010.

VII M. A. Omidiora, N. I Elkalashy, M. Lehtonen, M. H. Abdel-rahman and P. Hyvönen "Investigation of Lightning Arc between Conductor and nearby Tree under Artificial Rainfall", *IEEE Transactions on Dielectrics and Electrical Insulation*, Vol. 18, Issue 2, pp. 620-630, April 2011.

VIII M. A. Omidiora, N. I. Elkalashy, M. Lehtonen and M. H. Abdel-rahman "Modelling Evaluation of Lightning Arc between Power Line and nearby Tree", *European Transactions on Electric Power, ETEP,* published online on June 24th, 2011, DOI: 10.1002/etep.606.

This work was carried out in the Department of Electrical Engineering, Aalto University (Formerly Helsinki University of Technology, TKK), Finland, under the supervision of Professor Matti Lehtonen who has recommended the research topic. The author of the dissertation, who is the main author of the above publications, is responsible for the analysis and writing of the above publications. Laboratory setups were organized with technical support from Mr. Hannu Kokkola, Mr. Jouni Mäkinen, Mr. Joni Klüss, Mr. Tatu Nieminen and Mr. Veli-Matti Niiranen. The coauthors of other Publications [Publications VII and VIII] have assisted in the use of the right configuration for the experiments and also for the use of TACS systems in EMTP to model the arc. Their valuable comments and discussions have also helped in improving the quality of the publications. However, the experimental work and the modeling tasks, which involved the use of EMTP, FEM and MATLAB simulation software, were performed by the author.

Table of Contents

List of Symbols and Abbreviations

g	Time-varying arc conductance
G	Stationary arc conductance
τ	Arc time constant
G_i	Initial static arc conductance
G_c	Ultimate arc conductance
i	Arc current
I_p	Lightning current peak
U_o	Arc voltage gradient
r	Arc resistance per unit length
R_{arc}	Arc resistance for static and dynamic arc equations
A and B	Arc fitting coefficients
I_p	Lightning peak current (kA)
I_{50}	50% lightning current (kA)
$P(I_p)$	Probability that any peak return-stroke in any given flash will exceed I_p
ρ_s	Soil resistivity
N_{cd}	Number of underground cable damage times per year
N_g	Ground flash density
A	Underground cable attractive area
I_{min}	Minimum lightning current
R_g	Ground resistance
C_{sb}	Capacitance representation of substation
β	Calibration constant
r_{LC}	Striking distance from electrode to conductor
r_{LT}	Striking distance from electrode to tree
K_v	The factor for the ratio of the return stroke velocity to light velocity (v/c)
$U_t(w)$	Fourier transforms of the tree top potential
$I_t(w)$	Fourier transforms of the tree current
C_t	Tree's capacitance under the for dry-air and wet-air conditions
R_t	Measured tree dc resistance
$Z_t(w)$	Tree's frequency domain impedance
C_{tc}	Tree-to-conductor capacitance
C_{cg}	Tree-to-ground capacitance
U_{arc}	Arc voltage drop
U_t	Lightning impulse voltage
$U_{c,}$	Induced and conducted voltage on the conductor
TKK	Helsinki University of Technology
MV	Medium Voltage
EMTP	Electromagnetic Transient Program

ATP	Alternative Transient Program
TACS	Transient Analysis Control System
LV	Low Voltage
SW	Shield Wire
FMI	Finnish Metrological Institute
GFD	Ground Flash Densities
FEM	Finite Element Method
MOV	Metal Oxide Varistor
IEEE	Institutes of Electrical and Electronics Engineers
UC	Underground Cable
SD	Striking Distance
T	Thunderstorm days
BIL	Basic Insulation Levels
EA	Length of Exposure-arc
OGW	Overhead Ground Wire

1- Introduction

The fast increase in global climate change has been associated with a high rise in global lightning distributions and frequencies around the world. The implication is that distribution lines and equipment will continue to be vulnerable to this natural phenomenon if proper care is not taken. Lightning has been identified as the major cause of faults on medium voltage distribution lines [1]. In Finland, yearly reports of faults in all distribution lines have shown that lightning-related faults take the lead over other faults, despite substantial surge protection. This calls for a deep understanding of lightning electromagnetic interaction with distribution lines and the provision of adequate surge protection schemes for the total mitigation of lightning-caused faults in all medium voltage distribution line types, which include overhead lines, underground cables and covered conductors.

Surge performance of overhead lines can be minimized with adequate installation of surge arresters and shield wires. In addition, insulation enhancement can play a significant role in reducing the outage rates of the lines, though this is not the most effective. However, it has been proved that high and grounded structures such as trees or buildings can naturally protect the lines from direct lightning strokes [2-7], if the lines traverse the structures in such a way that there is adequate clearance between the lines and the structures. In the literature, critical studies have been made to understand the performance of lightning-induced voltage on lines from nearby strokes [1], [3]. As a matter of fact, very few investigations have been carried out to understand the influence of very close and tall structures, such as trees, buildings and other high structures, on the lightning performance of power distribution lines. It is revealed in this study that there exists some resulting induced overvoltage on distribution lines due to lightning strokes on nearby trees. Thus, induced voltage exists whenever a distribution line is perfectly shielded by a surrounding tree.

Rainstorms are the primary source of lightning [1]. Rainfall can play a number of roles in the electrical breakdown of an air interface between a tree and a nearby distribution line. Water is a stress enhancer because of its higher permittivity than ordinary air. A water drop deforms under the influence of the electric field - due to both Coulomb and field-gradient forces - thereby increasing its stress enhancing feature. Water can be a good conductor [8], [9], and so partly shorts out the some of the air insulation; as an extreme condition, the elongated water droplets can coalesce to form a ribbon of water between the electrodes. While it is well understood that the resistivity of air is higher than water, the presence of a substantial number of raindrops of air can be likened to an insulator (air) with several voids occupied with water thereby causing a reduction in the overall resistivity of the air insulation between electrodes. A water droplet can increase corona propagation and speed-up the breakdown period of air [10], thereby enhancing the arc formation between a lightning-struck tree and a nearby distribution line.

1.1 Problem Description

In order to make a thorough investigation of lightning overvoltage on a distribution network in a given area, good knowledge of the lightning activities within the area can be helpful. Other important considerations are the contribution of high structures, i.e. trees, and weather conditions on the persistent lightning faults within the area. Thus, the motivations and problem descriptions regarding this research work are briefly explained as follows.

1.1.1 Lightning Statistics in Finland

An understanding of lightning activities in an area where lightning protection is required is very important. The lightning data used in this work were made available by the Finnish Metrological Institute (FMI). As given in Figure 1.1, the inland part of southern Finland is the area where the rate of lightning strikes is very high when compared to other locations in the country, based on the statistical occurrence of lightning and other lightning related incidents. Multiple strokes from these flashes range from 1-15 strokes with a mean of 2 strokes per flash. In both the northern and coastal parts of the country, fewer flashes are detected than in the inland part of the southern region (inset of Figure 1.1). Distribution lines existing in this severe lightning area will be more susceptible to direct strokes than other network areas. Thus, the assessment of overvoltage due to direct strokes and the augmentation of surge protection to lines in this area are one of the subjects of this work.

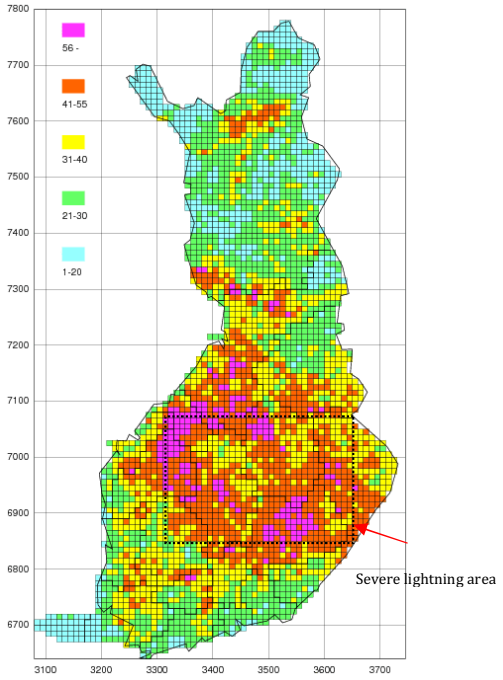

Figure 1.1. Average Ground Flash Densities (GFD) per 100 km^2 in Finland. There are 5 sensors plus 3 supporting sensors from Sweden, Norway and Estonia to boost the sensitivity of detection. The inset is the area with highest number of flash densities since 1998.

Based on the data collected from the FMI, the average GFD was estimated to be 0.786 stroke/ km^2/year. The field data analysis has shown that the cumulative distribution of lightning stroke magnitudes $P(I_p)$ can be represented as shown in Figure 1.2. After careful analysis, it was found that the probability density function given by *Klairuang et al* [11] fits the curve very well. This is given by (1.1). Hence, typical stroke in any lightning flash is expected to comply with (1.1) and Figure 1.2.

$$P(I_p) = \frac{1}{1+\left(\frac{I_p}{I_{50}}\right)^{3.09}} \tag{1.1}$$

Where;

$P(I_p)$ = Probability that any peak return-stroke in any given flash will exceed I_p,
I_p = Lightning peak current (kA),
I_{50} = 50% lightning current, (15 kA is the mean lightning current in Finland).

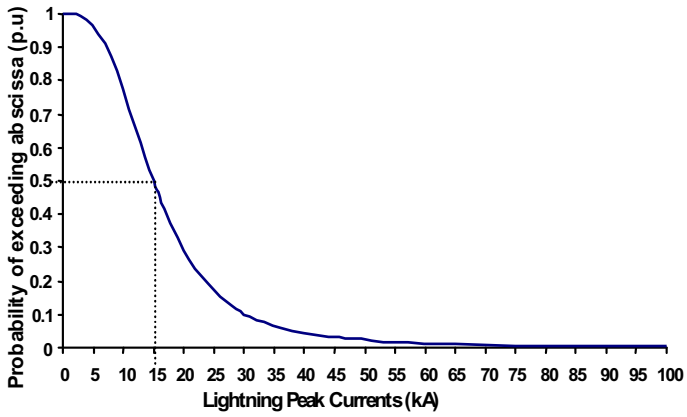

Figure 1.2. Cumulative distribution of lightning peak current in Finland according to lightning data collected from the Finnish Meteorological Institute (FMI).

1.1.2 Hypothesis of Natural Lightning Strokes to Trees

Lightning happens when strong negative charges in low clouds and strong positive charges on ground meet in air. The negative charges in the clouds descend in a series of chain reaction steps known as stepped leaders. The return stroke occurs as the positive charge in the cloud meets the negative charge in the air. Lightning stroke occur when these charges is within ionized air. Being one of the most abundant resources on earth without unrestricted growth in some countries like Finland, trees represent the tallest structures that are victims of natural lightning strokes (see Figure 1.3 adapted from [12]).

A wide misconception that lightning only strikes conducting materials like metal is a fallacy. Lightning finds the path of least resistance to the ground through the most conducting material in the areas such as wood or metal. Trees are mostly the victim of lightning because of their height; therefore, they appear as natural lightning rods. There is a higher probability of a tree being hit and damaged by lightning due to wetness of trees during rainstorms. However, trees often survive most lightning damage because of their extremely wet barks (the outermost layers), which allow the lightning current to flow into the ground. The following are other suppositions drawn from [12] that explain why lightning often strike trees: “The highest trees are most likely to be struck”, “Trees growing in the open, either alone or in a small group, or at the edges of forests, are more likely to be struck”, “Certain tree types are more likely to be struck than others”. “The presence of a good electrical ground will affect tree damage”, “Old trees are more likely to be damaged heavily”, “The presence of a good electrical ground will affect tree damage”, “Continuing lightning currents cause most damage”, “Strong positive flashes cause more damage”, “High peak current causes more damage”, “High-multiplicity flashes will cause more damage”.

Figure 1.3. Photograph of a natural lightning flash to a tree in Porvoo, Finland. The rainfall was about 15 mm in the 3 hours before the flash. The flash caused a temporary break in TV service to the area. The flash was uniquely tied to a -6 kA single stroke based on location and timing [12].

1.1.3 Influence of Rainfall on Lightning Arc from Tree to Conductor

One of the author's motivations for investigating the effects of rainfall on the lightning arc between trees and power conductors was the interesting work by *Rizk* and *Schneider et al,* which has revealed that rain significantly affect the switching flashover voltage of not only the solid insulators, but also the air insulation between air gaps:

- Test results by *Schneider and Turner* [9] showed a significant drop in the positive switching impulse flashover voltage of large-sphere plane gaps due to rainfall.
- Laboratory tests by *Rizk* [10] revealed that, for a large-sphere plane gap, the presence of raindrops in air between gaps could significantly reduce the 50 % flashover voltage under switching impulses for both positive and negative polarities. E.g. for a 1 m solid sphere plane gap, separation 2m and rain intensity 1 mm / min, the 50 % sparkover voltage of the positive switching impulse with a front of 240 μs for dry-air is 1400 kV as against 820 kV for wet-air – a reduction of about 40 %.

Since real lightning occurs during raining, rainstorms, snowstorms, and other natural phenomena [1], flashovers from nearby trees to power lines can be influenced by these weather conditions. This is particularly the case with lightning strokes to trees around the power lines in some densely forested countries, such as Finland. When the lightning-struck tree is close to the line, the amplitude of the lightning stroke is high, it is raining and the rain is accompanied by other natural phenomena, the coupling effect between the lightning-struck tree and the power line can be high enough to create a flashover.

1.1.4 Shielding and Lightning Arc by Trees

The vast majority of lightning faults in a power distribution network are from indirect strokes [1]. But not all these strokes terminate directly on the ground. In the Nordic countries, most distribution networks are installed in forest areas. In

Finland, about 70% of the permanent faults that occur in rural MV networks are caused by animals and weather conditions, such as thunderstorms (lightning), snow, icing, storms, strong wind and fallen trees [13]. Lightning can terminate on trees in most areas where the power networks traverse the forested areas, see Figure 1.4. Distribution lines and equipment around the forests can be protected naturally from direct hit by lightning strokes [5-7]. However, as shown in Figures 1.3 and 1.4, if the tree intercepts the lightning stroke, an arc may ignite due to the existence of mutual coupling between the tree and power line / equipment. One other factor that may cause arc ignition is the conductive properties of rainstorm during the lightning incidence. The surges from this incidence will transform into travelling waves that move in both directions along the power line to the transformers and other distribution equipment. Although the severe lightning energy may be shielded by the surrounding trees, it is also very important to devise a method to protect the lines against the lightning arcs from the trees.

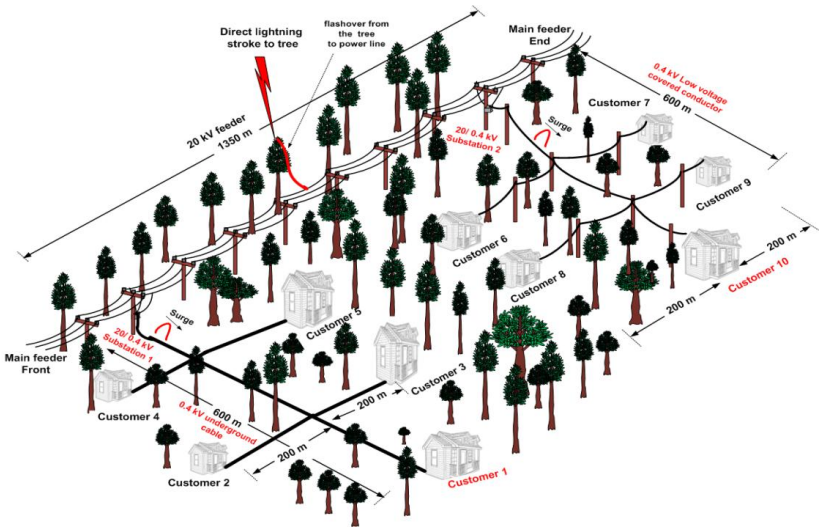

Figure 1.4. Typical 20/ 0.4 kV distribution network arrangement in Finland and the possible effect of a lightning arc. Direct strokes to a tree can cause severe damage to nearby power lines by initiating an arc channel through air to the bare conductors.

1.1.5 Arc Modeling for Lightning Arc Investigation

In the literature, a number of dynamic models have been developed to describe the behavior of electrical arcs; most of these models are used to model arcs in circuit breakers [14-18]. They have been proposed based on the theory of arc thermal equilibrium and they have become very useful for analyzing arcing phenomena. The thermal equilibrium method is one of the earliest dynamic arc models, proposed in [14], [15]. Also, they have been adapted to model long arcs on overhead transmission lines [18- 20] and to model short arcs [21]. The behavior of a lightning arc was simulated for further knowledge about the lightning performance of power lines. The lightning arc was initially modeled using the dynamic arc equation proposed by the *Kizilcay model*. However, there was a large error at the beginning time of the arc creation period. In order to reduce the error in the simulation results, the arc model was modified by combining a static equation [22] and the dynamic arc equation (*Kizilcay model*) [20]. This period was estimated by evaluating the error period in the dynamic arc equation with respect to the experimental waveforms.

1.2 Finnish Distribution Lines

In Finland, distribution line types include overhead conductors, underground cables and covered conductors. The distribution systems have traditionally been comprised of two voltage levels, e.g. 20/ 0.4 kV (medium voltage / low voltage). Apart from underground cables, lines are usually installed on impregnated wooden poles. Because of the low conductivity of the soil, the distribution poles are usually ungrounded, thus the flashover voltages between the phases to ground are very high. For the 20 kV class distribution lines, the Basic Insulation Level (BIL) between phases is 150 kV for overhead distribution conductors, 215 kV (125 kV, support insulation and 90 kV, conductor insulation) for covered conductors [Publication IV]. The 0.4 kV are usually aerial bundled cables (ABC cable; AMKA) with a BIL of 6 kV (IEC60664-1). All of these distribution lines are exposed to weather effects, such as rainstorms and windstorms, which cause faults and interruptions in the distribution network. This has led to a high number of outages during the past few years. The lightning performance of these lines can be influenced by their BILs and the ground flash density, lightning characteristics, among other things. Thus, the lightning protection for medium overhead conductors, underground cables and covered conductor are investigated in this work.

1.3 Economic Consideration for Lines with Surge Protective Devices

Medium voltage distribution lines are usually not shielded and are particularly vulnerable to direct lightning strokes. The success of surge arresters protection has been the subject of works with different objectives [1]. Surge arresters can be used, instead of overhead shield wires, to protect the distribution lines from lightning flashovers. The level and frequency of occurrence of discharge currents depends greatly on the exposure of the distribution system and the ground flash density. Arresters installed on exposed lines and located in areas of high ground flash density will receive large magnitude currents more often than arresters in shielded locations. In spite of the fact that the primary cause of flashover is in many distribution lines is a surge induced by a nearby stroke to ground, when the line is protected by surge arresters, only direct strokes to the nearby structures or to the unshielded lines becomes an issue, since only in such cases the energy discharged by arresters may be larger than energy withstand capability. Lightning flashes with multiple-strokes are another factor to be considered. Since strokes with any peak current magnitudes may reach a phase conductor of a distribution line, heavy-duty class arresters can be used to protect these lines [1]. Arrester damage caused by direct lightning strokes can be effectively prevented by installing overhead shield wires or by increasing arrester withstand capability. Also, surge protection can be achieved by lowering the grounding resistance, but this is not a decisive factor.

Thus, in order to achieve the most effective overvoltage protection of distribution systems, it is important to find the best agreement between the costs and benefits of the protection devices to be employed. Great effort should be made to achieve the technical-economic balance. The lightning overvoltage protection, which is correctly employed, lessen: (i) Outage of the distribution systems, (ii) Cost due to interruption in the energy supply, (iii) Electrical equipment replacement costs, (iv) Ageing of the insulation (i.e. cable, transformer), and (v) Maintenance labour. Thus, the costs of increasing the arresters withstand capability or adding a shield wire are not the most important factor, but the costs that may come up on a long-term basis if adequate surge protection is not employed.

1.4 Research Contribution

In this work, improvement in the lightning protection of Finnish distribution lines against multiple lightning strokes is proposed [Publication I]. The effects of surge arresters and of the combination of the surge arresters and shield wire on the protection of the overhead distribution lines are studied using the Electromagnetic Transient Program (EMTP) software. The true index of lightning severity in these power distribution areas is based on the ground flash densities and return stroke data collected from the Finnish Meteorological Institute. The presented test case is the IEEE 34-node test feeder injected with multiple lightning strokes and simulated with EMTP. The response of the distribution line to lightning strokes is assessed with a combination of shield wire and arresters.

The need for providing adequate lightning protection for medium voltage underground cables is discussed in this dissertation [Publications II and III]. Using analysis and Finite Element Method (FEM) software, the investigation shows the vulnerability of cables to lightning discharges to different soil structures. The effects of lightning stroke magnitudes, lightning stroke location, soil resistivity and soil structures are taken into consideration in the simulation. A new protection scheme is proposed by means of shield wire. The performance of the new protection scheme is examined with FEM and MATLAB software considering different soil structures and resistivity. The failure rates of the underground cable with and without a shield wire are compared based on the real lightning statistics in Finland.

This work examines the performance of lightning overvoltage due to real lightning discharges around medium voltage covered conductors [Publication IV]. Evaluation and simulation are based on real lightning data collected from the Finnish Meteorological Institute (FMI) from 1998 to 2008. The presented feeder is an overhead distribution line with a covered conductor subjected to indirect lightning strokes to ground and direct lightning strokes to a line support. With the Electromagnetic Transient Program (EMTP), simulations of lightning strokes are performed with different lightning current characteristics. The EMTP simulation cases consider the modeling guidelines for fast transients as specified in the lightning literature. Simulations are made to compare the resulting overvoltages and energy absorptions of surge arresters for all the analyzed cases.

In this dissertation, new knowledge is introduced in terms of the contributions of surrounding trees to the lightning performance of distribution lines. An experimental study and *Electro-geometric* model is used to investigate the shielding effect of the trees on lightning strokes to distribution lines [Publication V]. The shielding effect of a nearby tree on direct strokes to a distribution conductor is compared with that of a concrete building which has been previously investigated in the literature. For the first time, an experimental setup is made to investigate the induced voltages existing between a lightning-struck tree and a distribution line [Publication VI]. The effects of tree-to-line clearance, change in lightning time characteristics and the polarities of the lightning impulses on the induced voltages are investigated. The study is extended to compare the results of the laboratory experiment with the existing *Rusck* formula.

For the first time, the investigation of a lightning arc between a distribution conductor and a nearby tree under artificial rainfall is conducted [Publications VII and VIII]. At first, the investigation is made experimentally using a full-scale laboratory setup considering dry-air and wet-air conditions. The experimental results are then reproduced using a combination of EMTP models of a multi-stage impulse generator, a high-frequency RC model of a tree, a distribution conductor and dynamic arc equations. The arc is developed within the EMTP software with its Transient Analysis Control System (TACS) features. Furthermore, the research is extended to the modification of the existing dynamic arc model for the accurate

lightning arc simulation application. The modified dynamic arc model combines a static arc equation and the dynamic arc equations to reproduce a lightning arc involving a lightning-struck tree and a nearby conductor during rainfall. The EMTP simulation shows that the experimental results are reproducible by means of system modeling. It is expected that such a model can be included in the existing ATP/EMTP software packages for simulating power system transients.

The application of the modified dynamic arc model to a typical Finnish distribution network design is evaluated [Publication VIII]. The distribution network consists of a distribution feeder, distribution transformers, low voltage underground cable and covered conductor feeders and customer loads. The lightning arc characteristics of the distribution network elements are examined with EMTP software. By means of a simulation using the modified dynamic arc, the lightning arc performance of the MV/ LV network under the influence of nearby trees and the network characteristics is analyzed. Thus, the study provides strong evidence concerning faults related to lightning arcs, the consequent overvoltages on power lines and an option to subdue the arcs by means of proper grounding of distribution pole crossarms.

1.5 Dissertation Outline

The contents of this dissertation are a summary and Publications I - VIII. Brief illustrations of the contents are as follows.

- Chapter 2 presents an evaluation of lightning performance and the protection enhancement of different Medium Voltage distribution line types, which are overhead lines, underground cables and covered conductors.
- In Chapter 3, the effects of trees on lightning strokes to distribution lines are discussed, where shielding by trees and induced overvoltage involved are extensively covered.
- Chapter 4 summarizes the results of the modified dynamic arc model for representing the lightning arc between a tree and a nearby distribution line under artificial rainfall. A comparison of the existing arc model and the modified arc model is shown.
- By employing the modified dynamic arc model, Chapter 5 discusses the performance of a lightning arc on a typical 20/0.4 kV network.
- Conclusions and future considerations are given in Chapter 6.
- Publications I – VIII are included in the appendix.

2- Lightning Protection of Distribution Line Types

2.1 Protection of Overhead distribution lines against Lightning Overvoltages

Distribution lines within a high ground flash density (GFD) area could experience more lightning strokes than other lines. Thus, for a given voltage level, surge arresters installed on the lines are mostly of the same rating and energy capabilities. Surge protection of the lines against the excessive overvoltage can be more effective if a shield wire is combined with surge arresters to intercept the strokes and lower the excessive surge current into the ground.

The subject of discussion in this chapter is the enhancement of lightning protection in Finnish distribution networks in areas where lightning is most severe. Assessment was made to determine the effect of shield wires on lightning overvoltage reduction and the energy relief of surge arresters (MOV) from direct strokes to distribution lines. The true index of lightning severity in the areas is based on the ground flash densities and return stroke data collected from the Finnish meteorological institute (see Section 1.1.1). The presented test case is the IEEE 34-node test feeder injected with multiple lightning strokes and simulated with the Alternative Transients Program/ Electromagnetic Transients program (ATP/EMTP). The response of the distribution line to lightning strokes was modeled with three different cases: no protection, protection with surge arresters and protection with a combination of shield wire and arresters. Simulations were made to compare the resulting overvoltages on the line for all the analyzed cases.

A single lightning flash with multiple strokes was assumed to terminate on the test line section '816-824' of the IEEE 34-node radial distribution network shown in Figure 2.1c. The selection of the strokes was based on the mean values of multiple lightning strokes observed in Finland in 2006 [23] with amplitudes of 18.6kA, 15kA and 12kA for the 1^{st}, 2^{nd} and 3^{rd} strokes, with 1ms intervals. The strokes were represented by a Norton equivalent circuit of ideal sources (Heidler-type current sources [Publication I]) in parallel with a lightning-channel equivalent impedance of 2.5 kΩ [2].The *Test line section* '816-824' of length 3.112 km, was split into 9 spans and 10 poles. The line was modeled as a 10 pole distribution line of 9 equal spans, by taking into consideration, the physical configuration of Finnish distribution lines shown in Figure 2.1a. The whole line was simulated with the ATP line and cable constant (LCC) subroutine using the *Jmarti model*. This model considers the geometrical and material of the conductor including skin effect and conductor bundling and the corresponding electrical data are calculated automatically by the '*line constants'* subroutine file. Since distribution poles in Finland are usually ungrounded due to high ground resistivity, the ATP model of the distribution poles were considered without footing impedance (resistance). Surge arresters were employed for the protection of lightning surges at various locations on the test system. The characteristics of the arresters, as taken from the manufacturer's datasheet [24], are shown in Figure 2.1b. These arresters were connected to the ground without an additional grounding connection. Shield wire was positioned on top of the middle line (Phase B) of the three phase line (see Figure 2.1a. All the above configurations are modeled with EMTP. More explanation of the simulation is given in [Publication I].

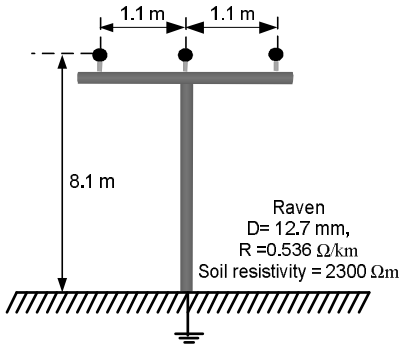

Figure 2.1a. Distribution line configuration.

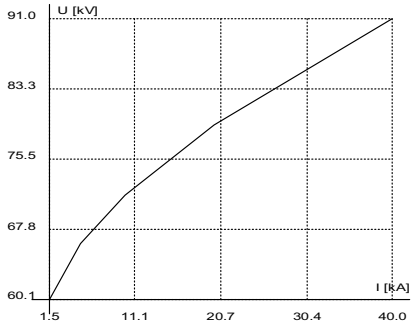

Figure 2.1b. V-I characteristic of a surge arrester [24].

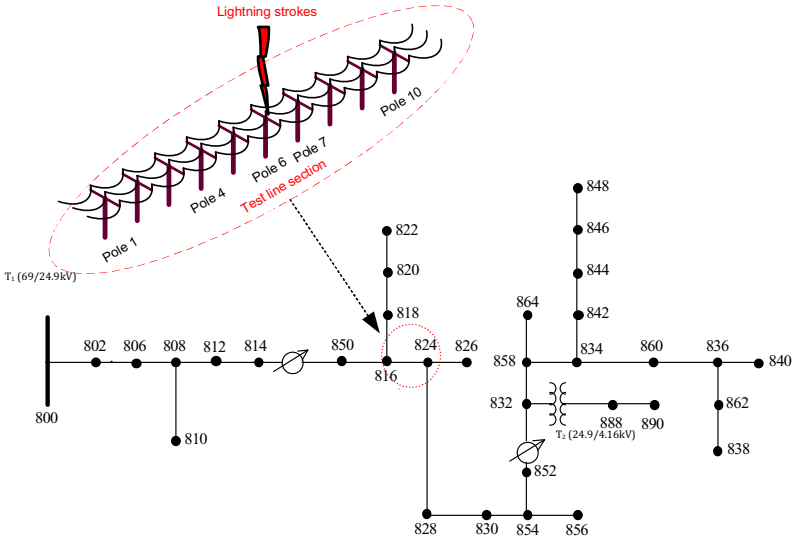

Figure 2.1c. IEEE 34-node Test Feeder.

2.1.1 Simulation Results

Three cases were taken into consideration in order to observe the lightning overvoltage performance of the distribution feeder and the suppression effect combined surge arresters and shield wire. *Case 1* was the multiple strokes on the line with no protection. Therefore direct strokes were terminated on phase B of pole number 6. *Case 2* considered the installation of surge arresters on phases A, B and C on each of the poles 1, 4, 7 and 10. In *Case 3,* the shield wire was combined with the surge arresters; therefore the pole configuration of distribution pole (see Figure 5 of [Publication I]) was modified with the inclusion of a shield wire 1.5 m above phase B on line 816-824. Simulation measurements were taken from phases A, B and C on each of the poles 1, 4, 7 and 10, and at the terminals of the substation transformer terminal (T_1) and the in-line transformer terminal (T_2) transformers.

For *Case 1*, Table 2.1 summarizes the results and Figure 2.2 shows the overvoltages wave-shapes at the pole number 6. It is obvious that the magnitudes of overvoltages measured were too high and that the flashovers will occur at the stroke point between the phases. However the flashover was disregarded based on the following points: Realistically, inter-phase flashover will occur depending on the overvoltage protection, also flashover to the ground is likely. The main focus is the characteristics of overvoltages on one (Phase B) of the phases struck by multiple lightning strokes, knowing that the overvoltage behavior is very important in the energy absorption requirement of surge arresters and, the location and placement on the arresters on the poles

Considering *Case 2* with surge arresters only, Table 2.2 summarizes the results and Figure 2.3 shows the remaining overvoltages clamped by the arresters at pole number 6. For Case 3 where the shield wire was combined with surge arresters installation of *Case 2*, Table 2.3 summarizes the results of the simulation and Figures 2.4 shows the remaining overvoltages at pole number 6. By using only surge arresters on line 816-824 at the designated poles, as in the *Case 2*, the overvoltages were minimized by 59%, 41.95% and 48.28% on phases A, B and C respectively, at the pole number 6 where the lightning flash was terminated. Overvoltage reduction was observed at every other pole including the two transformers. However, energies absorbed by the arresters at pole numbers 4 and 7 (see Figure 2.5), at the extremities of the strokes, were enough to damage the arresters even after successful operation, as they may require replacement for guaranteed protection in future. The energy handling capability of the 30kV class MOV arrester is 74.8kJ, 3.4 kJ/kV, where U_c= 22 kV [24]. With the use of shield wire on the lines and arresters at the designated poles, the overvoltages were reduced by 84.8%, 54.95% and 79.83% on phases A, B and C respectively, at pole number 6. In addition, the energies absorbed by the arresters on pole number 4 were reduced by 49.73%, 72.19% and 73.23%, and those of pole number 7 were also reduced by 77.79%, 48.02% and 78% for phases A, B and C respectively (see Figure 2.5). These results have shown clearly the effectiveness of adding shield wires to MOV-protected distribution networks in areas where power distribution lines are more prone to direct strokes. Considering the multiple lightning strokes, the combination of surge arresters and shield wire is very effective in suppressing to ground all overvoltages from the lightning strokes that the kind of network simulated in this study is frequently subject to. In distribution network areas where surge arresters are frequently damaged in spite of the installation of shield wires, surge arresters with larger energy handling capacity should be primarily installed.

Table 2.1. Peak Overvoltages at Poles -No Protection,
Direct Multiples Strokes on Phase B, at Pole 6

	Phase A (MV)	Phase B (MV)	Phase C (MV)
Pole 1	1.86	4.25	1.46
Pole 4	3.31	7.16	3.49
Pole 6	5.92	9.01	5.80
Pole 7	4.92	8.00	4.67
Pole 10	3.39	4.18	2.14
Transformer 1	1.52	2.74	0.93
Transformer 2	2.22	1.59	2.16

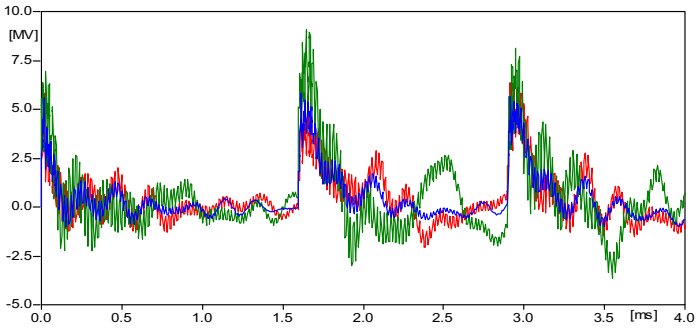

Figure 2.2. Case 1- Overvoltage waveshape at pole number 6 (No protection on the line).

Table 2.2. Peak Overvoltages at Poles –With Arresters,
Direct Multiples Strokes on Phase B, at Pole 6

	Phase A (kV)	Phase B (kV)	Phase C (kV)
Pole 1	43.50	54.90	31.70
Pole 4	67.87	79.36	66.74
Pole 6	2910	5230	3000
Pole 7	69.33	80.11	68.22
Pole 10	46.60	59.05	47.09
Transformer 1	20.32	73.73	56.40
Transformer 2	43.00	33.46	32.92

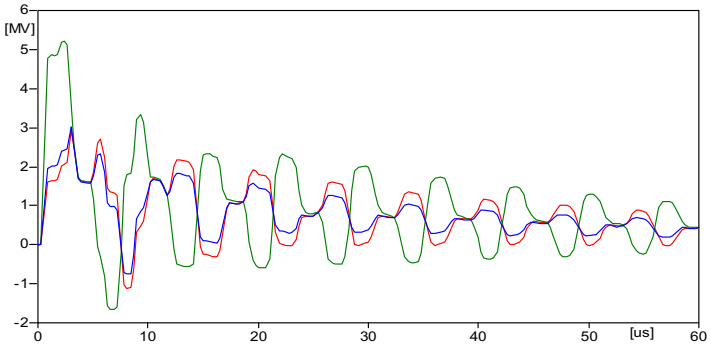

Figure 2.3. Case 2- Remaining overvoltages from 1st stroke measured at Pole 6. Phase B has the maximum overvoltage from the multiple strokes.

Table 2.3. Peak Overvoltages at Poles –with Arresters & Shield wire, Direct Multiples Strokes on Phase B, at Pole 6

	Phase A (kV)	Phase B (kV)	Phase C (kV)
Pole 1	43.29	56.52	33.29
Pole 4	60.50	79.64	58.70
Pole 6	900	4090	1170
Pole 7	62.27	80.46	60.50
Pole 10	47.79	57.82	49.53
Transformer 1	45.70	54.36	16.46
Transformer 2	75.71	50.75	51.99

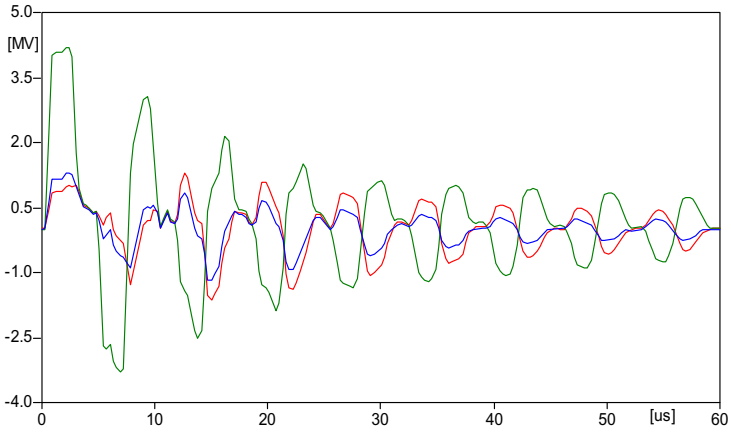

Figure 2.4. Case 3- Remaining overvoltages from 1st stroke measured at Pole 6. Phase B has the maximum overvoltage from the multiple strokes.

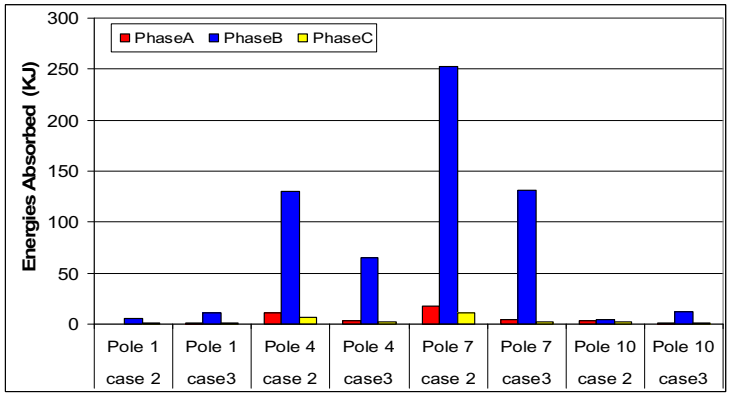

Figure 2.5. Energies absorbed by the Arresters installed at Poles 1, 4, 7 & 10. (Case 2- MOV only, Case 3 - MOV with Shield wire). The energy rating of the 30kV class MOV arrester is 74.8kJ, 3.4kJ/kV, where Uc= 22kV.

2.2 Protection of Medium Voltage Underground Cable against Lightning Overvoltages

The use of covered conductors in MV distribution lines is increasing day by day. After it was first researched in the 1970s in Scandinavian countries, the utilization of covered conductors began in Finland in 1984 [Publication IV]. Among the other benefits of covered conductor (CC) over bare conductor lines, covered conductors can tolerate temporary trees or branches leaning and eliminate disruptions due to conductor and tree clashes. However, the service reliability of covered conductors in our exposed climate is not quite clarified. Among other weather-related hazards, the ability of covered conductors to withstand conductor burn-down and insulation damages caused by lightning is uncertain. As a result of the low insulation level, lightning performance of covered conductor can be influenced by some factors including: the characteristics of lightning current, level of protection, distance between the protective devices and line span, among others.

Medium Voltage underground cables are more costly to maintain than any other type of power line. They are mostly used as connections from generating plants and substations to serve the loads for the life of the installation (see Figure 2.6.). They are also the predominant feeder type in urban distribution networks and are increasingly being considered even in rural MV networks. Lightning strokes can discharge to high structures such as trees, buildings, masts, overhead conductors, however, most lightning strikes the ground. These discharges can significantly affect underground cable networks nearby. Any direct stroke to an underground cable or indirect stroke nearby the cable can result in a high voltage build-up between the sheath and the core or high voltage punctures through the cable insulation, causing permanent damage. Lightning strokes to ground can cause overvoltage build-up or severe damage to any underground cables in their proximity. The most effective method of protecting a UC is by shield wire [25-32]. The impact of lightning strokes on underground cables can be minimized with shield wire [33- 34].

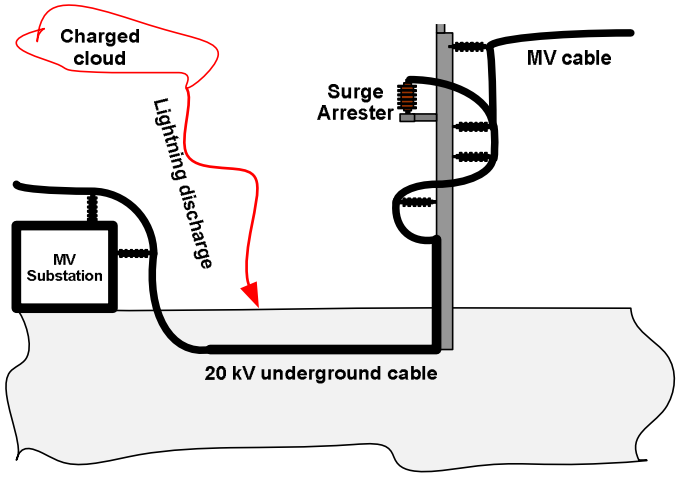

Figure 2.6. A schematic of Finnish 20 kV UC system for lightning analysis.

The basic idea of the proposed protection underground cable with shield is analytically established as follows; as shown in Figure 2.7, considering the underground cable (UC) with a striking distance (SD), the region of exposure of the UC to a lightning stroke is the part of the circle formed by the SD that intersects the ground surface at points X and Y. The shield wire must be positioned somewhere below this region (X-Y), to effectively protect the UC from direct strokes. The performance of this scheme, as established by the *Electro-geometrical*

method [25] is illustrated in Figures 2.7, 2.8 and 2.9. With the position of the SW indirectly above the UC and assuming that the striking distances (SD) of the two cables are equal, the intercept of the arcs of the two circles will be at point *P* above the ground surface. This will leave the SW and the UC protected from direct strokes to the surface of region C. Since only the arc of the SW covers region B (Figure 2.9), not the arc of the UC, any stroke to the surface in the region will be diverted to the SW. Similarly, the strokes to the surface of region D will be diverted to the UC. The probable attraction of lightning strokes in region A is to UC and to the SW in region F. Any stroke to the surface of region E can divert to either the SW or UC. For effective shielding, the intersection point P of the arcs of the SDs should meet underground rather than above ground. This can be achieved by installing the SW directly above the UC as demonstrated in Figure 2.10, where the UC is protected by the SW from direct lightning strokes to the surface of regions F, B or C.

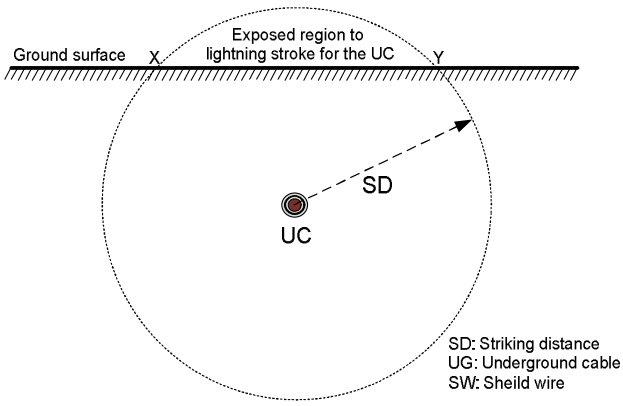

Figure 2.7. Exposed region of underground cable to lightning, X-Y.

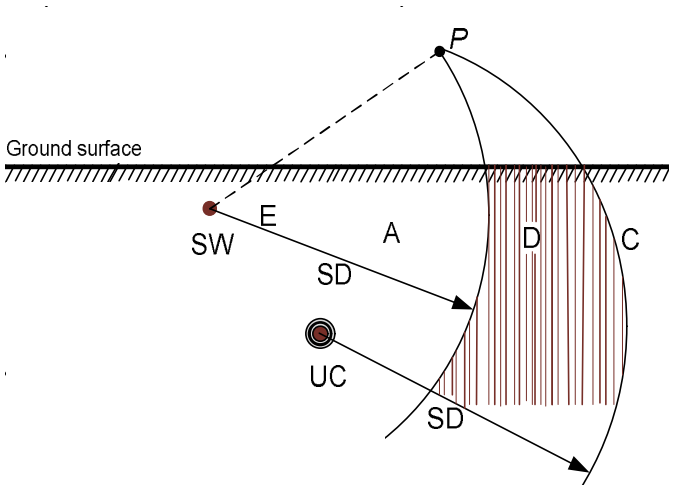

Figure 2.8. Ineffective protection with the shield wire on the right side of the UC.

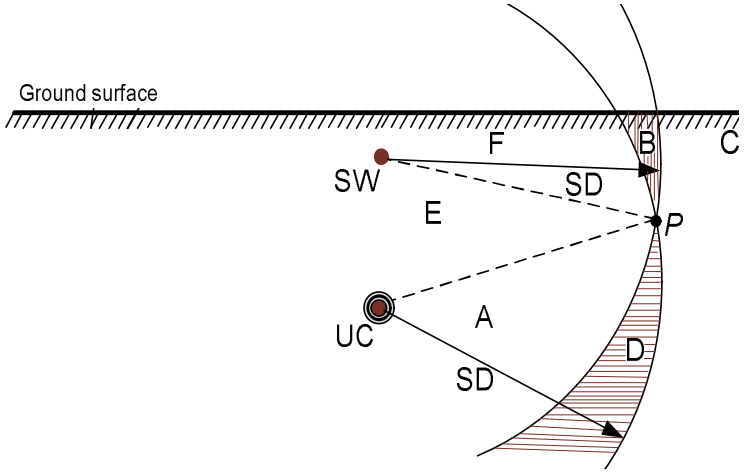

Figure 2.9. Effective protection with the shield wire directly above the UC.

2.2.1 Simulation Results

The lightning protection scheme of an underground cable with a shield wire, as indicated in Figure 2.10, is discussed here. Simulation of the underground cable with the shield wire is made to access the protection of the shield wire against lightning discharges around the cable. Figure 2.11 gives flowchart of the simulation and the calculation process. Figure 2.12 presents the configuration of the model for the simulation. The performance of the protection scheme is investigated with the Finite Element Method (FEM) considering different soil structures and resistivity. The other effort made was the comparison of the failure rates of the underground cable with and without the shield wire. Details about the simulation procedures have been reported in [Publications II- III].

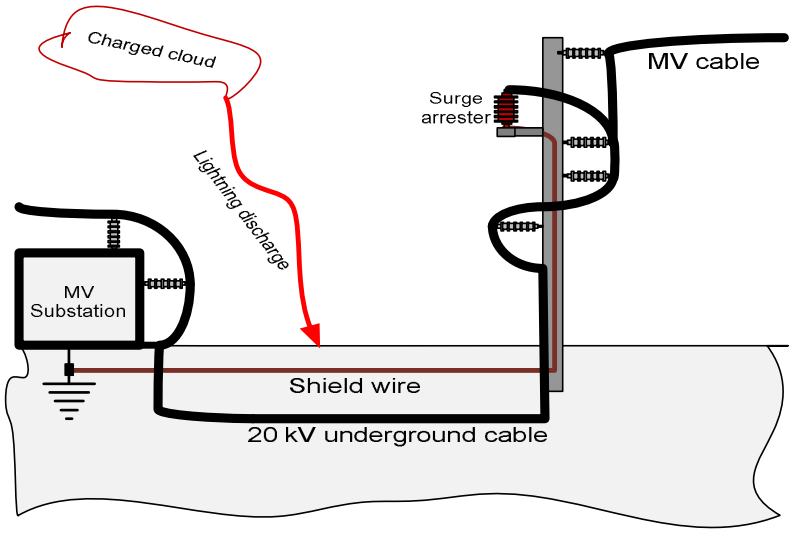

Figure 2.10. A schematic of a Finnish 20 kV UC system with the proposed shield-wire protection scheme.

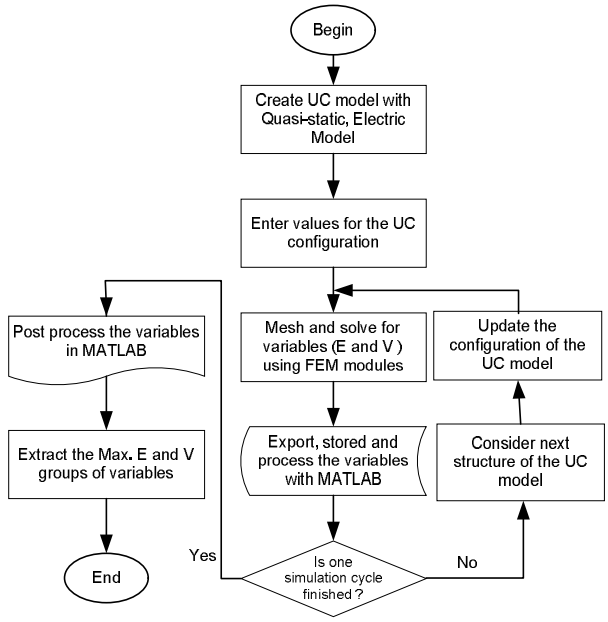

Figure 2.11. Flowchart for simulation and calculation process.

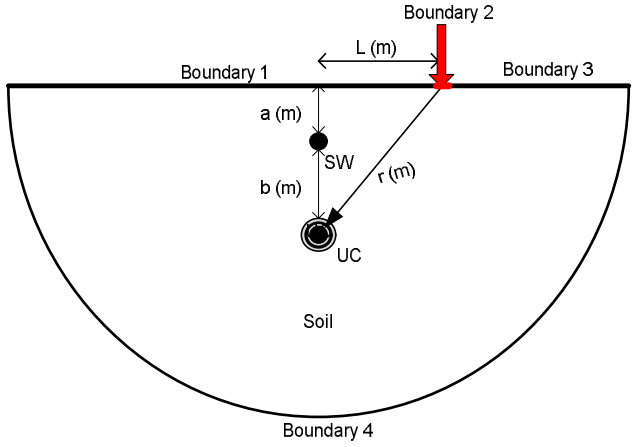

Figure 2.12. UC model configuration for simulation.

Potential distribution around the UC, with and without the shield wire

The comparison of the potential distribution around the UC, with and without the SW, is given in Figure 2.13. A lightning current of 15 kA (mean lightning current in Finland) was used. Homogenous soil (resistivity, ρ = 2300 Ωm) was considered and the depth of the SW and UC were 0.5 m and 1 m respectively. The visual appearance of the potential distributions have shown that the overvoltage stress reaching the UC from the lightning stroke point could be intercepted and suppressed by shield wire installation strategically on top of the cable.

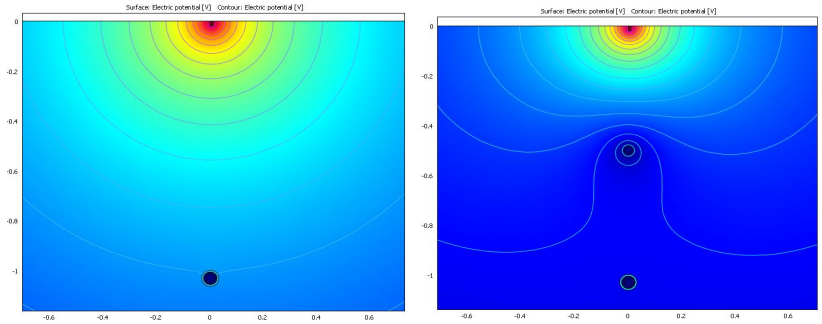

(a) UC without shield wire (b) UC with shield wire

Figure 2.13. Electric potential distribution around the lightning point, shield wire and UC cable

Effects of SW and lightning stroke location on overvoltage build-up on UC.

With the same configuration of the UC and SW as indicated above, Figure 2.14 demonstrates the effectiveness of shield wire protection of an underground cable against direct and indirect strokes. The aim of shield wire application is to intercept all lightning strokes [25]. This was shown in Figure 2.14, where the percentage of the lightning voltage (electric field) was minimized with the help of shield wire. About 81% of the electric potential and field intensity on the UC were suppressed by the SW (for a direct stroke, L = 0), though the reductions were less (45 %) as the lightning point's distance increases further than L = 1.5 m. However, the significance of the SW has been shown for a UC exposed to both direct and indirect lightning strokes.

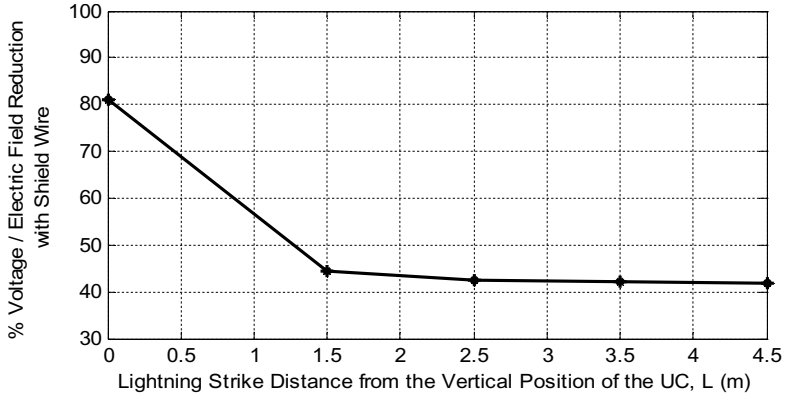

Figure 2.14. Percentage reduction in lightning voltage / electric field intensity on underground cable with shield wire.

Safe location of a shield wire around a cable for effective overvoltage protection

Since it has been demonstrated that a shield wire is able to intersect the most common stroke magnitudes, computation should be made to determine a reasonable spacing between the cables and the shield wire, to avoid sparkover between the two materials. The same configuration as the previous section was used except that two different lightning stroke points were considered, i.e. for direct strokes and for indirect strokes [Publication III]. Figure 2.15 gives the percentage reduction in voltage (or electric field intensity) on the cable considering

a change in vertical spacing between the underground cable and the shield wire. The SW can be more effective in intersecting direct strokes to the soil than distributing indirect strokes around the UC for all spacing examined. In the case of a direct stroke, the SW performed better by increasing the spacing between the two materials, whereas the reverse is the case for indirect strokes, as expected. Since most lightning discharges to underground cables are indirect in nature, a shield wire must be installed in the ground to take part of the lightning current rather than intersecting all of it. Thus, by creating enough spacing, at least 0.5 m for a 1 m cable burial, the two materials can be avoid from sparkover during severe lightning strokes, which in-turn will prolong the cable's lifetime.

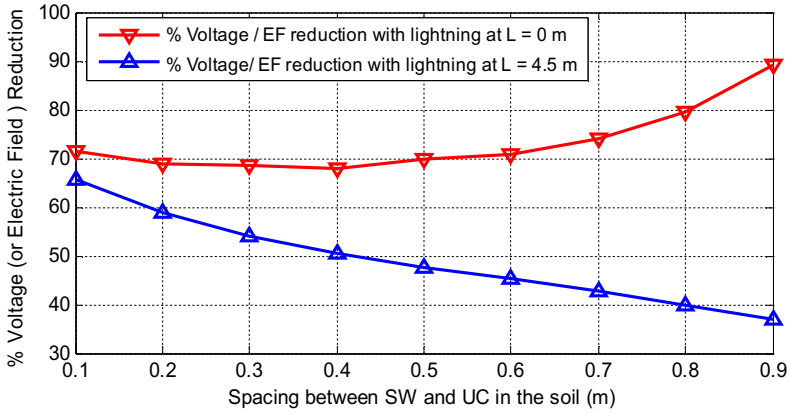

Figure 2.15. Effect of spacing between shield-wire (SW) and underground cable (UC) on voltage (or electric field) reductions around the cable.

Minimum lightning current to initiate breakdown in cable with and without a shield wire protection

The configuration in Figure 2.12 was considered with a shield wire depth of 0.2 m. By varying the soil resistivity values from 100 to 3000 Ohm-m [Publication III], a lightning current was increased from 1 kA to a minimum current that can cause breakdown in the UC insulation (i.e. when the lightning electric field intensity, E_c, exceeds the withstand strength, E (21.6 MV/m [11]) of the XLPE insulation of the UC, as demonstrated in Section 2 of [Publication III]. Figure 2.16 shows the calculated minimum breakdown currents to a UC both with and without SW protection, for different soil resistivity. Those minimum currents were assumed to initiate breakdown in the UC based on the voltage and withstand strength of the 20 kV cable. The shielding effect was very significant, with a *step-up* of the minimum damaging current by an average factor of 3.3, at all resistivity considered. This implies that the breakdown current in a UC with a SW is increased by a factor of 3.3 compared to a UC without SW.

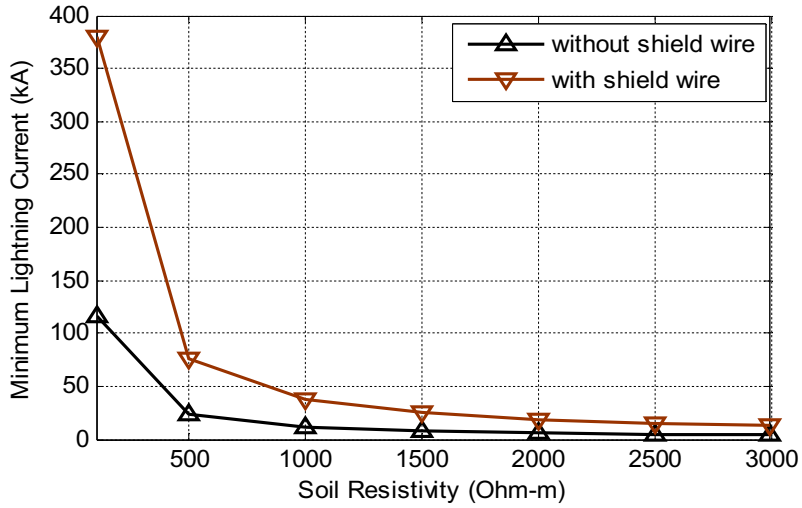

Figure 2.16. Minimum lightning current at which UC breakdown begins, with and without the presence of shield wire (SW)

Estimating failure rates of underground cables protected with a shield-wire in homogenous and inhomogeneous soils

Failure rates of underground cables with and without shield wire protection were compared based on actual lightning statistics from Finland [Publication III]. The homogeneous and inhomogeneous soil arrangements (see Figure 2.17) were used for the assessment. The homogeneous soil resistivity is ρ_s =2300 Ωm and depth 5m. For the 1st inhomogeneous soil: top-layer resistivity ρ_s =1500 Ωm and depth 0.5m, and bottom-layer resistivity ρ_s =2300 Ωm and depth 4.5m. For the 2nd inhomogeneous soil: top-layer resistivity ρ_s =150 Ωm and depth 0.5 m and bottom-layer resistivity ρ_s =2300 Ωm and depth 4.5 m. Lightning current peak was taken as *15 kA*. This current generated different electric potentials and field distributions at the struck point on the ground surface due to the different soil layer configurations. The number of UC damage times per year was calculated from (1.1) and (2.1) [Publication II]. Figure 2.18 shows the procedure proposed for the estimation of the failure rates of the cable. As illustrated in Figure 2.18, a minimum lightning current of I_{min} = 5 kA was selected to initiate the computation. This current was increased until the maximum breakdown current I_p was reached. The lightning distance, L was then increased to determine the attractive area under which this current would damage the underground cable. The corresponding attractive area, A is then calculated. Thus, any lightning current equal or greater than this maximum breakdown current will damage the cable if struck inside the area A. In paper [Publication II], the GFD in Finland is 0.786 stroke /square km/year or 0.393 flash / square km/year (1 flash = 2 strokes on average). Table 2.4 gives the failure rates of the UC protected with and without shield wire, for different soil types. Although the UC's failure rate is low irrespective of the soil types the value is minimized further as the top-layer resistivity decreases.

The results of [Publication II] indicate that, for 1 km length, the UC without shield wire may fail once in 137.95 years, 139.41 years, and 152.69 years for the homogeneous soil, the 1st inhomogeneous soils and the 2nd inhomogeneous soils respectively. However with shield wire, as estimated here, the UC may fail once in 1062 years, 1437 years and 159,534 years for the same soil types.

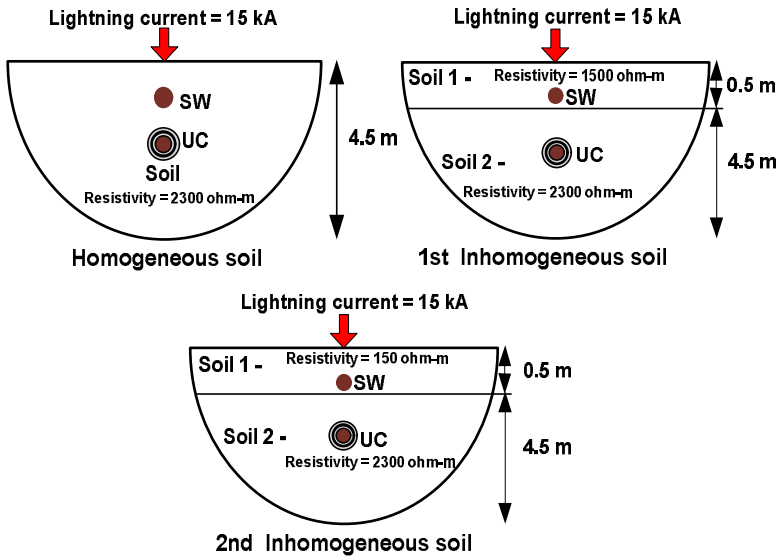

Figure 2.17. The configuration of homogeneous and inhomogeneous soils with shield wire placed around underground cable

$$N_{cd} = N_g * P(I_p) * A \qquad (times / year) \qquad (2.1)$$

Where;

N_{cd} *is the number of cable damages per year (times/year),*

N_g *is the ground flash density, GFD (stroke/km^2/year),*

$P(I_p)$ *is the probability that any lightning peak current (I_p) will cause damage to an underground XLPE cable. This is calculated by (1.1)*

A *is the maximum area around the underground cable at which the cable is unprotected from damage when the maximum peak current strikes the ground.*

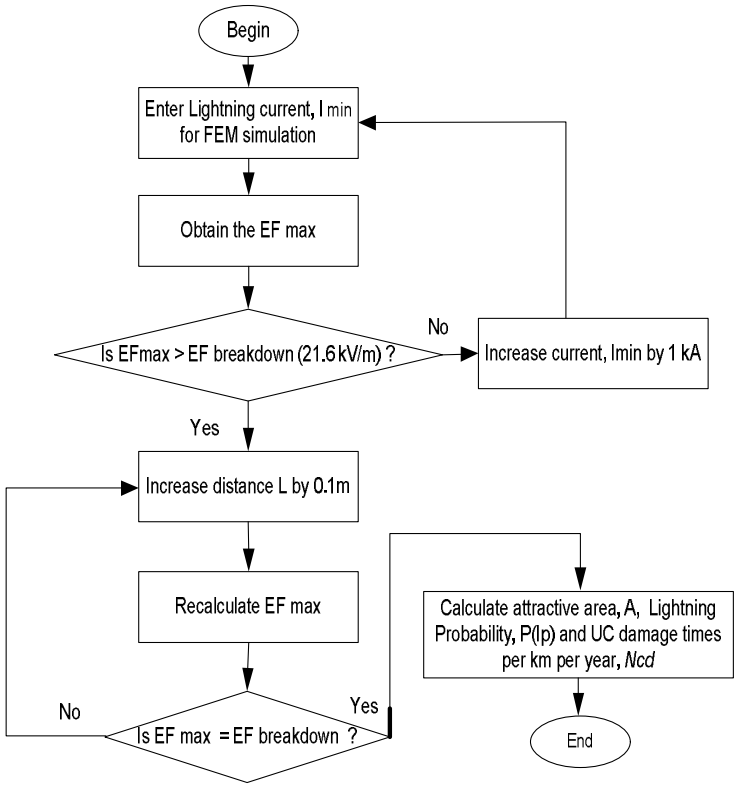

Figure 2.18. Flowchart for computation of UC failure rates.

Table 2.4. A comparison of the number of underground cable damages per year per km for cables with and without shield wire protected in different soil types.

Soil types	UC damage times/km/year	
	UC without SW	UC with SW
Homogeneous soil	0.00724	0.000943
1st Inhomogeneous soil	0.00717	0.000696
2nd Inhomogeneous soil	0.00655	0.0000063

2.3 Protection of Medium Voltage Covered Conductor against Lightning Overvoltages

The main goal of this study is to determine the number of direct strokes to covered conductors based on the already analyzed Finnish lightning data. The other task is to simulate the lightning performance of the conductors in order to determine the optimum distance at which a surge arrester must be installed on the distribution lines for the most effect protection against the overvoltage surges.

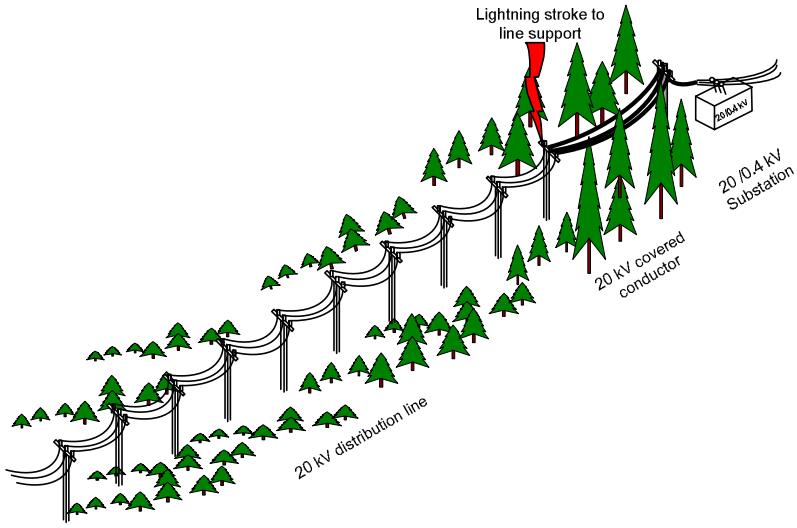

Figure 2.19. A schematic of part of a Finnish 20 kV MV network having a bare conductor, a covered conductor and a substation in series, assuming that a lightning stroke terminated on the pole that connected the covered conductors with the overhead lines.

2.3.1 Calculation and Simulation Results

The number of direct lightning strokes distribution conductors was estimated based on the lightning data in Finland (see Chapter 1). Between 1998 and 2008, the average thunderstorm days and ground flash density have been estimated to $T = 12$ days/year and $N_g = 0.786$ strokes/ km^2/year. The mean negative stroke is 15.2 kA (Figure 1.2). The frequency of direct strokes to a conductor of 1km length and average height $h = 10$m is defined with $N = N_g\ (0.028lh^{0.6})$ [35] as 0.08761 strokes/km/year. Therefore, by assuming condition in which, the value of the characteristic impedance of the covered conductor overhead distribution line is 480 Ω [36], the line-support earth resistance is 10Ω [Publication I], the Basic Insulation Level (BIL) of the conductor insulation is 90 kV for 20 kV class covered conductors, the average lightning stroke per flash is 2 [Publication I] and, the expected probability distribution of lightning currents is as in Figure 1.2. Then, the conductor is prone to approximately 9 direct lightning strikes a year for a 100 km power line. Each stroke, to either a covered conductor or line support, is expected to cause an interruption or outage, or damage to the covered conductor.

Induced overvoltages have been computed for the simulated network of Figure 2.19, consisting of a bare conductor in series with the covered conductor and the substation. By simply treating the line support as a neutral wire, the network shown in Figure 2.19 is simulated in ATP/ EMTP as in Figure 2.20. A lightning stroke of 15.2 kA with maximum rates of rise of current of (i) 30 $kA/\mu s$ and (ii) 3 $kA/\mu s$ was terminated on the line support where the covered conductor and the overhead line meet. The V-I characteristic curve of the arrester used for the simulation is given in [Publication IV]. Details of the simulation procedures are

given in [Publication IV]. One of the simulated induced overvoltages on the covered conductor is given in Figure 2.21. The resulting overvoltages are far higher than the Basic Insulation Level (BIL) of the conductor insulating layer (90 kV). Thus, any distribution line with a covered conductor is prone to breakdown when a lightning of this nature struck the line support, unless it is well protected with surge protective devices, such as surge arresters, arc gaps or other devices. By installing surge arresters on each pole (100 m pole span) as in Figure 2.22, the maximum overvoltages were suppressed to the values less than the BIL of the conductors (Figure 2.23). Also the energies absorbed by the surge arresters closer to the conductor are displayed in Figure 2.24.

The study has shown that the stress from lightning overvoltages on distribution conductors due to lightning stroke on the line support can be so intense. Also, a change in the characteristics of far distant strokes affects the conductor much more than the strokes to the line supports. However the induced voltage distortion increases with an increase in the rate of rise of the lightning current. Energy dissipation in surge arresters increases as the rate of rise of the lightning current decreases. Good protection of the conductor against any slow or fast rising surges could be achieved if the arresters are installed on every pole, for a 100 m line span.

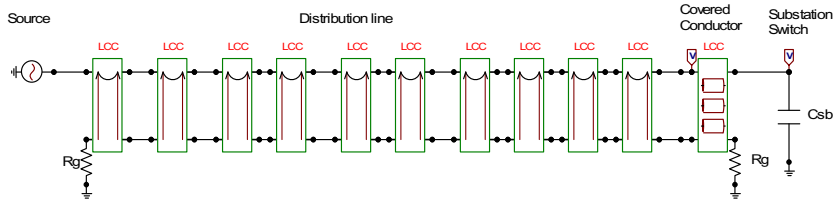

Figure 2.20. A single-phase ATPDraw model of a 20 kV MV network, consisting of a bare conductor in series with a covered conductor and substation. R_g is the grounding resistance and C_{sb} is a substation switch represented with a capacitance.

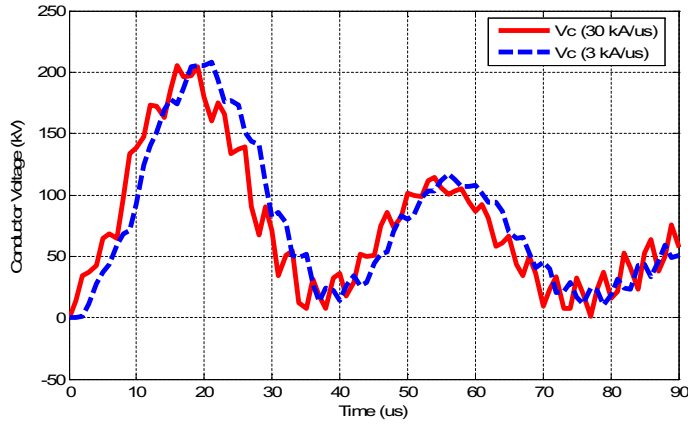

Figure 2.21. Induced voltage on covered conductor *head* for different maximum rates of rise of lightning current

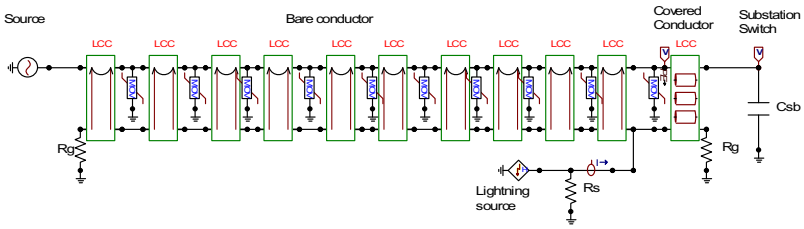

Figure 2.22. ATPDraw model of the power line configuration with arrester at every pole.

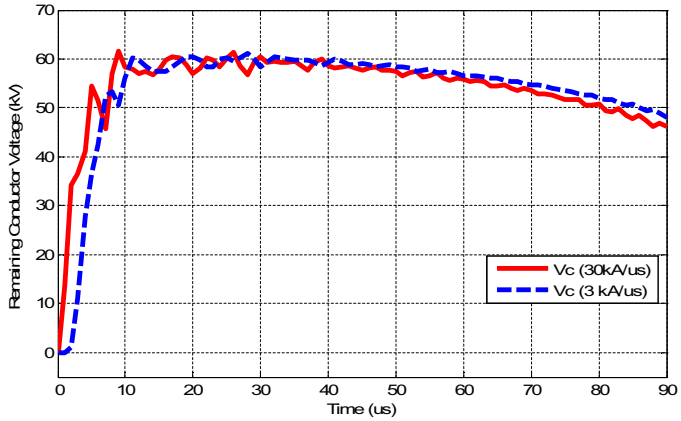

Figure 2.23. Remaining induced voltage on covered conductor for different maximum rates of rise of lightning current.

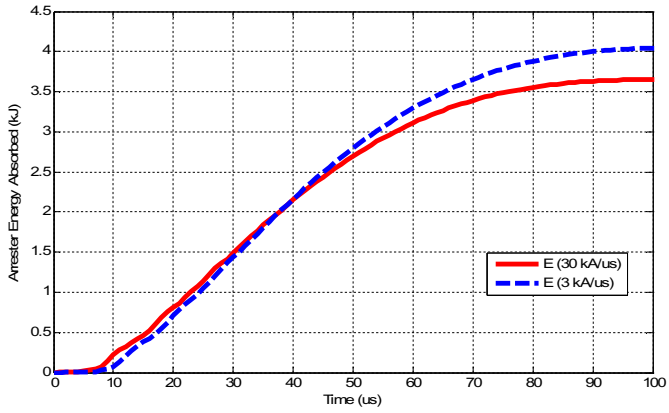

Figure 2.24. Energy absorbed by MOV arrester installed on the connecting point of the bare conductor and covered conductor for different maximum rates of rise of lightning current. The energy rating of the 30kV class MOV arrester is 74.8kJ, 3.4kJ/kV, where Uc= 22kV [24].

3- Effects of Trees on Lightning strokes to Medium Voltage Lines

3.1 Shielding Effects of nearby Tree on Direct Lightning Stroke to Distribution Line

Surge protection of distribution lines can be enhanced either with adequate installation of surge arresters or a combination of the arresters and shield wire [35][37-40], [Publications I and II]. Insulation enhancement also serves as another method of reducing equipment failure rates, thereby prolonging the life span of the equipment [39]. However, naturally, distribution equipment is protected from direct strokes when sited around high and grounded structures, such as buildings and trees [37], [35]. The expected overall failure rate can be minimized by the shielding objects [Publication V], though the induced flashovers due to the nearby strokes will increase considerably when such a situation arises [Publication VI].

The shielding effect of a tree on a direct lightning stroke to nearby distribution lines can be explained further with the *Electro-geometric* model [41]. The heart of the electro-geometric model is the striking distance of the lightning stepped leader to a grounded object. According to the model, the striking distance, r_s, is a function of the peak return stroke current; the higher the stroke current, the longer the striking distance r_s. The theory of this model has been extensively addressed by Armstrong and Whitehead [41], and also by [37]. A simple illustration of the model will be used for proper understanding of this study. From Figure 3.1, with a known value of striking distance r_s, arc a_1-a_2 can be drawn by taking the center point from the conductor (C). The line b_1-b_2 parallel to the ground surface is then drawn with the striking distance, r_{sg}, separating the ground and the line. Now, the arc is intercepted at points a_1 and a_2 by the straight line b_1-b_2. Thus, if there is any stroke tip within the exposure-arc a_1-a_2, then it will strike the conductor. Research done by Armstrong et al [41] has suggested a formula for the relationship between the striking distance and return-stroke current. The return-stroke current, I, which corresponds to striking distance r_s is given by (3.1). Moreover, the relationship between the striking distance r_s (m) and the striking distance to ground r_{sg} (m) has been suggested by Armstrong *et al* as in (3.2).

$$r_s = 6.72\, I^{0.8} \tag{3.1}$$

$$r_{sg} = \beta\, r_s \tag{3.2}$$

Where ß is a calibration constant which depends on the ground's shape.

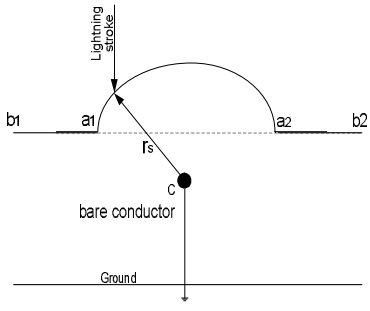

Figure 3.1. Electro-geometric model for estimating the least distance of ground strike.

This study aims at the enhancement in the surge analysis of MV distribution lines with the shielding effect of trees. To achieve this aim, a reduced-scale laboratory test has been carried out to estimate the rate of lightning flashovers to a medium voltage bare conductor and a grounded tree (see Figure 3.1). The tree used is a fresh and mature Norway spruce (*Picea abies*) with 10 branches. Taken to the laboratory in good condition, the tree was mounted near the conductor as shown in Figure 3.2. As indicated in Figure 3.3, at first, the dependence of the configuration parameters, such as *d,* r_{LT} and r_{LC}, on the flashovers to the tree and the conductor were determined by means of breakdown tests. This task was followed by incorporating the test results in the *Electro-geometric model* [41] for the estimation of the length exposure-arc (EA) of the conductor using different magnitudes of lightning strokes. Finally, the shielding performance of the tree was compared with that of a concrete building which has already been established in the literature [42].

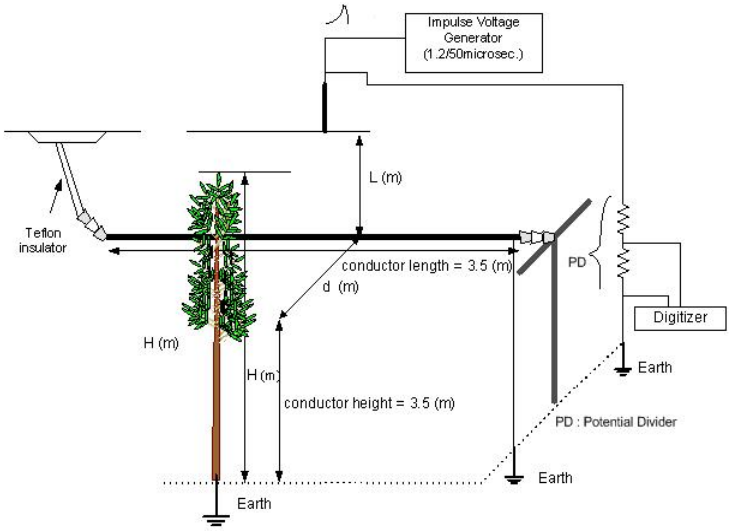

Figure 3.2. Schematic diagram of laboratory experimental setup.

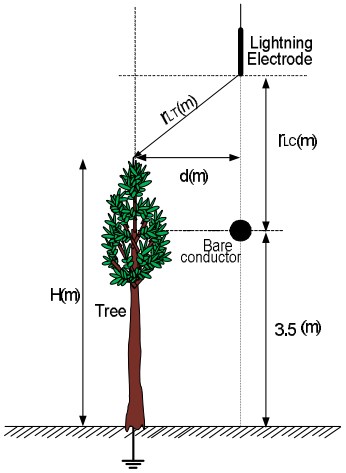

Figure 3.3. Configuration of the tree, bare conductor and lightning electrode. Tree-to-line clearance = d, striking distances from the lightning electrode to the tree is r_{LT} and to the line is r_{LC},

Table 3.1. Experimental cases and their parameters

Case No.	Lightning Impulse (V)	Conductor height (m)	H (m)	d (m)	r_{LC} (m)	r_{LT} (m)
1	1000 kV 1.2/50 µs	3.5	5	1.60	1.60	1.60
2				1.20		1.20
3				0.80		0.81
4				0.80	1.70	0.83
5					1.86	0.88
6					1.90	0.89
7	1200 kV 1.2/50 µs		5	1.60	1.60	1.60
8				1.20		1.20
9				0.80		0.81
10				0.8	1.70	0.83
11					1.86	0.88
12					1.90	0.89
13	1200 kV 1.2/50 µs		3.5	1.60	1.60	2.30
14				1.2		2.00
15				0.8		1.79
16				0.8	1.70	1.88
17					1.86	2.03
18					1.90	2.06

3.1.1 Experimental and Analytical Results

With two standard lightning impulses of 1 MV and 1.2 MV, the analysis of the shielding effect of a tree on direct strokes to a conductor has been made with breakdown tests (see Figure 3.2).This is considered the first scenario in [Publication V]. The tests were carried out by varying the configuration parameters shown in Figure 3.3. Detailed explanations on the experiment have been reported in [Publication V]. By considering the experimental cases of Table 3.1, the estimated rates of flashover to the tree and bare conductor are shown in Figures 3.4, 3.5 and 3.6. The results have clearly indicated that flashovers to distribution lines are significantly dependent on the attraction to nearby trees and the nature of the incoming lightning current. What determines the attraction are the height and clearance of the tree while the nature of the current is related to the magnitude and the point of final jump of lightning to the distribution lines.

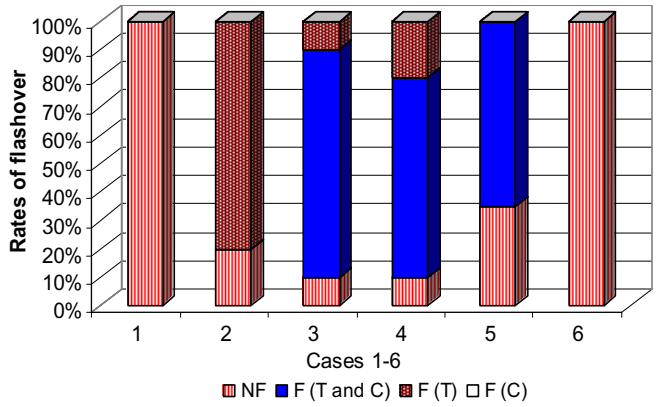

Figure 3.4. Estimated rates of flashover under electrical breakdown test. V = 1000 kV and tree height = 5 m. NF: Non-flashover, F (T and C): Flashover to tree and conductor, F (T): Flashover to tree, F (C): Flashover to conductor.

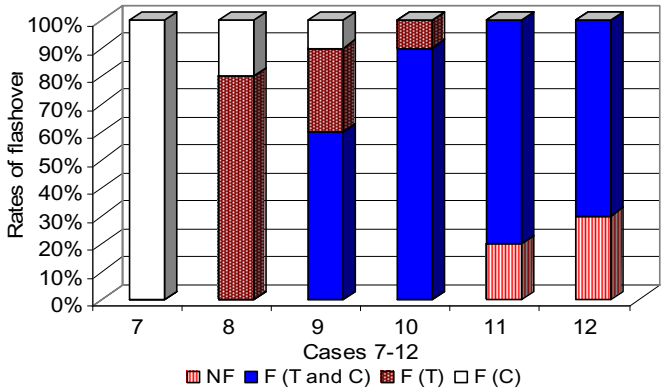

Figure 3.5. Estimated rates of flashover under electrical breakdown test. V= 1200 kV and tree height = 5 m. NF: Non-flashover, F (T and C): Flashover to tree and conductor, F (T): Flashover to tree, F (C): Flashover to conductor.

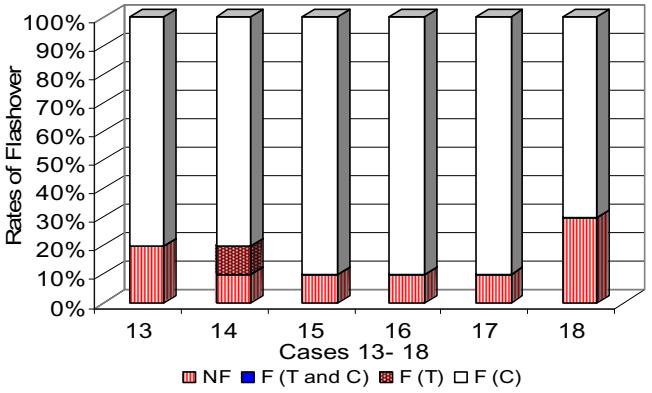

Figure 3.6. Estimated rates of flashover under electrical breakdown test. V= 1200 kV and tree height = 3.5 m. NF: Non-flashover, F (T and C): Flashover to tree and conductor, F (T): Flashover to tree, F (C): Flashover to conductor.

The second scenario investigates the protectiveness of a distribution line from lightning discharge due to the presence of a nearby tree [Publication V]. In order to determine the protectiveness in terms of the exposure-arc of the line, two different configurations of Figure 3.7 were employed to determine the equal probability (50%) of lightning strokes to the tree and the conductor. Accordingly, the occurrence probability was examined under a positive impulse voltage of 1200 kV (waveform, 1.2/50 µs) by changing the horizontal position of the lightning leader point. The relationship between the r_{LT} and r_{LC}, as expressed in (3.2) [Publication V], is equivalent to (3.3), where $\beta = 0.42$ is the calibration constant.

By using the electro-geometric (explained in [Publication V]), the r_s was obtained by substituting the lightning current, I, into (3.1) of [Publication V]. Since the calibration constant is estimated to $\beta = 0.42$, the r_{sg} was then calculated by inserting the β and r_s into (3.3). This (3.3) was then used to determine the shielding effect of the tree on lightning strokes to the conductor. Therefore, the Figure 3.8 gives the estimated results of the length of Exposure Arc (EA) of a grounded conductor with regards to the height of a tree, for different magnitudes of lightning currents, i.e. 5 kA and 50 kA. The EA length is greatly dependent on the magnitude of the lightning current. An increase in the lightning current will increase the EA length of the grounded conductor. In the same figure, as the height of the tree is increased, the EA length of 50 kA decreased faster than the EA length of 5 kA, up

to the point at which the height of the tree is double the height of the grounded conductor (tree 20 m & conductor 10 m). Nevertheless, the *EA length* tends to remain constant for the two events even as the height of the tree is further increased. Thus, the tree has offered some protection to the conductor by greatly reducing the length of the exposure arc of the conductor to the upcoming lightning discharge. However, the situation where the exposure arc disappears (i.e., Perfect shield = EA length = 0) is not realized for this scenario.

By comparison, the shielding performance of the tree with that of the concrete building on a distribution conductor is shown in Figure 3.9 (a) and (b). In their experiment [42], *Yamamoto et al* have made some calculations based on the *electro-geometric* model on the exposure-arc of grounded conductor for different positive lightning impulses due to the nearby concrete building. They obtained a calibration constant of $\beta = 1$ for 50 % occurrence probability of strokes to the building structure and the grounded conductor. In contrast to [42], this experimental work produced the same 50% occurrence probability of strokes to the tree and the grounded conductor, where the calibration constant is $\beta = 0.42$. As indicated in the Figure 3.9, the EA length of the conductor for the case of the nearby tree is longer than that of the conductor for the case of the building structure. The reason is that, the calibration constant obtained here is less than the one obtained by *Yamamoto et al*. Thus, a tree can offer a shield on a conductor to some extent but a perfect shield may not be realized as in the case of a building structure.

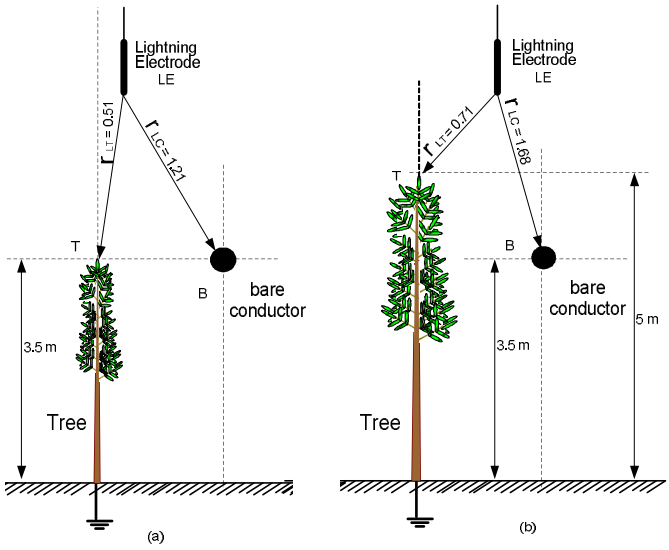

Figure 3.7. (a and b). The configuration of striking distances to bare conductor and tree which gives 50% lightning occurrence probability to the bare conductor or the tree. The condition at which the events of flashovers to the tree (T) equaled the events of flashovers to the bare conductor (C).

$$r_{LT} = 0.42 r_{LC} \tag{3.3}$$

Where; r_{LT} is striking distance from the lightning electrode to the tree, r_{LC} striking distance from the lightning electrode to the line and calibration constant (β) is 0.42

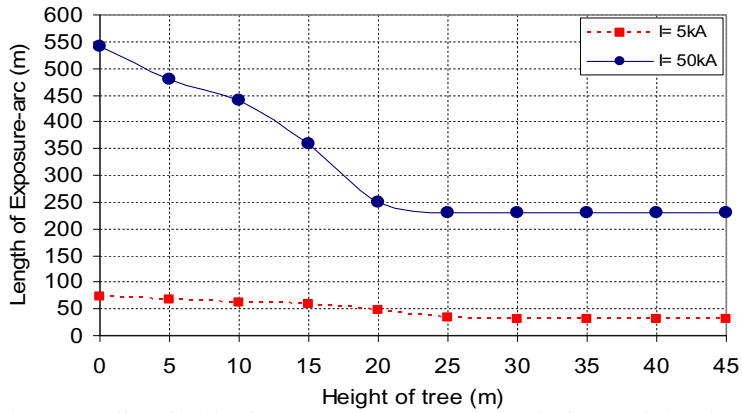

Figure. 3.8. Effect of height of a tree on exposure-arc (EA) length of a grounded conductor for two different lightning currents. *Height of the conductor (10 m). Horizontal distance between the tree and the conductor (4 m)*

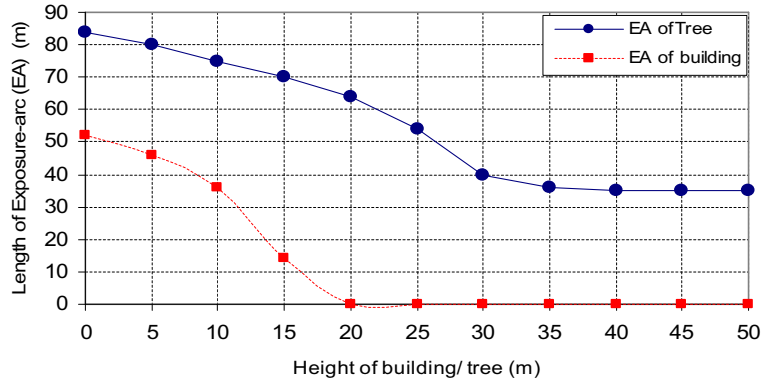

(a) The case of lightning stroke current I = 6kA

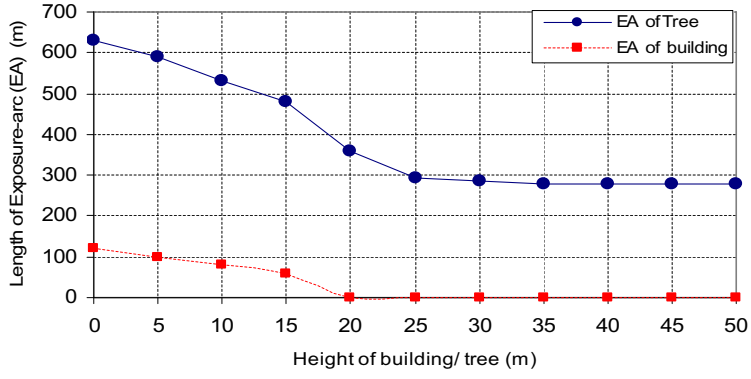

(b) The case of lightning stroke current I = 60kA

Figure 3.9 (a) and (b). Effect of height of tree and building structure on Exposure-Arc (EA) length. Tree/ building height= 11 m, clearance = 4 m, Calibration constant (β) is 0.42 for the case of the tree in this study and 1.0 for the case of the building in [42].

3.2 Induced overvoltages on distribution line from lightning stroke to nearby tree

Recent measurements have revealed that a tree can sometime intercept a lightning stroke within the vicinity of a power line [Publication V]. However, induced voltage may exist even when the power line is perfectly shielded by the nearby tree. Therefore, the performance of overvoltage build-up on distribution lines from indirect strokes to trees should be considered as an important issue for the safety of the lines. In addition to frequently growing emphasis on the reliability of power systems, more understanding of the sources of lightning faults in medium voltage lines is required for effective protection. Lightning-induced voltage on power distribution lines or telecommunication lines has been a subject that has received critical attention in the literature for years. However, very few investigations have been carried out on the influence of very close and tall structures, such as trees, buildings and other high structures on the lightning performance of power distribution lines. The analytical study [43], simulation studies [44] and experimental studies [Publication V], [5], [45] have proved that power lines that traverse through forests are naturally protected by the nearby trees. The main reason is that the lightning will strike the tree instead of the line because of the higher attractiveness of the tree to the lightning stroke. However, in the event that the stroke is directly terminated on a tree, the resulting overvoltage can be high enough to create flashover(s) between the tree and the power lines, which can possibly lead to a permanent fault.

3.2.1 Experimental and Analytical Results

The performance of induced overvoltage on a distribution line due to lightning discharge to a nearby tree has been accessed by means of a full-scale laboratory experiment, which has been reported in [Publication VI]. The configuration and schematic diagram of the experimental facilities are shown in Figure 3.10 and 3.11. The employed tree is a fresh and mature Norway spruce (*Picea abies*) with 30 branches. Taken to the laboratory in good condition, the tree was mounted near the conductor as given in Figure 3.11. The tree was equidistant from the line termination and was at 1 m from the center of the line. A detailed explanation of the experimental setup is given in [Publication VI] which examines the effect of change in tree-to-line clearance, change in lightning time characteristics and polarities of the indirect lightning strokes. Evaluation of the induced overvoltage from the tree to the power conductor has been made for larger clearance by using a *Rusck* model.

In order to study the response of the line to a direct stroke to the nearby tree, a lightning impulse voltage of peak value of 400 kV and waveform of 1.2/ 50 µs (see Figure 3.12) was applied on the tree. The overvoltage response of the line to the impulse voltage on the tree is shown in Figure 3.13. The experimental result reveals that the induced voltage waveform was characterized by faster rise-time and shorter duration with regards to the originating lightning impulse waveform on the tree. The tree was able to limit the induced voltage by a factor of 29 (i.e. 400 kV / 14 kV), though the some induced voltage exists after the shielding. Dependence of the induced voltage on the lightning voltage class is given in Figure 3.14, where the induced voltages on the conductor are practically proportional to the direct impulse voltages on top of the tree. Figure 3.15 shows the effect of clearance on the induced voltage on the line by varying the clearance from 1 m to 3 m. Thus, of course, by increasing the clearances, the induced voltage decreases marginally. This indicates that in reality, the variation in the clearance between trees and distribution lines within the practical range of 3 m to 5 m would have a limited effect on the induced voltage performance of the lines.

The effect of front-time of impulse voltages of Figure 3.16 is significant on the induced voltage of Figure 3.17, measured on the line. For the two different time

characteristics of the lightning impulse, the resulting induced voltages revealed from the figure (Figure 3.17) that the induced voltages are very short compared to the applied impulses (Figure 3.16). Also, a direct stroke with different time characteristics on a tree can induce a different magnitude of overvoltages on a power line within the vicinity of the tree. As the rate of voltage increase in a real lightning voltage discharge often exceeds several hundreds of megavolts per second, the discharges with a shorter front-time will produced larger voltage difference across the air insulation causing "side flashes" to nearby power lines, which can subsequently damage the equipment connected to the lines. The effect of the lightning polarities of Figure 3.16 is also observed on the voltage induced on the line, as the results indicate in Figures 3.18 and 3.19. The voltage induced for the positive impulse voltage is more than double the induced voltage for the negative lightning impulse. Thus, line insulation could be more stressful for the positive lightning impulse than the negative one. However, higher oscillation was observed on the negative induced voltage waveform, this may be harmful also to the equipment which is closer to the stroke location.

Analytical results by *Rusck model* [46] have been compared with the experimental results obtained in this work. The model is straight forward in the sense that it presents a simplified equation to describe the maximum value of induced voltage at an infinitely long line. In the experimental setup, there were restrictions in the used impulse voltages and therefore, limitations in the clearance between the tree and the conductor. A detailed explanation of this model has been shown in [Publication VII]. For a distance that is within the range of the clearance between a tree and a power line in the field, Figure 3.20 gives the measured induced voltages on the line as a comparison with the *Rusck* model, for larger clearance. Comparing the two results at a shorter clearance of 1 m, the induced voltage magnitude was about 4 % smaller than that predicted by the *Rusck*, whereas, at a larger clearance of 5 m the induced voltage magnitude was about 75 % larger than that predicted by the *Rusck model*. The higher impedance of the tree might be responsible for the higher voltage induction on the line at the wider clearance.

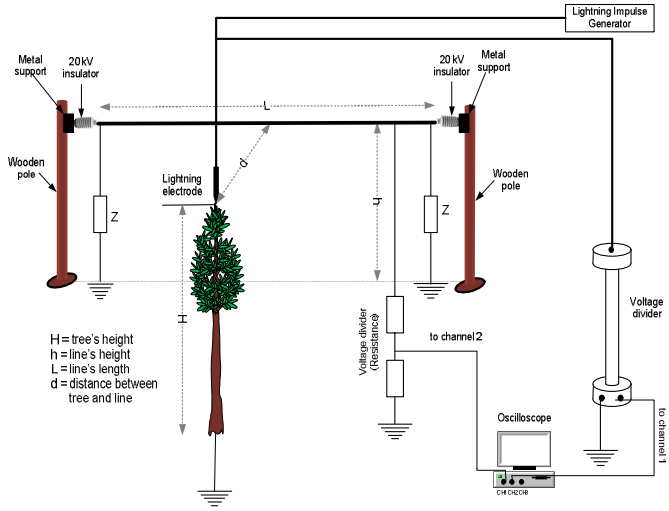

Figure 3.10. Experimental configuration. Line length = 16 m, Line height of 8 m, Z= 400 Ω, Tree height 9.5 m.

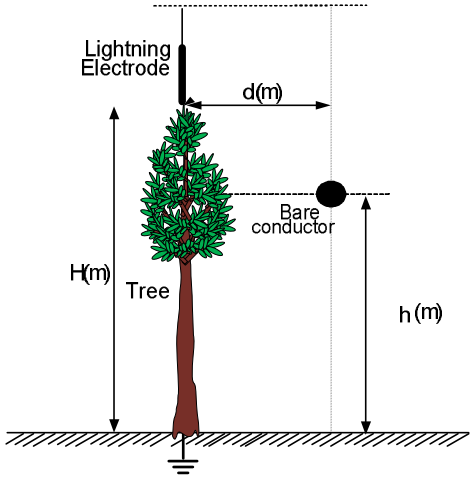

Figure 3.11. Schematic of the tree and the MV bare conductor.

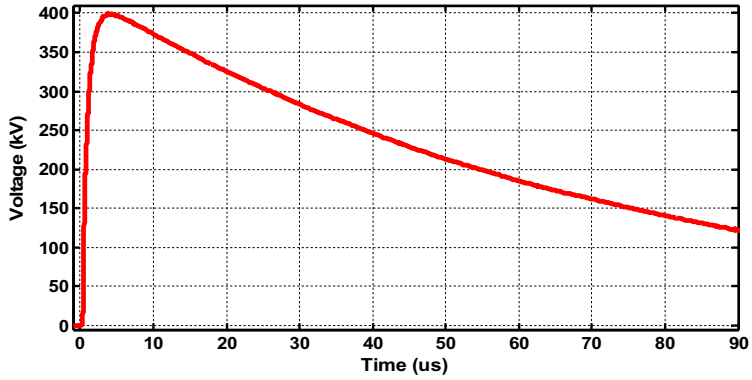

Figure 3.12. Lightning impulse applied on top of the tree close to the bare conductor (1.2 / 50 μs).

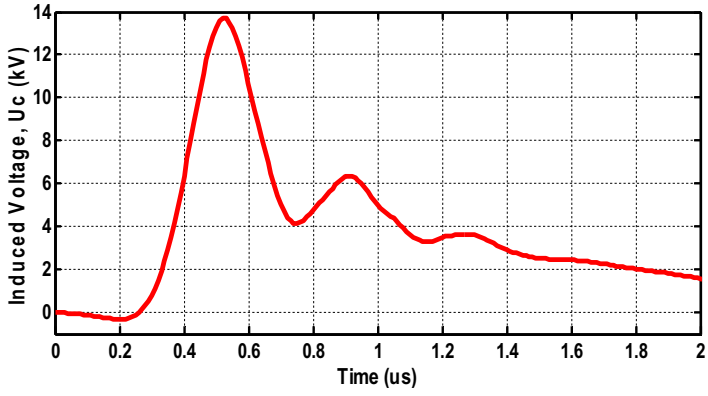

Figure 3.13. Measured induced voltage on the conductor. Tree height , H = 9.5 m, conductor height h = 8 m and clearance, d = 1 m.

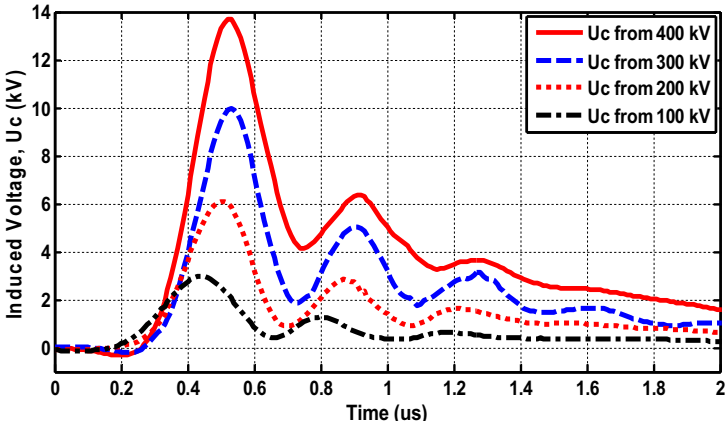

Figure 3.14. Measured induced voltages on the conductor as a function of the applied impulse on the tree. Tree height, H = 9.5 m, conductor height, h = 8 m and tree-conductor clearance, d = 1 m.

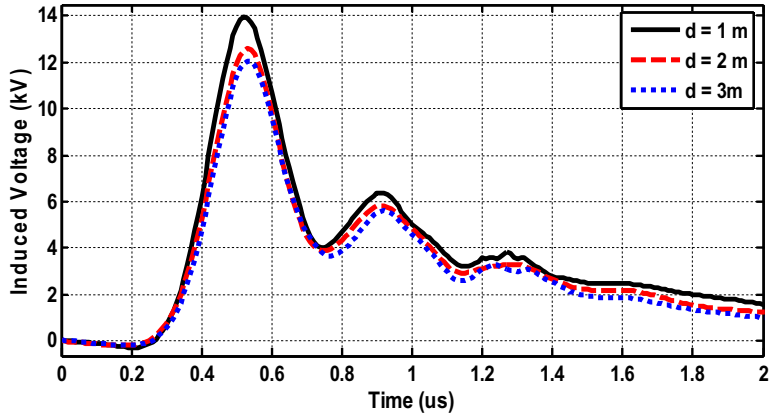

Figure 3.15. Measured induced voltages on the conductor as a function of the tree-conductor clearance. Tree height, H = 9.5 m, conductor height, h = 8 m and clearance.

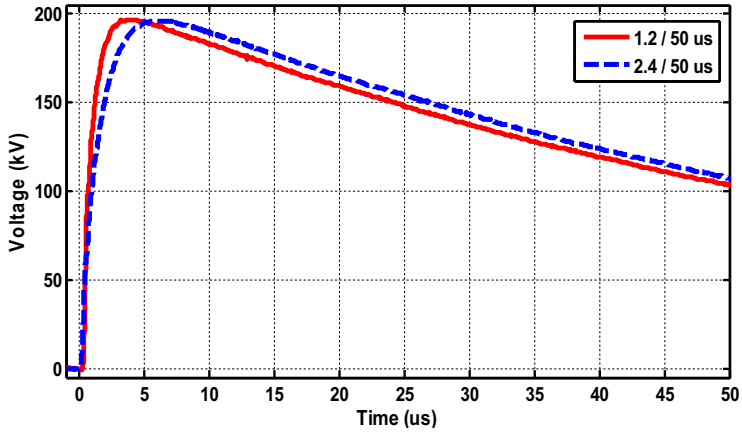

Figure 3.16. Lightning impulse with different time characteristics applied on top of the tree close to the bare conductor.

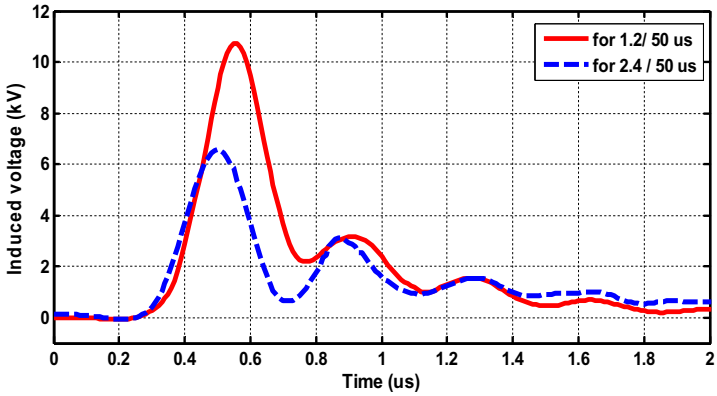

Figure 3.17. Measured induced voltages on the conductor as a function of time characteristics of the applied impulse (see Figure 3.16) on the tree. Tree height, H = 9.5 m, conductor height, h = 8 m and clearance, d = 1 m.

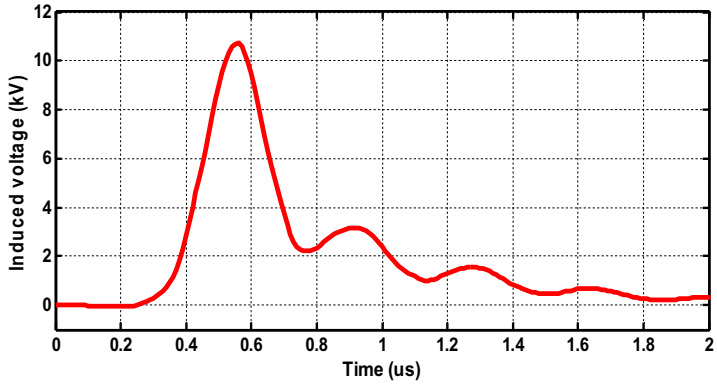

Figure 3.18. Measured induced voltage on the conductor as a function positive polarity of the applied impulse (see 200 kV, 1.2/50 µs of Figure 3.16) on the tree. Tree height, H = 9.5 m, conductor height, h = 8 m and clearance , d = 1 m.

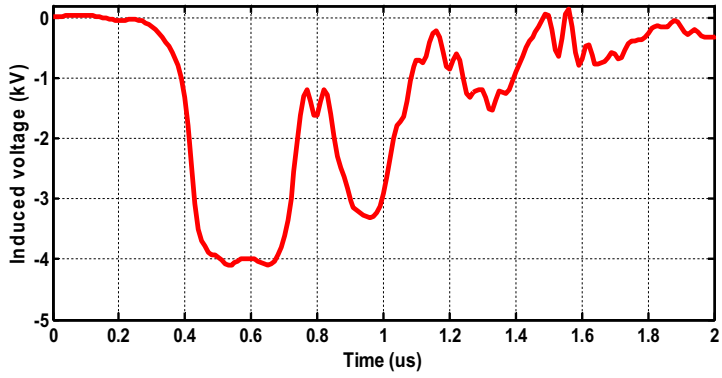

Figure 3.19. Measured induced voltages on the conductor as a function of negative polarity of the applied impulse (see 200 kV, 1.2/50 µs of Figure 3.16) on the tree. Tree height, H = 9.5 m, conductor height, h = 8 m and clearance, d = 1 m.

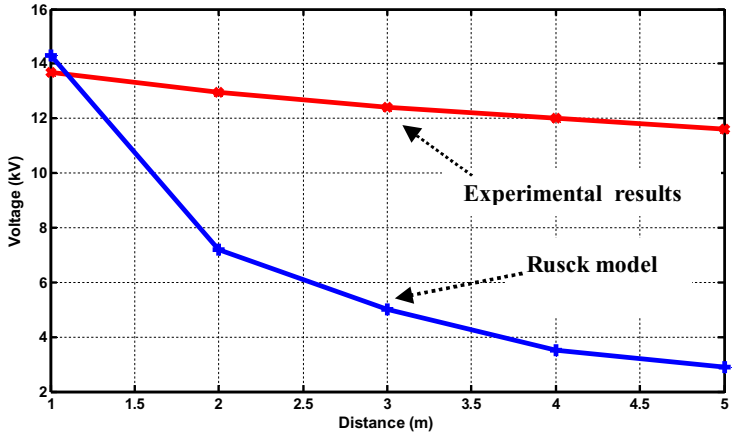

Figure 3.20. Induced voltage on the line with the Rusck model and the experimental results. Impulse voltage peak= 400 kV. K_v =38.8, Tree height= 9.1 m, line height 8.1m.

It is noteworthy to discuss here about the differences between the experimental results and the calculated results from the *Rusck* coupling model. The lightning induced electric field consists of two major components such as the horizontal component and vertical component. The vertical electric field has three components such as electrostatic, induction and radiation. Therefore, one reason that may lead to this difference is the capacitive coupling (electrostatic field) between the tree and the conductor, which marginally decreased from 1 m to 5 m. It is obvious that the electric field due to the electrostatic field was enhanced by the high impedance of the tree. In *Rusck* formula, lightning channel is considered perfectly conducting; therefore, higher contribution to induced voltage build-up on the conductor comes by induction and radiation. If lightning strikes a 'poorly' conducting tree, the lightning channel (tree) will be raised to a high voltage compared to the surroundings. Other factors which may contribute to the results margin are soil resistivity, physical and electrical arrangement of the experimental configurations. However, thorough investigation would be required to better clarify the difference in the results.

4- Modeling of Lightning Arc between a Tree and a nearby Distribution Line under Artificial Rainfall

Overvoltages due to indirect strokes to a nearby distribution line are invariably lower than those resulting overvoltage due to direct strokes to the line. However, the incident of indirect strokes is much more frequent and can influence significantly the lightning performance of the overhead distribution lines [47- 52]. The frequency and nature of the lightning strokes collected by lines in the forest area differ from the data associated with power lines on bare land. Those differences are particularly important for distribution lines in Finland, where the power lines traverse the forests that cover 86 % of its land area. As a matter of fact, lightning occurs during raining, rainstorms, snowstorms, and other natural phenomena [1], these phenomena could be responsible for the persistent lightning interaction with power networks. This is particularly the case with lightning strokes to trees around the power conductors in some densely forested countries, such as Finland. When the lightning-struck tree is close to the line, the amplitude of the lightning stroke is high, it is raining and the rain is accompanied by other natural phenomena, the coupling effect between the lightning-struck tree and the power line can be high enough to create a flashover.

This study has been carried out to investigate the existence of a lightning arc between a lightning-struck tree and a distribution line under artificial rainfall. A full-scale laboratory experiment confirmed that a direct stroke to a tree can cause severe damage to nearby power lines by initiating an arc channel through the air to the bare conductors. In a number of the experimental runs performed, it was found that the conducting arc path allows the establishment of a large long-duration lightning current from the lightning-struck tree to the bare conductor under the wet-air condition. Consequently, a higher overvoltage is measured on the conductor. The lightning-triggered arc phenomenon was monitored closely. It was confirmed that lightning strokes to a nearby tree can be more intense during wet-air rather than in dry-air conditions, and cause a flashover on power lines. A complete model of this phenomenon is accomplished through a modified dynamic arc model. The arc model is a combination of the existing static and dynamic arc equations, which have been tested and proven accurate in some literature [17], [19], and [53]. The model is accomplished by the bilateral interaction between the ATP/EMTP network and Transient Analysis Control System (TACS) field. The computer simulation using the arc model shows that the experimental results, one of which has been photographed and reported in the paper, are reproducible by means of system modeling. Both results of the dynamic arc model and the modified dynamic arc model have been compared with the experimental arc characteristics.

4.1 Experimental and Modeling Results

The configuration of the experimental setup is shown in Figure 4.1, with its detail explanation in [Publication VII]. The full scale experiment took place under different atmospheric conditions i.e. dry-air (laboratory weather condition) and wet-air conditions (artificial raining condition), as shown in the schematic diagram of Figure 4.2. In order to simulate natural rainfall, de-ionized water was generated using water spraying equipment placed at 2 m above and 3 m away from the configuration. The nominal conductivity of the water is 0.01 S/m and the intensity of the water droplets was constant at 1 mm/min. Thus, the schematics of Figure 4.1

were considered with and without the artificial rainfall.

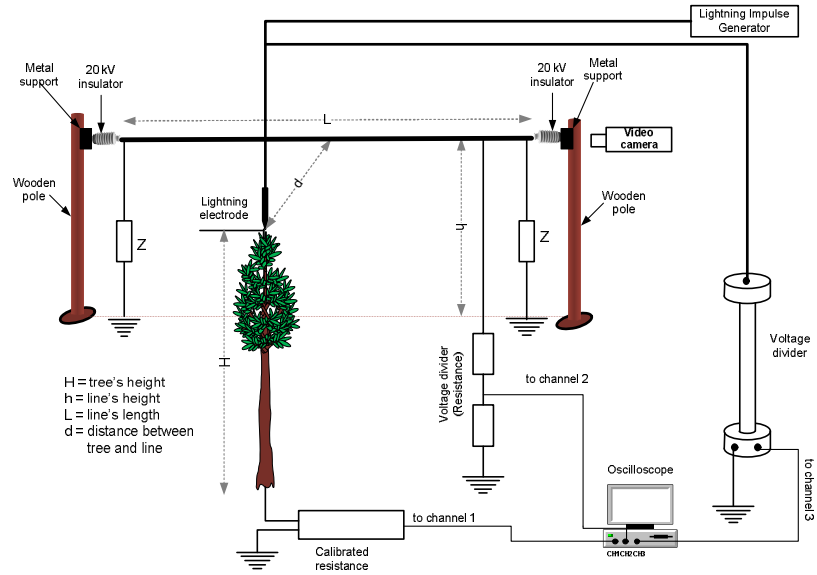

Figure 4.1. Experimental configuration. H = 9.5 m, h = 8 m, d = 1 m, Z = 400 Ω.

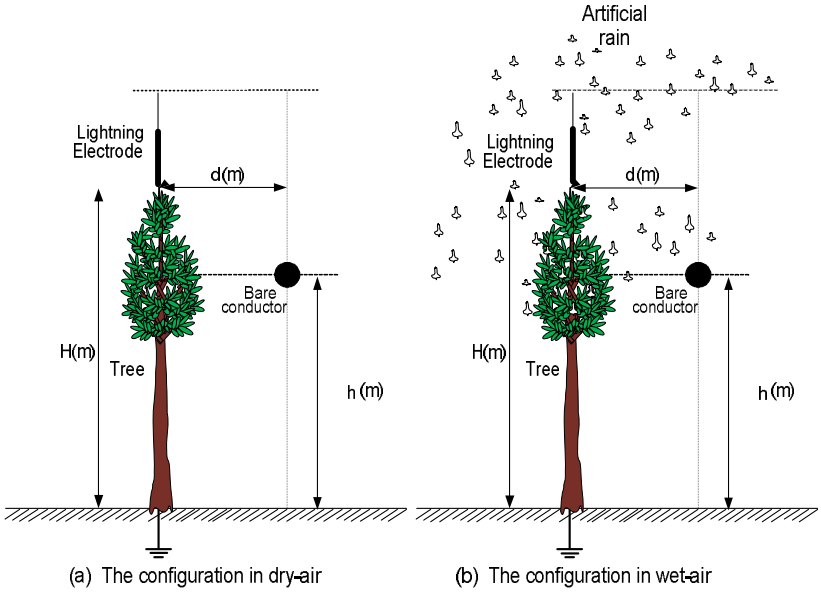

Figure 4.2. The configurations of the tree, the bare conductor and the lightning electrode under two weather conditions.

4.1.1 Measured Tree Impedance

Firstly, the measurements of tree impedance have been carried out, in this work, to determine how the impedance varies with weather conditions. Other task was to develop a simple RC model which is equivalent to the impedance of the tree. The employed tree is a fresh and mature Norway spruce (*Picea abies*) with 30

branches. Taken to the laboratory in good condition, the tree was mounted near the conductor as shown in Figure 4.1. The tree's dc resistance was estimated to be 3.3 MΩ at -10 ^{o}C. The tree was left grounded inside a water bowl in the laboratory for 24 h, and then its resistance decreased to 830 kΩ for the dry-air condition. Under the application of the artificial rainfall for 15 min, with an intensity of about 1 mm/min, the resistance was noticed to have slightly lowered to 810 kΩ under the wet-air conditions. The laboratory temperature was 20 ^{o}C. Thus, it was concluded that trees resistance changes according to weather condition [21].

Next, the author developed a simple RC model to represent the tree, by computing the frequency dependent characteristic impedance of the tree (see Figure 4.3) subjected to lightning strokes under dry-air and wet-air conditions, based on the physical and electrical representation of Figure 4.3a and (4.1). Since the dc resistance of the tree has been determined, a simple RC model of the tree was established and the expressions of the tree's capacitances were obtained for the modeling phase of the work. A range of impulse voltages, U_t, from 100 kV to 400 kV were applied to the tree and the current through the tree to the ground was measured. Figures 4.4 and 4.5 show one of the impulse voltages applied and the current flowing through the tree to ground respectively, in the time domain. In order to determine the impedance of the tree for the two weather conditions, the time dependent surges were converted by Fourier transform into frequency dependent surges (see Figures 4.6 and 4.7). The results indicate that the tree's impedance is highly dependent on the surge frequency. Shown in the table the average tree's impedance, from a high frequency range of 0.5 MHz to 1 MHz, is higher under the wet-air condition being almost double the impedance under the dry-air condition for a lower impulse voltage. As the impulse strength increases, a very marginal difference is observed for the two conditions. The higher the impedance the higher the possibility of side flashes from the trees to the power line.

The physical orientation and the experimental results suggest a simple RC-model as a suitable first order approximation for representing the tree, as shown in Figure 4.3. The conditions for assuming the representation are based on the fact that the lightning frequency is usually within a few MHz and the inductive effect of the tree can be neglected for the highly resistive object, such as the tree. The selection of RC parameters is simple. The frequency domain impedance, Z_t , as in (4.1) is expressed as (4.2). Based on the measured impedances of the tree under the two weather conditions for the impressed voltage of 400 kV on the tree (as indicated in Table 4.1), Table 4.2 presents the measured dc resistances and the computed capacitances of the tree under the dry-air and the wet-air conditions. Therefore, the two capacitances were included in the modeling of the tree under the two weather conditions.

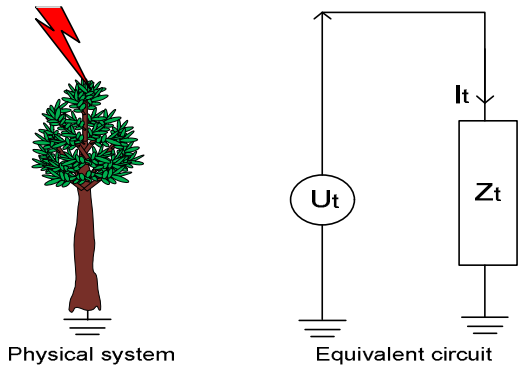

Figure 4.3. Physical system and equivalent electrical circuit representing the tree.

$$Z_t(w) = \frac{U_t(w)}{I_t(w)} \tag{4.1}$$

where the $U_t(w)$ and $I_t(w)$ are the Fourier transforms of the tree top potential and the tree current, respectively.

$$Z_t(w) = \frac{1}{\frac{1}{R_t} + (-jwC_t)} \ (\Omega), \tag{4.2a}$$

where R_t is the measured tree dc resistance and C_t represents the tree's capacitance under the for dry-air and wet-air conditions. The lightning frequency is $w = 2\pi f$. From the above complex impedance, the capacitance of the tree is computed at the high frequency range of 1 MHz by

$$C_t = \sqrt{\frac{1}{w^2}\left(\frac{1}{Z_t^2} - \frac{1}{R_t^2}\right)} \ \text{(Farad)} \tag{4.2b}$$

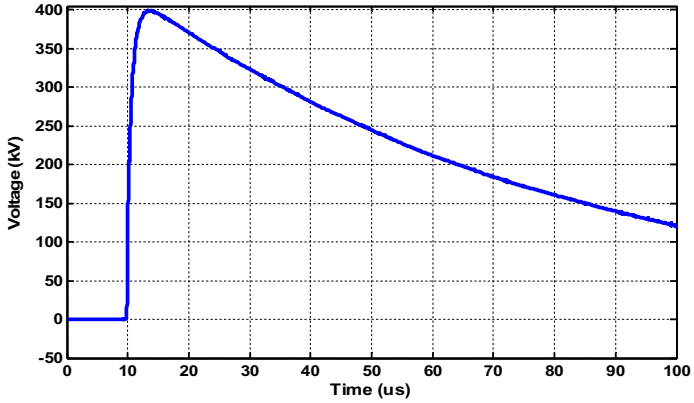

Figure 4.4. Experimental lightning impulse injected on top of the tree close to the bare conductor under the dry-air condition.

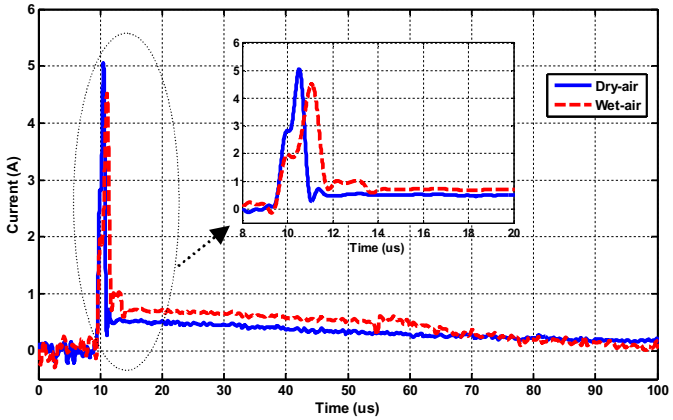

Figure 4.5. Measured tree currents under the dry-air and wet-air conditions.

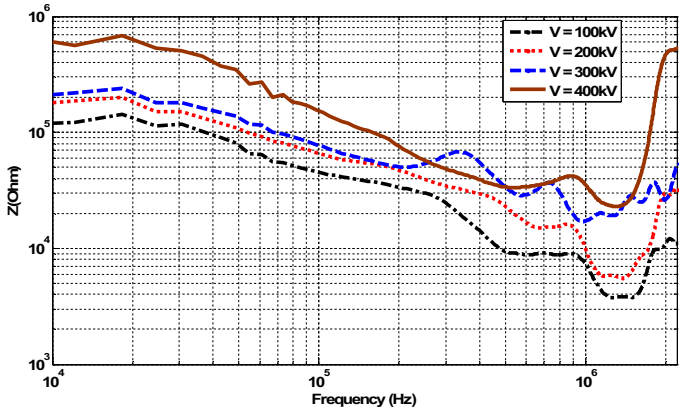

Figure 4.6. Characteristic impedance (magnitude) of the tree in the dry-air condition for different impulse voltage magnitudes.

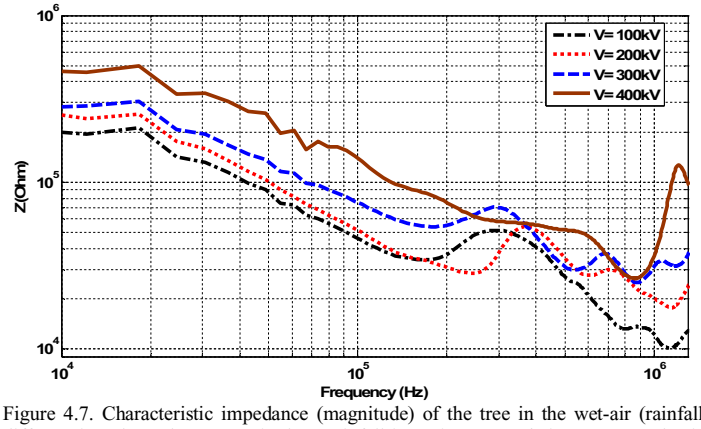

Figure 4.7. Characteristic impedance (magnitude) of the tree in the wet-air (rainfall) condition for different impulse voltage magnitudes. Rainfall intensity= 1 mm/min, water conductivity, σ = 0.01 S/m.

Table 4.1. Measured characteristic impedance of the tree

Tree impedance (kΩ)	Dry- air condition			
	100kV	200 kV	300 kV	400 kV
Zc ($0.5MHz \leq f \leq 1MHz$)	8.70	15.70	27.30	35.00
Zc (at 1 MHz)	7.22	9.50	17.32	36.80
	Wet- air condition			
Zc ($0.5MHz \leq f \leq 1MHz$)	16.80	26.50	30.50	38.50
Zc (at 1 MHz)	12.20	20.00	31.23	38.00

Table 4.2. Measured and estimated RC parameter of the tree

	Impedance and RC Parameters (at f = 1 MHz)		
	Zc (kΩ)	R_t (kΩ)	C_t (pF)
Dry- air condition	36.80	830	4.32
Wet- air condition	38.00	810	4.18

4.1.2 Experimental Induced Voltage for Dry-air and Wet-air Conditions

In this part of the experiment, the induced voltages on the line have been measured for the purpose of extracting its features for modeling phase. The impulse voltages were applied at the top of the tree as shown in Figure 4.1 where d = 1 m is the minimum distance between the tree and the bare conductor. Figure 4.8 shows the recorded induced-voltage on the power conductor for different applied impulse voltages under the dry-air and wet-air conditions. Within the voltage range of 100-300 kV, the induced voltages were slightly higher for the wet-air compared to the dry-air. The reason is because of increasing the coupling capacitance during the rainfalls [Publication VII]. However, with an impulse voltage of 400 kV, there was a significant difference in the voltages. For the dry-air conditions, the induced voltage measured was 13.65 kV and its waveform is shown in Figure 4.9.

For the 400 kV impulse applied to the tree during rainfalls, the voltage is extensively higher because the dielectric of the wet-air between the tree and the conductor could not withstand the electric field and then the voltage was finally accompanied by a flashover as shown in Figure 4.10. The luminous channel in the figure explains the path through which the lightning followed from the lightning-struck tree to the power conductor. The recorded waveforms of this experiment are shown in Figures 4.11, 4.12 and 4.13. In Figure 4.11, the voltage source waveform is affected due to arc conduction from the tree to the conductor. At the steepness of the applied voltage, there is an induced voltage of 13 kV observed in Figure 4.12a where it is similar to the one observed under the dry-air condition shown in Figure 4.9. When the arc was created and its conduction started between the tree and the conductor, the voltage measured was 110 kV. Figure 4.13 shows the channel current that was used for the arc modeling that will be discussed in Section 4.1.5.

The arc ignition in the wet-air condition can be attributed to a reduction in the dielectric strength between the tree and the conductor. With the wetness of the environment, the occurrence of the arc at this voltage level may be explained in terms of the higher electron attachments in the wet-air [54]. A Higher affinity of water molecules to electrons makes the rainwater to have much greater conductivity than ordinary air. Therefore, it is very obvious that the presence of wet-air around the highly stressed tree and nearby power conductor will intensify the electric field between the objects (lighting-struck tree and bare conductor). The wetness of the surrounding air favors the induced and arc conducting of voltage (Figure 4.12) during the rise time and the tail time of the applied impulse voltage (Figure 4.11).

Since the lightning activities often occur during rainfall and the possibility of lightning strokes to high objects like trees is higher than to the ground surface, it is therefore important to consider the protection of power lines, substations and other equipment against overvoltages characterized by double voltages with shorter time parameters typical of Figure 4.12, rather than the one in Figure 4.9 and in [12], [55-57]. As revealed here and with the experimental and simulation results in [12], [39], [55- 59], a nearby lightning stroke can illuminate a nearby conductor with overvoltage having much shorter front and tail time than the SLI values that are around a few microseconds.

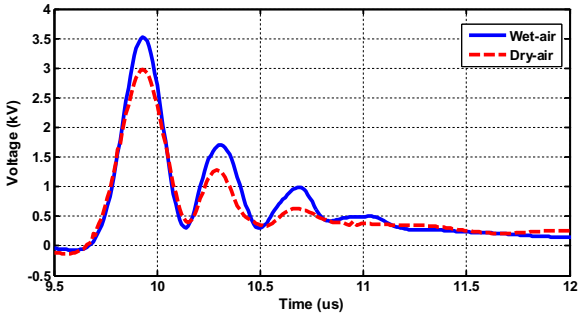

(a) Induced voltages from 100kV

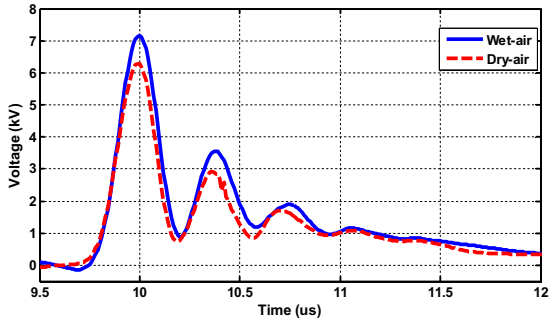

(b) Induced voltages from 200kV

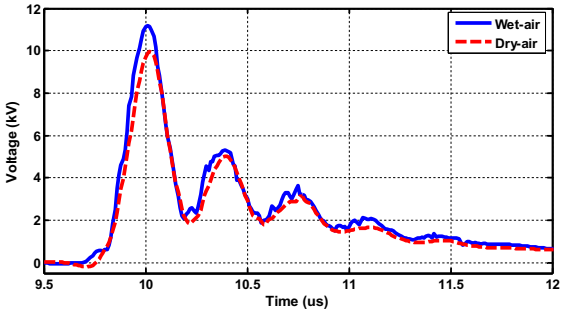

(c) Induced voltages from 300kV

Figure 4.8. A comparison between the induced voltages magnitudes measured on the power conductor for the dry-air and the wet-air conditions.

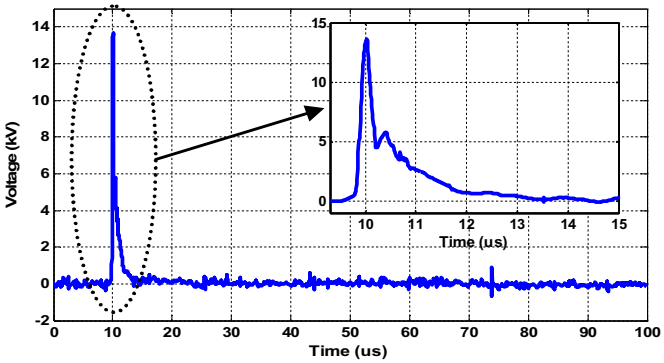

Figure 4.9. Experimental lightning induced voltage measured under the dry-air condition.

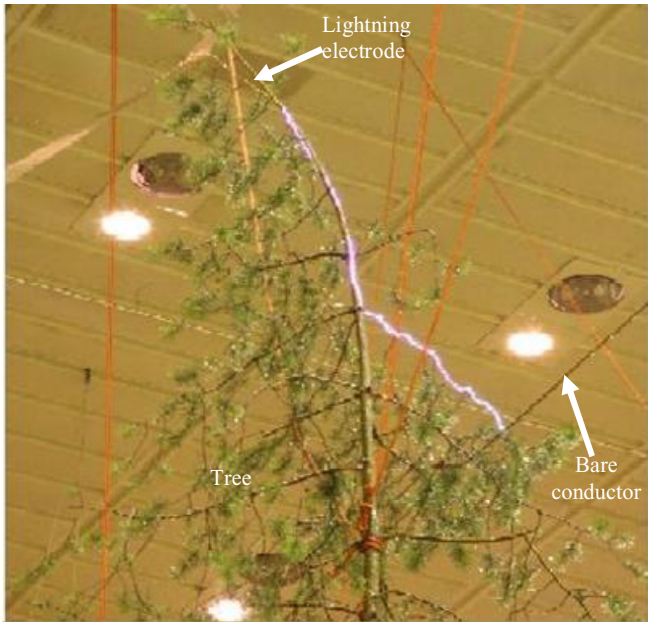

Figure 4.10. Arc generated between the lightning-struck tree and the bare conductor during artificial rainfall.

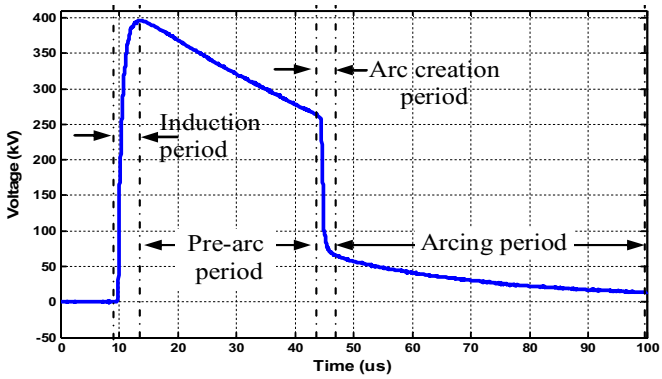

Figure 4.11. Experimental lightning impulse voltage injected on top of the tree close to the bare conductor under the wet-air condition.

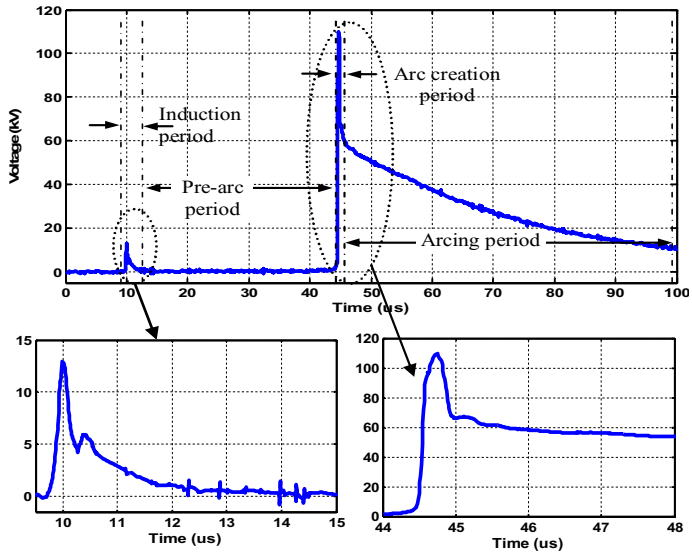

Figure 4.12. Experimental lightning induced voltage measured under the wet-air condition. (a) During the induction, (b) During arc creation.

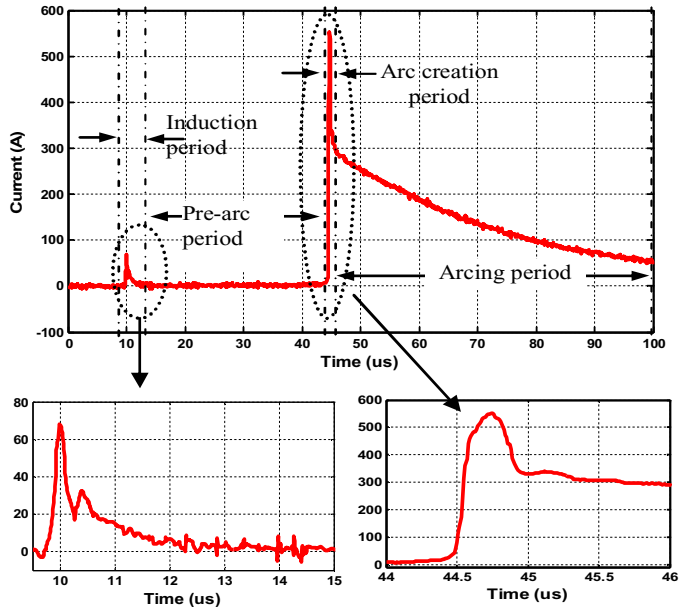

Figure 4.13. Experimental arc current measured under the wet-air condition. (a) During induction, (b) During arc creation.

4.1.3 Simulated Induced Voltage for Dry-air Condition

Simulated results of the experimental configuration have been made with the ATP/EMTP program where ATPDraw was used for the realization of the model objects. Details about the modeling of the impulse generators are given [Publication VII], while the tree impedance modeling has been explained in the previous section. The power conductor was modeled according to the experimental configuration explained earlier. The line was represented by the frequency dependent Jmarti model [61]. In order to represent the line in the same way that it was presented in the experiment, the 16 m bare conductor was matched at both ends with a corresponding resistance of 400 Ω. A capacitance, C_{cg} = 3.32 pF was also added between the conductor and the ground. Due to the small distance between the tree and the power line, the coupling effect between the tree and the conductor was represented with a coupling capacitance, C_{tc}. Therefore the tree-conductor capacitance was estimated to be C_{tc} = 110 pF. The tree-to-ground capacitance is C_{tg} = 4.32 pF (Table 4.2). Discussions on the calculation of the capacitances and other parameters in the Figure 4.15 are given in [Publication VII]. The simulation of the combined model of the impulse generator (source voltage), the tree, the power line and the coupling capacitances between the test object, as in Figure 4.14, is presented here. The ATPDraw of the configuration is illustrated in Figure 4.15. Considering the applied impulse voltage of 400 kV (Figure 4.4) on the tree (Figure 4.3), the experimental induced voltage on the bare conductor is given in Figure 4.16. The amplitude of the induced voltage in the experiment is 13.65 kV and the simulated value is 13.74 kV, with an error of 0.66%.

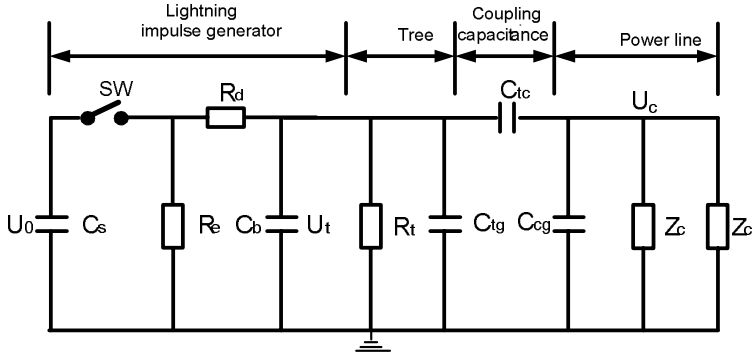

Figure 4.14. Equivalent circuit diagram for the induction.

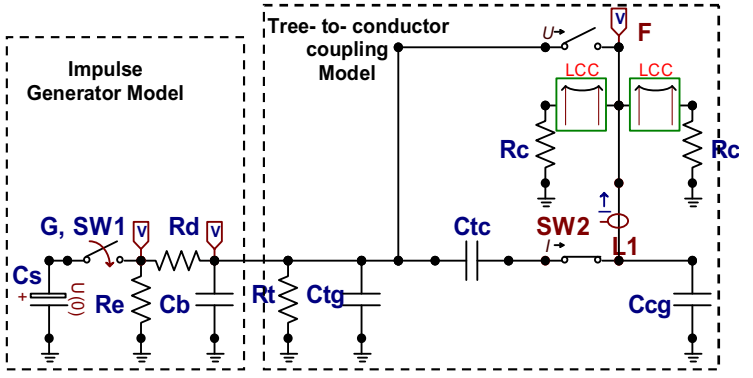

Figure 4.15. ATP-EMTP model of the experimental setup for the dry-air condition.

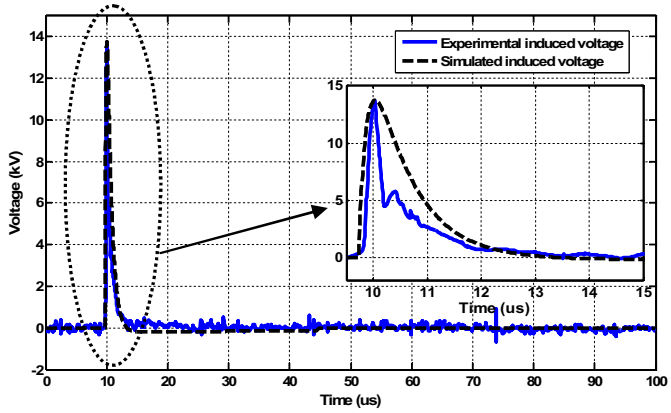

Figure 4.16. The simulated and the experimental induced-voltage measured on the bare conductor for the dry-air condition.

4.1.4 Experimental Arc Characteristics

Here, the performance of the experimental arc characteristics is evaluated for the purpose of modeling the arc characteristics. Three important parameters that should be known beforehand are the arc voltage drop and the current flow and the conductance within the arc channel. The arc current is shown in Figure 4.13 with known lightning impulse voltage, U_t, (see Figure 4.11) on the tree and the induced and the conducted voltage on the conductor, $U_{c,}$ (see Figure 4.12) before and after the arc period, the arc voltage drop, U_{arc} , in Figure 4.17 was extracted by

$$U_{arc}(t) = U_t(t) - U_c(t), \ (t = 0 \text{ to } 100\ \mu s) \qquad (4.3)$$

Thus, the experimental V-I characteristics of the arc is presented in Figure 4.18. The experimental arc conductance which also played a major role in the modeling task is shown in Figure 4.19. This conductance was extracted by

$$g = \frac{i_{arc}(t)}{U_{arc}(t)} \quad , \qquad (\text{where } t = 44.5 \text{ to } 100\ \mu s) \qquad (4.4)$$

In the Figures 4.13 and 4.17, the waveforms were separated into four periods for accurate modeling. The first one is the induction period (first period) that appeared in the same manner of the dry-air condition with different amplitude. The coupling capacitor, C_{tc} = 119 pF [Publication VII], was effective between 9.5 to 15 µs. The second period was denoted as the pre-arc period at no induced voltage observed on the conductor. It was assumed that no coupling exists between the tree and the bare conductor, though the coupling capacitance C_{tc} was left in the circuit for the whole simulation period in order to confirm the initial assumption. However, in the third and fourth periods, there was an arc interaction, which was accompanied by a heavy current flow through the arc channel; this resulted in a higher conducting overvoltage on the conductor.

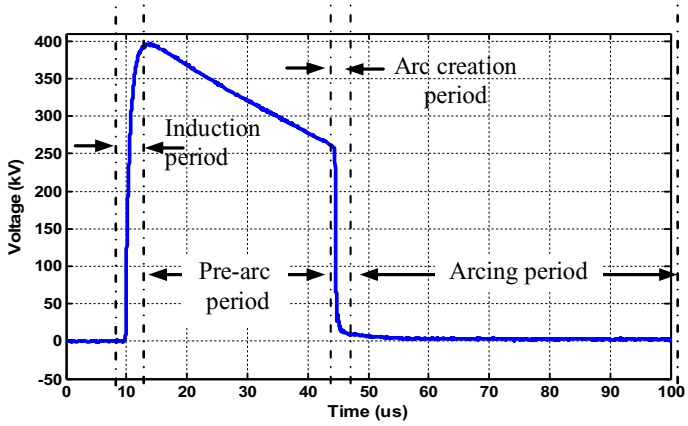

Figure 4.17. Resulting experimental arc voltage within the arc channel for the wet-air condition.

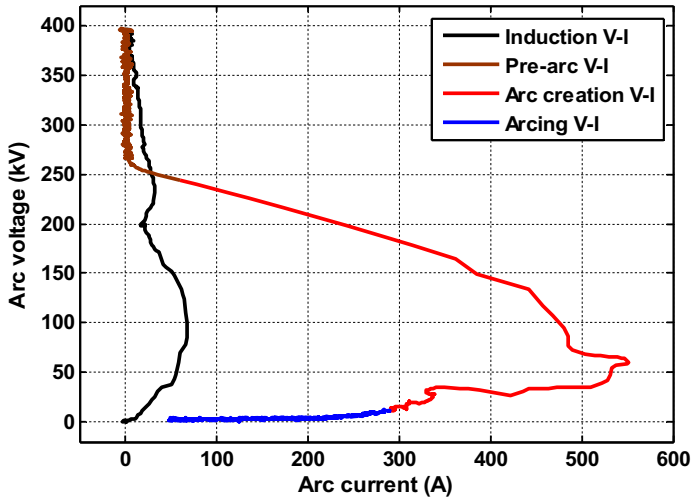

Figure 4.18. Experimental arc characteristics for the lightning voltage and current between the tree and the bare conductor.

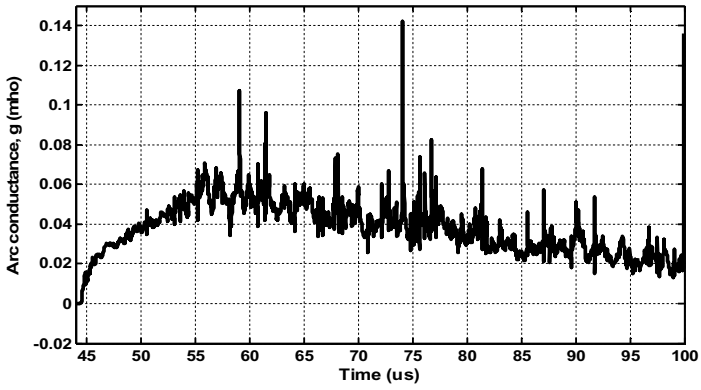

Figure 4.19. Experimental arc conductance for during the arc creation and the arcing period.

4.1.5 Modeling Arc Characteristics with Dynamic Arc Model

In order to represent the arcing phenomenon between the tree and the line in ATPDraw, the coupling capacitance C_{tc} shown in Figure 4.14 is automatically replaced by a dynamic arc conductance, which is controlled by the universal arc representation. First, the dynamic arc model was used, with the help of TACS, to model the V-I characteristics of Figure 4.18. This dynamic arc model was then modified with the inclusion of a static arc equation in order to improve the model accuracy. The comparison with reference to the experimental arc characteristic was carried out. For these two modeling concepts, the coupling capacitance $C_{tc,}$ (see Figure 4.14) was replaced automatically by a dynamic arc conductance, g, controlled by the universal arc representation. Since their introduction, dynamic arc equations have been further modified to increase the model accuracy and to reduce the computational burden. The thermal long arc models [19] and [20] have been introduced to model the arcing fault. The dynamic arc model by *Kizilcay et al* [20], which is a well trusted model based on its experimental proved performance, was introduced here for the dynamic arc modeling. Considering the dynamic model, the equation of dynamic arc conductivity adapted for the arcing period is given as (4.5).

$$g = \int \frac{1}{\tau}(G - g)dt \tag{4.5}$$

where t is the time and g is the time varying arc conductance. $G = |i|/U_{arc}$ is the stationary arc conductance, where $|i|$ is the absolute value of the arc current, $U_{arc} = (U_o + r|i|)l$ is a constant arc voltage parameter, U_o is the arc voltage gradient, r is the arc resistance per unit length and τ is the arc time constant which influences the arc voltage-current characteristic. The arc time constant τ is considered in the form [21]:

$$\tau = Ae^{Bg} \tag{4.6}$$

where A and B are two fitting coefficients and they can help to accurately track the arc nature. The arc parameters were identified using the measured arc characteristics during the arcing periods shown in Figure 4.18 and considering the arc conductance shown in Figure 4.19. For this experimental case, the arc length depicted in Figure 4.10 was l = 230 cm and the corresponding arc parameters were found U_o = 4.1 kV/cm and r = 0.0085/cm. However, the parameters A and B were tuned that A = 9 x 10^{-6} and B = 50000. Figures 4.21 and 4.22 give the Equations flowchart and the ATPDraw circuit for the dynamic arc model respectively, without considering the static arc modeling phase. A comparison of the simulated dynamic arc and the experimental arc characteristics in the V-I domain is shown in Figure 4.20. It can be seen clearly from the figure that the modeling of the arc creation period (third period) was extremely difficult using the dynamic arc equations.

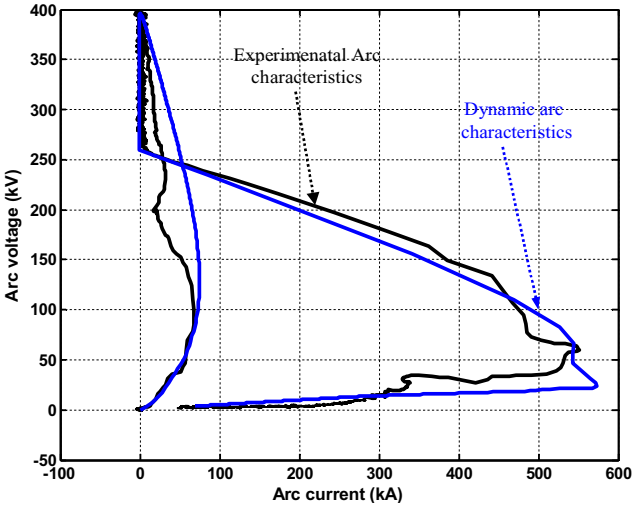

Figure 4.20. Comparison of a dynamic arc model with the experimental arc characteristics.

4.1.6 Modeling Arc Characteristics with Modified Dynamics Arc Model

The great task of the work was the modeling of the arc characteristics during which the heavy flashover current flows from the lightning struck-tree to the power conductor as all the lightning voltage appeared across the arc channel as the arc voltage within the duration of the constant arc current. Therefore the static model was employed to reproduce the arc variables within the period before automatically switching to the dynamic model for the four periods.

The static arc model proposed in [53] and evaluated in [22] was used to model the transition from the dielectric to arcing. The modified dynamic arc model incorporated the static arc equation and the dynamic equation for reproducing the experimental arc characteristics. Therefore, the arc conductance per unit length, *G (t)*, during this constant arc current flow into the network which according to [22, 53], translates to

$$G(t) = G_c + (G_i - G_c)e^{-t_D/\tau} \tag{4.7}$$

In the equation, t_D is the arc creation period, G_i and G_c are the initial and ultimate conductance values during the arc creation period, respectively. The initial static arc conductance, G_i, and initial dynamic arc conductance, G_c , were then taken out from the experimental time-varying arc conductance, *g* (see Figure 4.19). From the figure, G_i was estimated to be 0.0008 S/m and G_c was estimated to be 0.013 S/m. The time constant,τ, between the static arc period, whose value is normally assumed [22], was taken to be τ = 90 μs.

The steps for the calculation of the arc conductance using the static arc (4.7) and the dynamic (4.5) are shown in Figure 4.21. The static and dynamic models were used sequentially with the help of the Controlled Integrator (Type 58). The static model (4.7) and the dynamic arc (4.5) are easily introduced to TACS in ATP-EMTP, and the result of the two equations is the time dependent arc conductance, g, the reciprocal of which is introduced as the arc resistance, $R_{arc,}$ into the system circuit. Based on the nature of the experimental arc phenomenon shown in Figure 4.19, the static arc equation was applied to the arc creation period (44.5 μs to 45.5 μs). The interpretation of determining this time length of the arc creation period is as follows. When the arc was modeled using only the dynamic arc equation, unfortunately there was high error at the beginning time of the arc creation, called

the arc creation period (see this period in Figures 4.11- 4.13, 4.17 and 4.18). This error was not compensated by tuning the model parameters of the dynamic arc (4.5). This arc creation period has a different time constant to the arcing period, i.e. the static time constant was 90 μs and the dynamic time constant was determined by the (4.6). The period of the static arc creation was considered as 1 μs (from 44.5 to 45.5 μs) for the case under study. So, in order to reduce the error in the simulation results, the arc was divided into two periods; the arc creation and arcing periods as in Figures 4.11-4.13 and 4.17. This period was estimated by evaluating the error period in the dynamic arc equation with respect to the experimental waveforms.

Immediately after the arc creation period, the dynamic arc model was applied to model the decaying of the current from 45.5 μs to 100 μs. The control signal was generated by the help of the Logical FORTRAN expressions in order to differentiate the arc creation and arcing periods. When the control signal is negative, the integrator output equals to the reset signal, that is, the time domain solution of the static model (4.7). When the control signal changes from negative to positive, the integrator output becomes the integration of the dynamic arc model (4.5). In TACS, both the equations are solved for each time step with the Controlled Integrator (Type 58). The steps considered in the modeling of the arc are as follows. For the static modeling phase, the time t_D is zero until the arc started. The current flowing in the static arc is transposed into the TACS using the time –varying element (Type 91 current sensors) of the ATP/EMTP. The arc (4.7) is solved in the TACS and the static arc conductance is calculated. The inverse of the conductance value is transferred through the time-varying resistance element (Type 91 TACS controlled resistance) into ATP/EMTP. The node equations are solved in the ATP/EMTP. The arc conductance for the dynamic modeling phase is calculated as follows. The current flowing in the arc is transposed into the TACS using the time –varying element (Type 91 current sensors) of the ATP/EMTP. Its absolute value is divided by the constant arc voltage parameter, $V_{arc,}$ and then the outcome minus the arc conductance computed in the previous step is divided by the arc time constant τ (4.6). The resultant dynamic arc conductance is imputted into the Controlled Integrator (Type 58) and solved with (4.5). Thus, the arc conductance is updated at each time step. The inverse of the conductance value is transferred through the time-varying resistance element (Type 91 TACS controlled resistance) to ATP/EMTP. The node equations are solved in the ATP/EMTP. Thus, the arcing phenomena, their interaction with the power line, and the transients involved, were simulated successfully. Figure 4.22 gives the ATPDraw network of the experimental setup that was used for the simulation. The overall model consists of the following: the lightning impulse generator, in which, its components data were collected from the laboratory; the tree-to–conductor model, which is a combined model of the tree, bare conductor and the capacitive coupling between the two objects; and the modified dynamic arc model (universal arc representation). The simulated arc characteristics of the dynamic model and the modified model with reference to the experimental arc characteristics are shown in Figure 4.23. A better agreement in these comparisons was achieved for the modified dynamic model and this confirms its modeling accuracy with reference to the experimental arc characteristics. Thus, such a model can be included in the existing software packages for the simulation of lightning arcs.

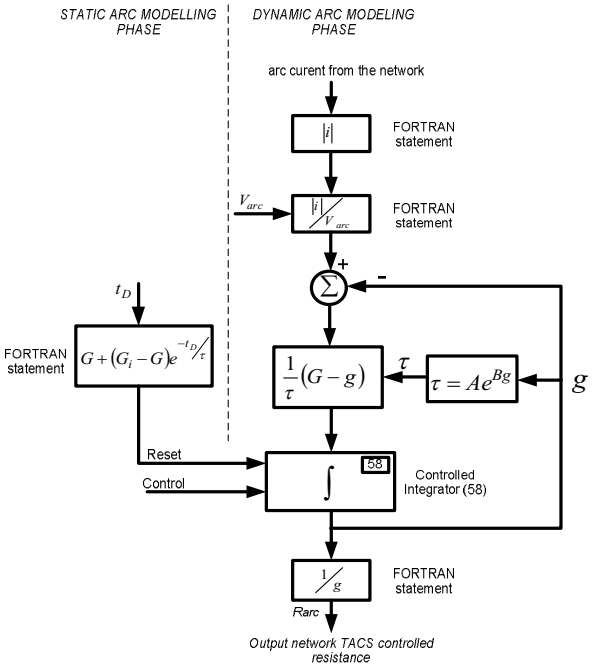

Figure 4.21. Equations flowchart for the modified dynamic arc model.

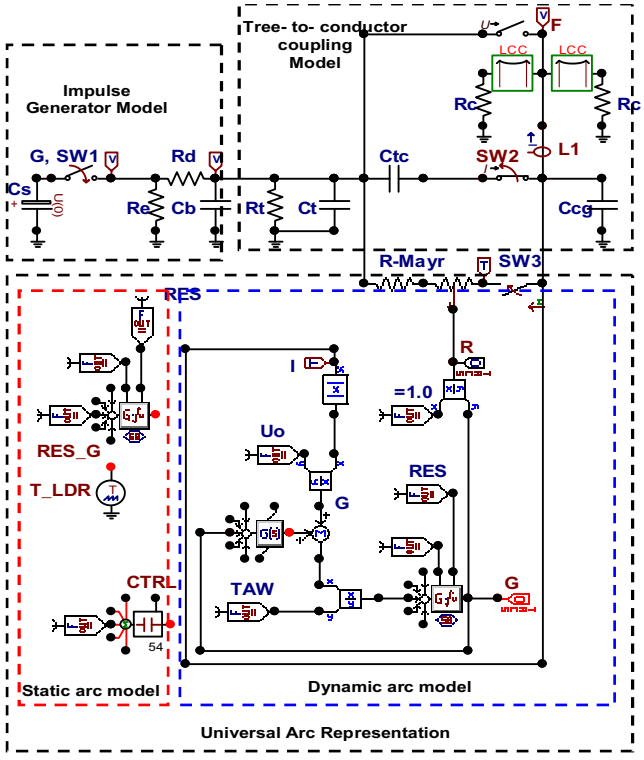

Figure 4.22. ATP-EMTP model of the experimental setup with modified dynamic arc model

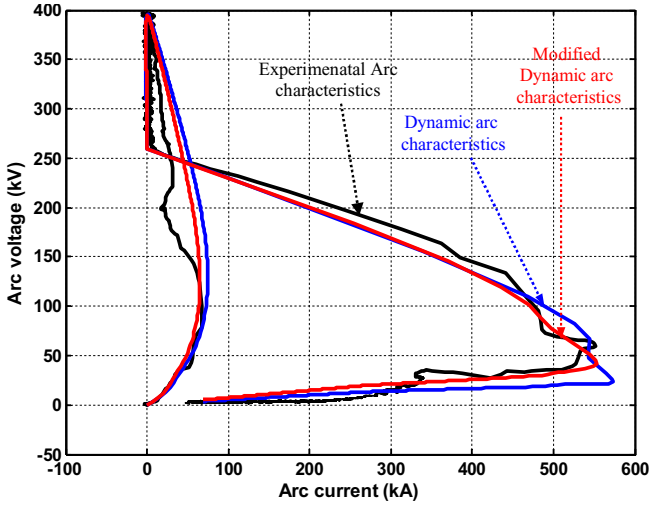

Figure 4.23. Performance comparison of the dynamic arc model and the modified dynamic arc model with the experimental arc characteristics.

5- Evaluation of Lightning Arc between a Tree and a Distribution Network

In this study, the response of a typical Finnish distribution network to the arc phenomenon was examined [Publication VIII]. The modified arc model that was presented in the previous chapter has the capability of reproducing the dynamic arc interaction of a lightning arc between a tree and a distribution network. Shown in Figure 1.4 is the distribution network, the corresponding one-line diagram of the network is given in Figure 5.1. The ATPDraw circuit of the complete distribution network (MV bare conductor feeders, transformers at substations 1 and 2, LV underground cable feeder, LV overhead covered conductor feeder and customer loads) is shown in Figure 5.2. The network was simulated based on an ATP/ EMTP theory book [60] and the Finnish distribution network configuration as follows: all the feeders were represented by the *Jmarti* frequency-dependent model with distributed parameters [61-62]. All segments of the feeders, as in Figure 1.4, were represented in ATPDraw accordingly. To avoid reflections, the main feeder were terminated to the ground, at the front and the end feeder sections, through a 3-phase distributed parameter (Clarke) having characteristic impedances of 400 Ω [61]. Accurate modeling of distribution transformers is required in order to determine the correct high frequency overvoltage response of the network. Thus, an experimentally verified 20/0.4 kV distribution transformer model reported in [63] was adapted for this study. The two 3-phase transformers connected the MV line to two different types of LV networks; one is an LV underground cable feeder (600 m) and the other is an LV overhead covered conductor feeder (600 m). The customer loads were modeled, in these two LV feeders, as 3-phase balanced impedance loads. The same customers and load characteristics were connected to the two LV feeders. The coupling capacitance from the tree to the conductor phases, considering 5 m clearance, was calculated based on the formula introduced in [Publication VII] and the modified dynamic arc model of Figure 4.22 was simulated with the network (Figure 5.2). Therefore, by employing the modified dynamic arc model, the performance of the lightning arc on the MV/ LV network under the influence of the nearby tree and the network characteristics is evaluated with the following simulated cases.

Simulated cases and calculation points
With reference to Figures 1.4 and 5.1, the following are the simulated cases:
Case 1: Lightning arc performance on Finnish MV/ LV distribution network
Case 2: Shielding effect of tree on the distribution network
Case 3: Lightning arc protection by crossarm grounding.

The arc was generated with a lightning current of 15 kA which is the mean lightning current in Finland [23]. The positive and standard lightning characteristics of 1.2 /50 μs [1] was represented using a single-stroke, *Heidler-type* [61] current source, with a parallel lightning channel surge impedance of 400 ohms [61]. The calculation locations are as follows: The overvoltages at the midpoint of the MV feeder were recorded. Since the two substations, i.e. *Substation 1* and *Substation 2*, are the same distance (525 m) from the lightning fault point, the overvoltages arriving either of the substations are the same. Thus, only the overvoltages on the MV side of *Substation 1* were reported. Due to the different characteristics of the LV feeders, the overvoltages on the LV side of *Substation 1* and *Substation 2* were also reported. The transfer overvoltages from these substations to the LV underground cables and LV covered conductor lines connecting *Customer 1* and *Customer 10* respectively were measured. It should be

noted that both customers (*Customer 1* and *Customer 10*) are located at the same distance, which is 1125 m from the lightning fault location (middle point of the MV feeder).

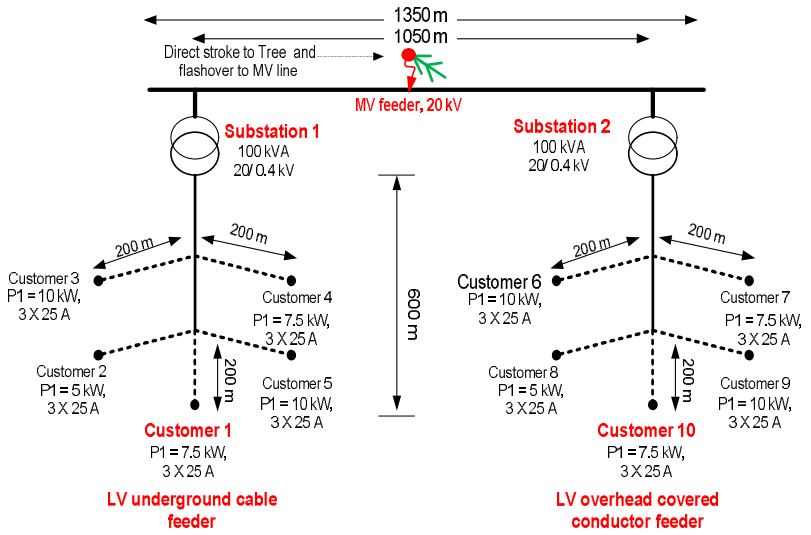

Figure 5.1. One line diagram of the MV/ LV distribution network of Figure 1.4 for the simulation studies.

5.1 Simulation Results

Case 1- Lightning arc performance on Finnish MV/ LV distribution network

Arc simulation was realized by assuming a direct stroke to the tree (see Figures 1.4 and 5.1) and a lightning arc creation between the tree and *Phase A* at the midpoint of the MV feeder. Shown in Figure 5.3 are the induced and arc-conducted overvoltages measured at the midpoint of the 3-phase distribution feeder. The overvoltages on the *Phases B* and *C* are based on mutual coupling among the three phases. Thus, the induced overvoltages on the conductors were proportional to their distances from the tree, the arcing overvoltages were more than double the resulting overvoltages on *Phase B* or *C*. Both the induced and arc-conducted overvoltages appeared in the time characteristics are surprisingly different from the standard lightning impulse characteristics. There was a noticeable reflection on Figure 5.3 (ii) in spite of the main feeder matched with the characteristic impedance of 400 Ω. The probable reason is the reflections from the ends of the feeder or from other parts of the network. Figures 5.4, 5.5 and 5.6 show the overvoltages at MV and LV sides of the *Substation 1* and *2*. Though the same overvoltage waves arrived at the two substations at the same time as in Figure 5.4, the overvoltages at the substations were slightly lower than the overvoltages at the feeder midpoint (see Figure 5.3). There was a higher overvoltage peak at the entrance of the covered conductor feeder (LV Figure 5.6) than the underground cable feeder (Figure 5.5). This appreciable suppression of overvoltages at the underground cable entrance can be ascribed to its much lower surge impedance compare to the covered conductor.

In order to evaluate the attenuation characteristics of both the LV feeders, the overvoltage profiles along the two LV feeders were recorded accordingly. It should be noted that the two feeders are of the same load densities and arrangements. The *Customers 1* and *10* have the same loads and distances (1125 m) from the lightning arc point. The propagated surges to *Customers 1* and *10* through the underground cable and the covered conductor are shown in Figures 5.7 and 5.8 respectively.

Figures 5.9 and 5.10 show the overvoltage profile at various points along the two LV feeders. With reference to the two distribution substations, the overvoltage decreases as the feeder length increases but much faster on the covered conductor feeder. The percentage overvoltage peak reduction was 98 % for the covered conductor and 93 % for the underground cables of the same length 600 m. The higher frequency attenuation of the covered conductor shows its substantial impact on the lower overvoltages to which *Customer 10* is subjected to. However, the lower surge impedance of the underground cable and the much lower overvoltages on *Customer 1* clearly depict its considerable impact on power network reliability, especially in areas where lightning flash density is high.

Case 2: Shielding effect of tree on the MV/ LV distribution network

The assumption made here is that without the presence of the tree, there is no shielding and the 15 kA stroke will terminate directly at the line. Therefore the case of direct lightning impact on *phase A* of the MV line was examined; the lightning contact point was the same as in *Case 1*. The resulting overvoltages on *Phase A*, due to the direct hit were compared with the case of the overvoltages due to arcing, as in given Figures 5.11, 5.12, 5.13 and 5.14. Of course, the overvoltages from the direct stroke were much more than from the arcs, since much of the lightning energy has been suppressed by the tree. Thus, the presence of the tree allowed reductions of about 60 % (on MV feeder midpoint and substations), 33 % (on *Customer 1* through underground cable) and 41 % (on *Customer 10* through covered conductor) of the overvoltage peak values. This explains the benefit of allowing trees around the corridors of power distribution lines. One other observation is the rise time of the direct overvoltages that was faster than the rise time of the lightning arc overvoltages.

Case 3- Lightning arc protection using crossarm grounding

The main purpose of grounding systems is to suppress fault currents into the ground, which can be caused either by internal faults or by external sources, such as lightning. Lightning performance by crossarm grounding or shield wire has been demonstrated to be effective for the protection of power line [64-74]. Therefore, the effectiveness of grounding on a distribution pole crossarm to minimize the overvoltage caused by a lightning arc is assessed here. Recalling that the resulting overvoltages from *Cases 1* and *2* are much more than the MV distribution *BIL* (150 kV). Thus, any insulation that is exposed to these overvoltages will flash over as long as the overvoltage exceeds the withstand voltage level of the line. However, much of these overvoltages will be lowered if there is flashover and the pole crossarms are effectively grounded. Since the grounding wire is short, it was modeled with a single inductance using $L = \mu_0 l/(2\pi)\{\ln(2l/r_g) - 1\}$ [66], where the wire length, l = 8 m and radius, r_g= 1.3 mm were taken from [66], hence, the inductance was estimated to L =15 μH. The grounding resistance of the pole was taken as 17 Ω [64]. Thus, *Case 1* was simulated with all the MV distribution poles cross-arms grounded. Figures 5.15 and 5.16 give the resulting overvoltage reductions as a comparison with the original overvoltages at the arcing point and the substations respectively. The grounding of the pole crossarms was very effective; the overvoltages were suppressed accordingly at the feeder midpoint, the substations and the customer entrances (see Figures 5.17 and 5.18).

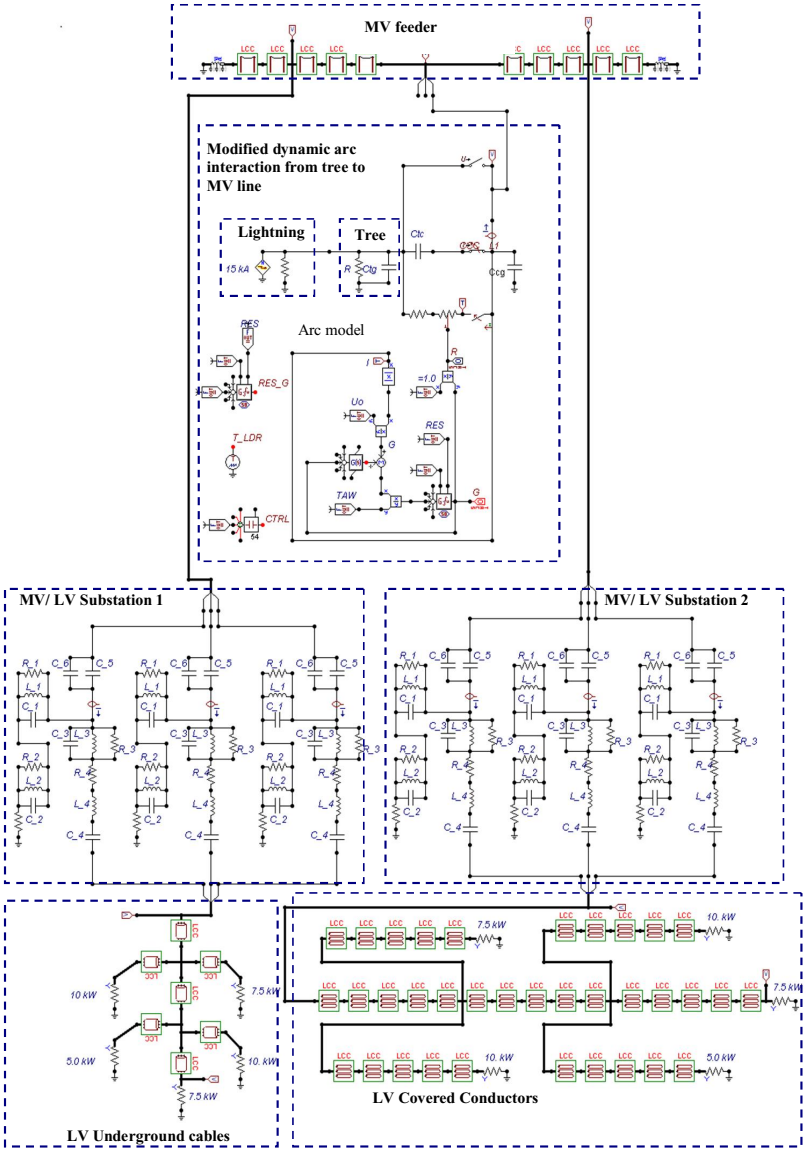

Figure 5.2. ATP/ EMTP Model of the MV/ LV distribution network of the *Case 1* with; 15 kA (mean lightning current in Finland), tree, with modified dynamic arc, high frequency transformer model (at substation 1 and 2), the LV underground cables, LV covered conductors and customer loads. Note that the *Case 2* has no inclusion of the tree and the arc model; *Case 3* is the same as *Case 1* but with all the MV poles grounded.

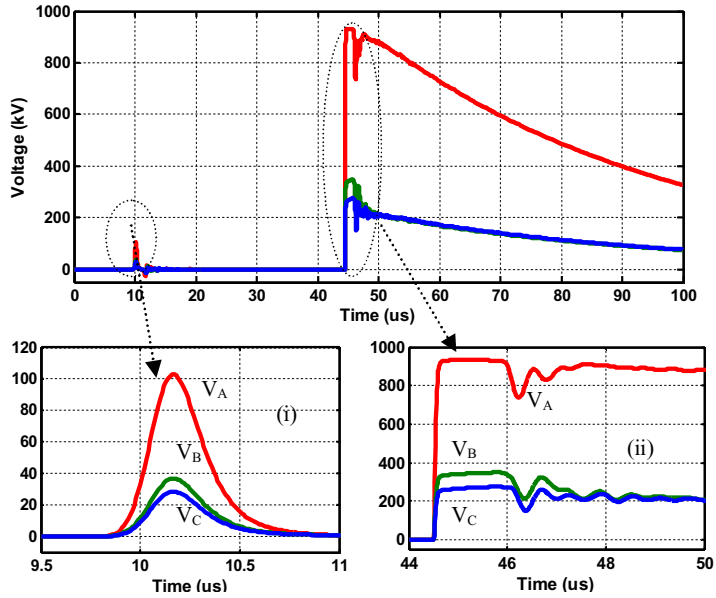

Figure 5.3. Simulated lightning overvoltages measured on the 20 kV feeder midpoint. (i) the voltage peak during the induction (V_A = 102 kV) (ii) the voltage peak during arc creation (V_A = 930 kV).

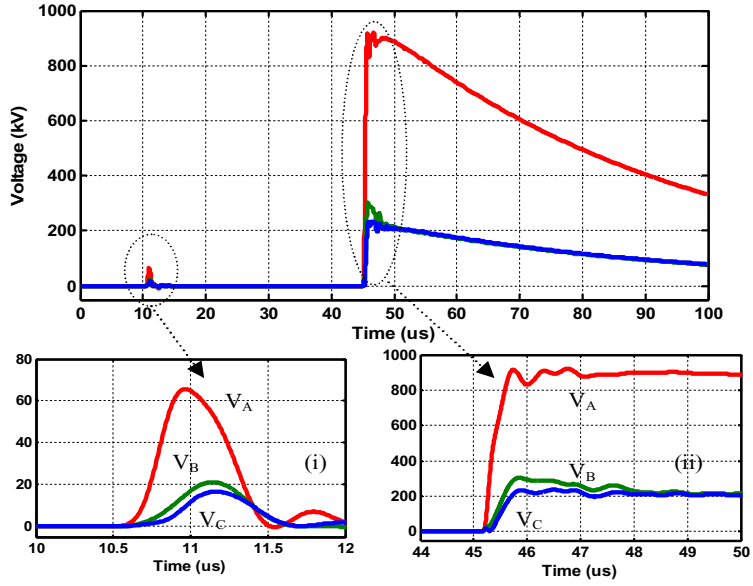

Figure 5.4. Simulated lightning overvoltages measured on the MV side of substation 1 or 2. (i) the voltage peak during the induction (V_A = 66 kV) (ii) the voltage peak during arc creation (V_A = 910 kV).

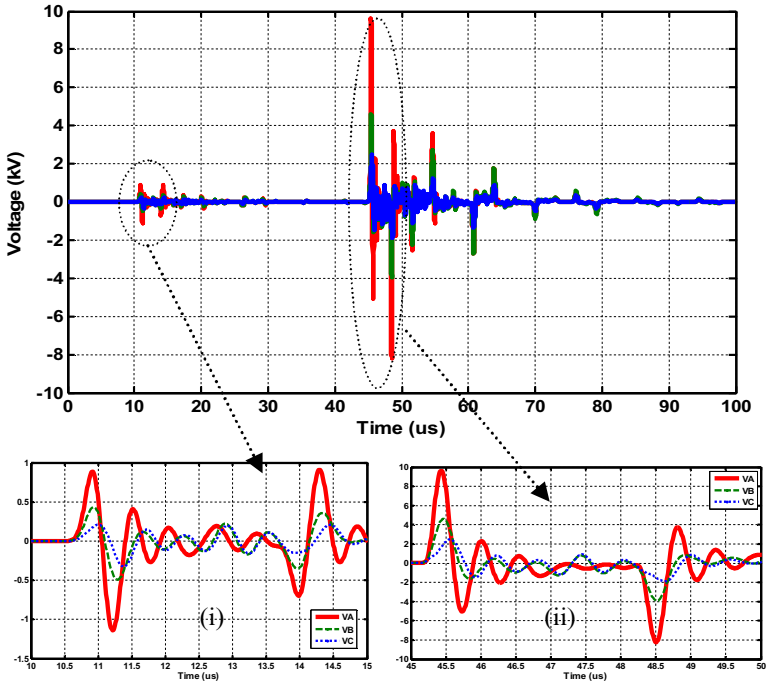

Figure 5.5. Overvoltages on *LV side of Substation 1* connecting LV underground cable. (i) the voltage peak during the induction (V_A = 1140 V) (ii) the voltage peak during arc creation (V_A = 9540 V).

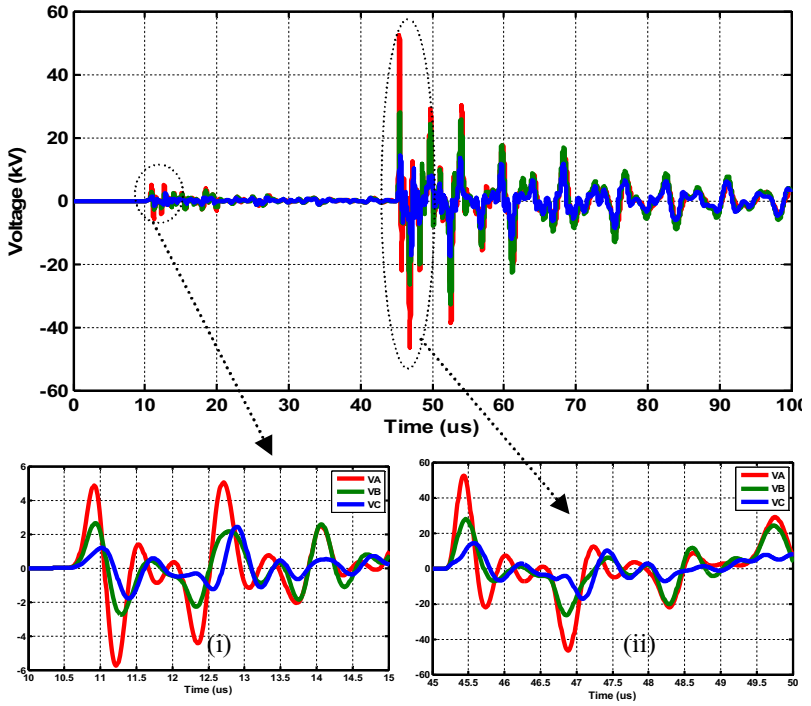

Figure 5.6. Overvoltages on *LV side of Substation 2* connecting LV covered conductor. (i) the voltage peak during the induction (V_A = 5750 V) (ii) the voltage peak during arc creation (V_A = 50450 V).

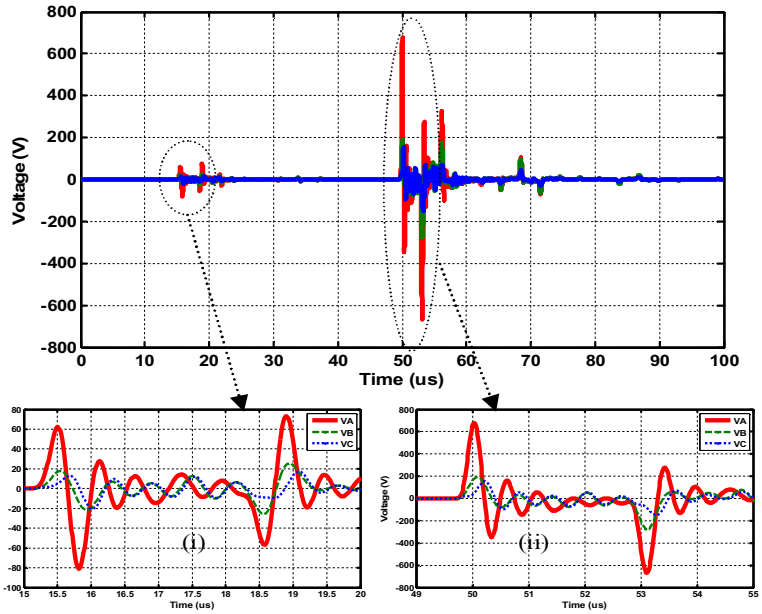

Figure 5.7. Entrance overvoltages on *Customer 1* connected through underground cable. (i) the voltage peak during the induction (U_A = 80 V) (ii) the voltage peak during arc creation (U_A = 680 V).

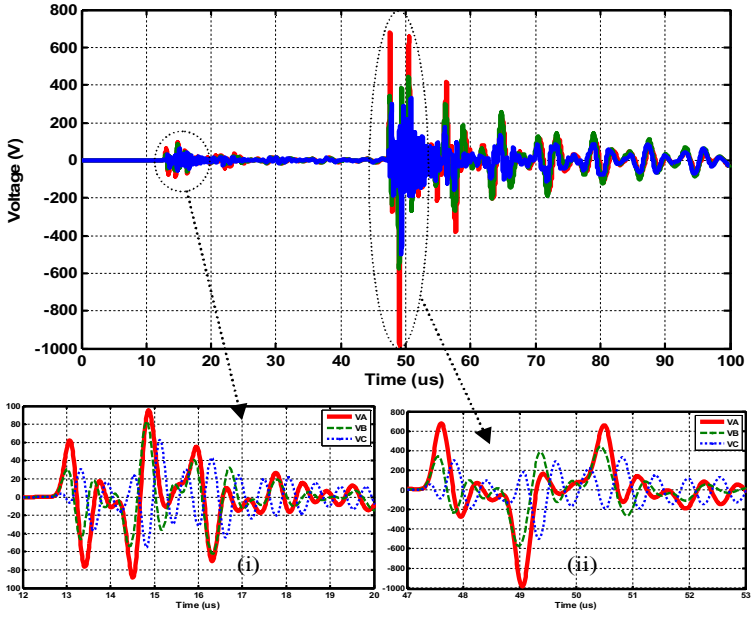

Figure 5.8. Entrance overvoltages on *Customer 10* connected through covered conductor. (i) the voltage peak during the induction (U_A = 99 V) (ii) the voltage peak during arc creation (U_A = 1000 V).

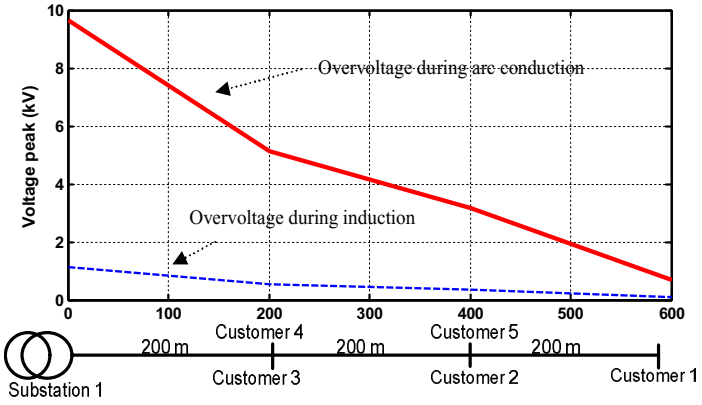

Figure 5.9. Overvoltage profile along the 600 m, LV underground cable feeder during the induction and arc creation at the MV feeder midpoint.

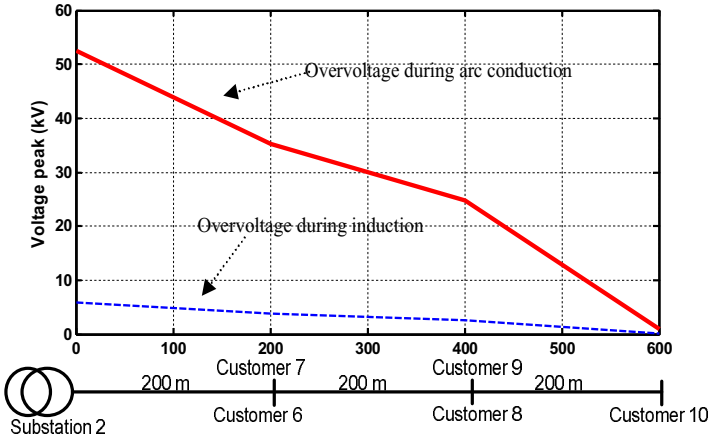

Figure 5.10. Overvoltage profile along the 600 m, LV covered conductor feeder during the induction and arc creation at the MV feeder mid-point.

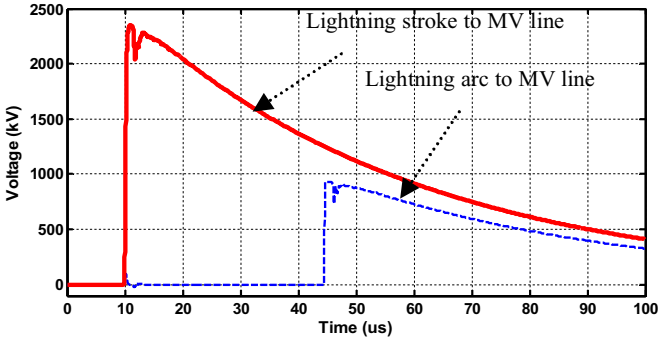

Figure 5.11. Comparison of overvoltages on the *midpoint* of the 20 kV feeder from direct stroke to line (Voltage peak, U_A = 2350 kV) and direct stroke to tree (Voltage peak, U_A = 930 kV).

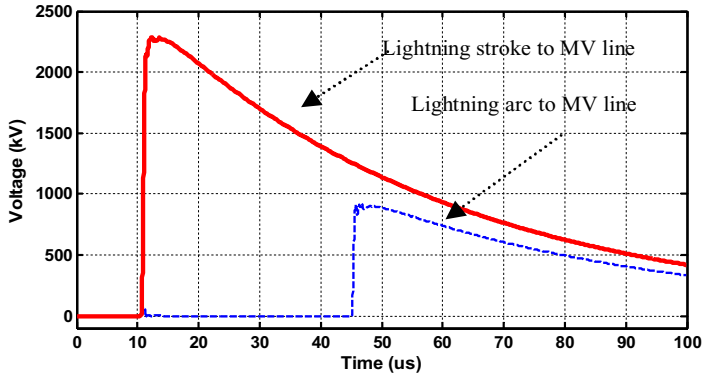

Figure 5.12. Comparison of overvoltages on MV side of *substations* 1 and 2 due to direct stroke to line (Voltage peak, U_A = 2230 kV) and direct stroke to tree (Voltage peak, U_A = 910 kV).

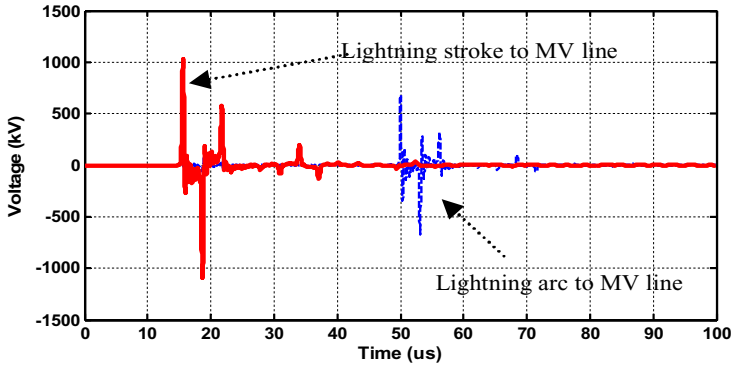

Figure 5.13. Comparison of the entrance overvoltages on *Customer 1* connected through underground cable for the direct stroke to line (Voltage peak, U_A = 1030 V) and direct stroke to tree (Voltage peak, U_A = 680 V).

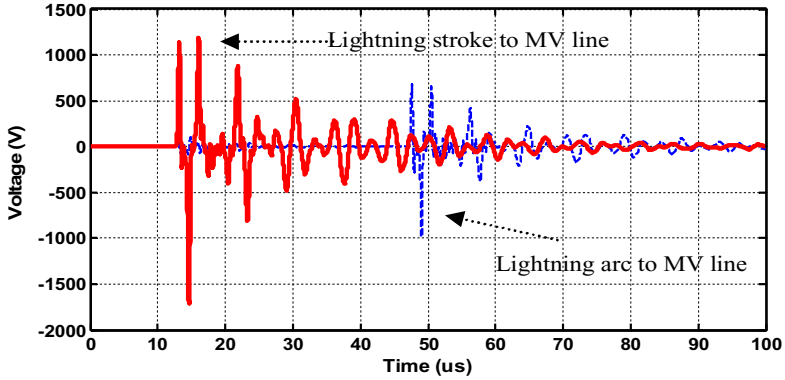

Figure 5.14. Comparison of the entrance overvoltages on *Customer 10* connected through covered conductor for the direct stroke to line (Voltage peak, U_A = 1700 V) and direct stroke to tree (Voltage peak, U_A = 998 V)

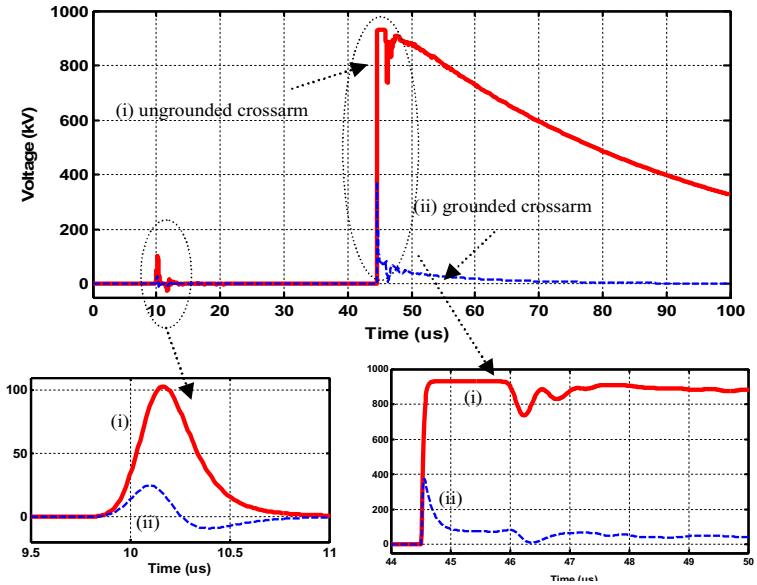

Figure 5.15. Comparison of overvoltages on the feeder midpoint for the grounded and ungrounded pole cross-arms. (i) ungrounded crossarms (ii) grounded crossarms

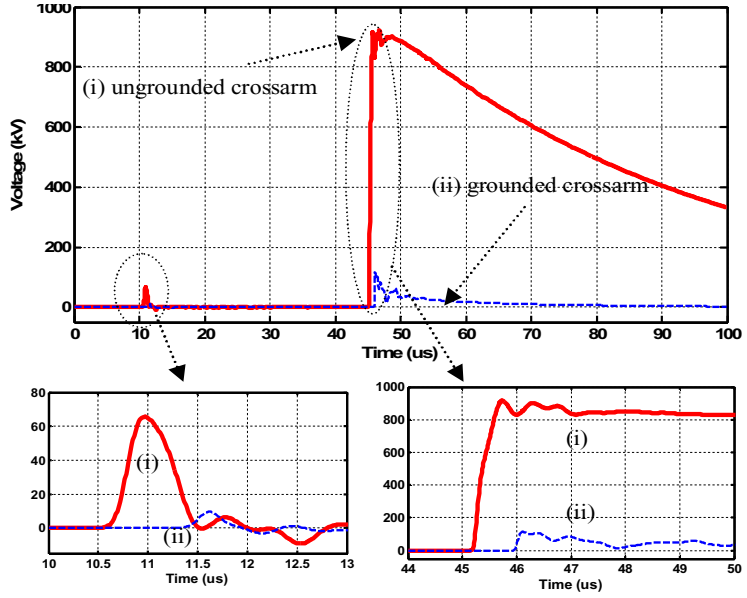

Figure 5.16. Comparison of overvoltages on the substations 1 and 2 for the grounded and ungrounded pole cross-arms. (i) ungrounded crossarms (ii) grounded crossarms.

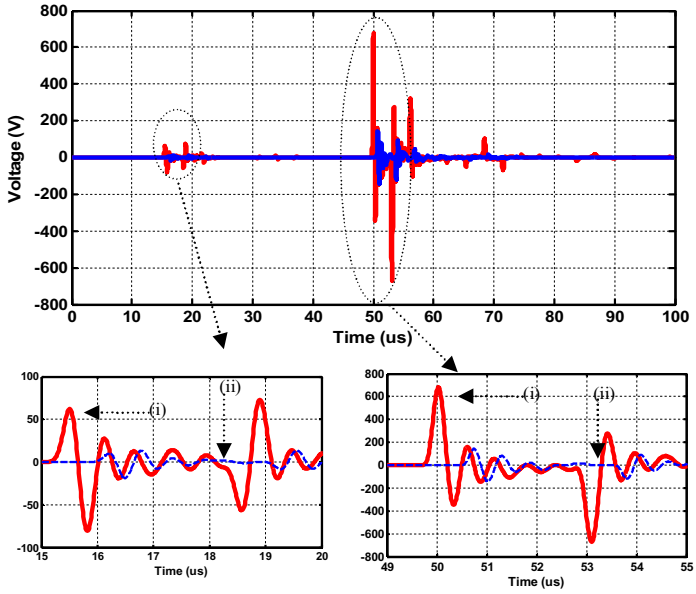

Figure 5.17. Comparison of the entrance overvoltages on *Customer 1* connected through underground cable for grounded and ungrounded MV pole crossarms. (i) ungrounded crossarms (ii) grounded crossarms

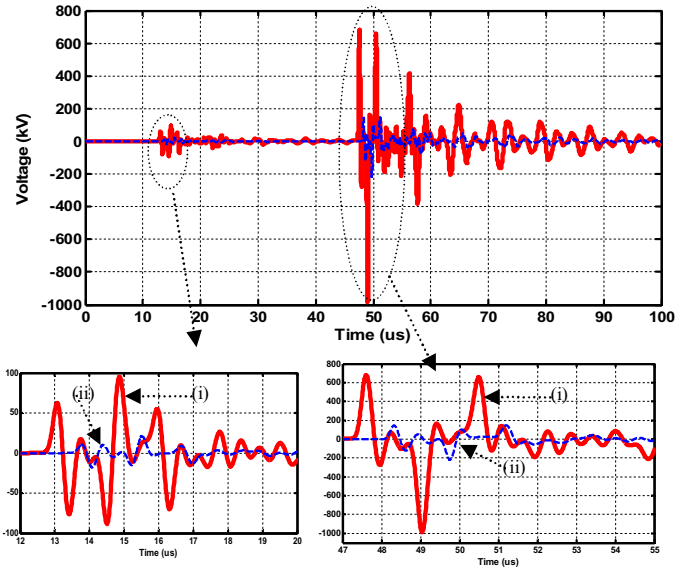

Figure 5.18. Comparison of the entrance overvoltages on *Customer 10* connected through covered conductor for grounded and ungrounded MV pole crossarms. (i) ungrounded crossarms (ii) grounded crossarms.

6- Conclusions and Future Work

6.1 Conclusions

Considering a typical direct lightning flash with multiple strokes in Finland, the effects of surge arresters and of the combination of surge arresters and shield wire on the protection of overhead distribution lines have been studied using EMTP software. For the stroke magnitudes simulated in this work, surge arresters on their own were not effective in suppressing the overvoltages due to the direct strokes. The arresters at the extremities of the lightning struck point may therefore suffer physical and electrical damage even after successful operation. However, shield wires can help relieve the surge arresters from overvoltage stress if installed in severe areas, such as were tested in this study. The simulation has established the need for an augmented protection scheme against lightning overvoltages in distribution networks where lightning incidence is most severe.

Further, lightning protection of medium voltage underground cables was proposed in this work. With the Finite Element Method (FEM), the study has revealed the susceptibility of underground cables to direct and indirect lightning discharges to different soil structures. Possible protection of the cable with the use of shield wire has also been demonstrated. The study revealed that any increase in soil resistivity will increase the lightning disturbance in underground cables. However, with the shield-wire protection, an underground cable can withstand more than 3 times the damaging current compared to the same cable without a shield-wire. Regarding the soil structures examined, although the number of cable damage times per year is very low for soils without a shield wire, i.e. for a 1 km cable length, damage occurs once in 137.95 years, 139.41 years, and 152.69 years for homogeneous soil, the 1st inhomogeneous soils and the 2nd inhomogeneous soils respectively, this study has further demonstrated that, with a shield wire, the UC may fail once in 1062 years, 1437 years and 159,534 years, for the same soil types. Therefore, increasing cable depth for protection against lightning is not necessary if the protection of the cable includes a shield wire with a suitable clearance from the underground cable.

Evaluation of direct strokes to MV distribution covered conductors has been made using numerical studies by considering the Finnish lightning data. The study was extended to simulate the lightning performance of the conductors in order to determine the optimum distance at which a surge arrester must be installed on the distribution lines for the most effective protection against overvoltage surges. With 15.2 kA and 0.786 strokes/ km^2/year taken to be the peak value of the return stroke current and ground flash density in Finland respectively, a direct lightning discharge to either a covered conductor or a line support is expected to cause an interruption or outage, or damage to the covered conductor. Also, good protection of the conductor against any slow or fast rising surges could be achieved if the arresters are installed on every pole, for a 100 m line span.

With experimental study and electro-geometric modeling, an improved lightning analysis of overhead distribution conductors with the shielding effects of trees has been carried out. The shielding effect of a nearby tree on an MV distribution conductor is compared with that of a concrete building which has been previously investigated in the literature. The investigations proved that distribution conductors that transverse the forests will be protected from direct lightning strokes, depending on the nature of the magnitude of the strokes, the height of the trees and the clearance between the lines and the trees. However, further experimental study

has revealed that perfect shielding by trees will not eliminate the resulting induced overvoltage on the lines, which can be sufficient to disrupt the power supply.

An investigation was carried out to understand the phenomenon of lightning interaction with distribution lines in different weather conditions with the aid of full-scale laboratory experiments. Therefore, experimental results revealed that tree resistance significantly changes with weather conditions. The surge impedance values of the tree under the wet-air condition are greater than under the dry-air condition. The higher surge impedance of the tree and decrease in the voltage strength of air due to raindrops could be responsible for the most persistent lightning faults on distribution lines that traverse forests. In the experiment conducted with artificial rainfall, a direct stroke to the tree initiated an arc channel through the wet-air to the bare conductors. This confirmed that raindrops could considerably lower the flashover voltage between a lightning-struck tree and nearby distribution conductor, in reality.

This work has carried out experimental and simulation analyses to investigate the lightning arc existing between a lightning-struck tree and a distribution conductor under rainfall. A modified dynamic arc model to evaluate the lightning arc characteristics between a power line and nearby tree considering rainfall has been presented and validated. The arc characteristics were successfully modeled by capturing the features of the experimental results in the existing dynamic arc equations, which were later incorporated in the TACS field of the EMTP software as a Universal Arc Representation to reproduce the experimental arc. Due to the strange characteristics of the experimental lightning arc recorded, the dynamic arc equation was not sufficient to model the arc, thus a modified arc model that combines a static and the dynamic arc equations was employed to reproduce the arc characteristics with better agreement. The accuracy of the arc model has been tested with the experimental arc characteristics. The arc model can be used generally for the simulation of the lightning-arc or flashovers between a lightning-struck tree and distribution line or substation equipment.

Features of the modified arc model have been used to evaluate the performance of a lightning arc in a typical Finnish distribution network design under the influence of a nearby tree. The distribution network consists of a distribution feeder, distribution transformers, low voltage underground cable and covered conductor feeders, and customer loads. The lightning arc characteristics of the distribution network characteristics were examined. The shielding by nearby trees on distribution lines is very necessary but not sufficient to subdue the lightning overvoltage performance of the lines. For one of the examined cases, the overvoltage performance of the power line was affected by the presence of the tree. Thus, for lines that traverse forests, lightning arcs from trees are likely. Aside from the use of surge arresters and spark gaps to protect the power infrastructure against lightning overvoltages, the proper grounding of distribution pole crossarms can further suppress the lightning arc overvoltages and relieve the arresters from the need to dissipate excessive amount of energy.

6.2 Future Research

Briefly, the following list contains ideas for future work that could be pursued in this field of research.

1. Considering the low specific ground conductivity in Finland, more investigation should be carried out on the effect of shielding wires and arresters on lightning protection considering arresters' locations, grounding and lightning parameters.
2. The wetness of the ground can influence the lightning performance of underground cables; therefore, experimental verification of this scenario

should be established.

3. Now that covered conductors are gradually replacing the existing bare conductors for higher reliability in most MV distribution networks in the Nordic countries and elsewhere, further work should examine the effect of rainfall on the performance of lightning overvoltages on these covered-conductor lines, which are also supposedly protected by nearby trees.
4. The lightning arc modeling should be implemented further to study the lightning arcing phenomena in substations and large power networks, and to access the protection performance of surge arresters, spark gaps and other protective devices. A field scenario of the arcs should be compared to the digital modeling.
5. Since most standards of lightning overvoltage protection do not take into consideration the contribution of rainfall, wind and other environmental variables in their investigations, it would be sensible to carry out further research in this area with the aim of incorporating the results into the existing standards.
6. Further investigation would be required to create a mathematical formula or modify the existing models for the accurate calculation of induced voltage resulting from lightning strokes to nearby high-impedance trees and other structures.

References

[1] IEEE Guide for Improving the Lightning Performance of Electrical Power Overhead Distribution Lines, *IEEE Standards*, IEEE Std 1410-1997.

[2] V. A. Rakov and M. A. Uman, Lightning: Physics and Effects, Cambridge Univ. Press, New York, 2003.

[3] Joint CIGRE/CIRED Working Group 05 "Lightning Protection of Distribution Networks. Part I: Basic Information", *14th Intern. Conf. Exposition on Electricity Distribution*, Birmingham, UK, No. 438, pp. 2.21.1-2.21.7, 1997.

[4] A. M. Mousa and K.D. Srivastava, "Effect of Shielding by Trees on the Frequency of Lightning Strokes to Power Lines", IEEE Trans. Power Delivery, Vol. 3, pp. 724-732, 1988.

[5] M. Sakae, A.A. Asakawa, K.Ikesue, T.Shindo, S. Yokoyama and Y. Morooka, "Investigating on Lightning Attachment Manner by Use of an Experimental Distribution Line and a Tree", *Transmission and Distribution Conf. Exhibition,* Asia Pacific, IEEE PES, Vol. 3, pp. 2217- 2222, 2002.

[6] M. Sakae, A.A. Asakawa, K. Ikesue, T. Shindo, S. Yokoyama and Y. Morooka and K. Ikesue, "Characteristics of Impulse Discharge on Lightning Attachment to an Open Wire and a Tree", *Intern. Sympos. High Voltage Eng. (ISH)*, Vol. 12, pp. 119-125, 2001.

[7] A. M. Farouk, "Modeling of Transmission Line Exposure to Direct Lightning Stroke", *IEEE Trans. Power Delivery*, Vol. 5. 1990.

[8] J. Slepian, C.L. Denault, A.P. Strom "Dielectric Strength of Water in Relation to Use in Circuit Interrupters", *Transaction of the American Institute of Electrical Engineers,* 1941; 60(6):389-395.

[9] H.M. Schneider, F.J. Turner "Switching-surge flashover characteristics of lon sphere-plane gaps for UHV station design, *IEEE Transactions on Power Apparatus and Systems,* 1975; PAS-94(2):551-560

[10] F.A.M. Rizk "Influence of rain on switching impulse sparkover voltage of large-electrode air gaps", *IEEE Transactions on Power Apparatus and Systems,* 1976; PAS-95(4):1394-1402.

[11] N. Klairuang, W. Pobpom and J. Hokierti, **"**Effects of electric fields generated by direct lightning on ground to underground cables", *2004 International Conference on Power System Technology - POWERCON* 2004 Singapore, pp. 21-24, November 2004.

[12] J. Mäkelä, E. Karvinen, N. Porjo, A. Mäkelä, and T. Tuomi, "Attachment of Natural Lightning Flashes to Trees: Preliminary Statistical Characteristics", *Journal of Lightning Research,* Vol. 1, pp. 9-21, 2009.

[13] P. Heine, J. Pitkänen , M. Lehtonen "Voltage Sag Characteristics of Covered Conductor Feeders", *38th International Universities Power Engineering Conference, UPEC 2003*, Greece, September 1-3, 2003.

[14] A. M. Cassie, Theorie Nouvelle des Arcs de Rupture et de la Rigidité des Circuits, Cigre, *Report 102*, pp. 588-608, 1939.

[15] O. Mayr, "Beitrage zur Theorie des Statischen und des Dynamischen Lichthogens", *Archiv für Elektrotechnik*, Vol. 37, pp. 588-608, 1943.

[16] CIGRE Working Group 13.01 “Applications of Black Box Modeling to Circuit Breakers”, *Electra*, No. 149, 1993.

[17] P. Schavemaker and L. Sluis, “An Improved Mayr-Type Arc Model Based on Current-Zero Measurements”, *IEEE Trans. Power delivery*, Vol. 15, pp.580-584, 2000.

[18] H. Darwish and N. Elkalashy “Universal Arc Representation Using EMTP”, *IEEE Trans. Power Delivery*, Vol.2, pp. 704-709, 2005.

[19] A. Johns, R. Aggarwal, and Y. Song, “Improved Techniques for Modeling Fault Arcs on Faulted EHV Transmission Systems”, *IEE Proc. Gener. Transm. Distrib.*, Vol. 141, pp. 148-154, 1994.

[20] M. Kizilcay and T. Pniok “Digital Simulation of Fault Arcs in Power systems” , *European Transactions on Electrical Power System, ETEP*, Vol. 4, No. 3, pp. 55-59, January/February 1991.

[21] N. A. Elkalashy, M. Lehtonen, H. A. Darwish, M. A. Izzularab and A. I. Taalab , “Modeling and Experimental Verification of High Impedance Arcing Faults in Medium Voltage Networks”, *IEEE Trans. Dielectric Electr. Insul.,* Vol. 14, pp. 375-383, 2007.

[22] F. A. M. Rizk, “A Model for Switching Impulse Leader Inception and Breakdown of Long Air-Gaps”, *IEEE Trans. Power Delivery*, Vol. 4, pp. 596-606, 1989.

[23] T. Tuomi, Mäkelä A., *Lighnting Observations in Finland*, Report of Finnish Metrological Institute, Helsinki, No. 6, 2006.

[24] Ultrasil Housed VariGap Arresters, *Cooper Power Systems Electrical Apparatus I235-39*, April 2003.

[25] H. Chang “Protection of Buried Cable from Direct Lightning Strike”, *IEEE Trans. on Electromagnetic Compatibility*, Vol. EMC-22, n. 3, August 1980.

[26] F. M. Tesche, A. W. Kalin, B. Brandli, B. Reusser, M. Ianoz, D. Tabara, and P. Zweiacker, “Estimates of Lightning-Induced Voltage Stresses within Buried Shielded Conduits”, IEEE Transactions on Electromagnetic Compatibility, Vol. 40, No. 4, Nov. 1998.

[27] M. E. Petrache, F. Rachidi, M. Paolone, C.A.Nucci, V.A Rakov, M.A. Uman “Lightning induced disturbances in buried Cables-part I: theory”, *IEEE Trans. on Electromagnetic Compatibility*, Vol. 47, pp. 498-508, 2005.

[28] B. Vahidi, S. Taghipour Boroujeni, S. M. Ahadi “An Investigation of the Applicability of Barbed Shield Wires to Protect Transmission Lines Using Charge Simulation Method”, *International Review of Electrical Engineering (IREE)*, Vol. 4., pp. 102-107, n. 1, February 2009.

[29] N. Theethayi, R. Thottappillil “On Reducing the Lightning Transients in Buried Shielded Cables Using Follow-On Earth Wire”, *IEEE Transaction on Electromagnetic Compatibility*, Vol. 49, pp. 924-927, 2007.

[30] J.D. Nordgard, C. Chin-Lin “Lightning-Induced Transients on Buried Shielded Transmission Lines”, *IEEE Transaction on Electromagnetic Compatibility*, Vol.21, pp. 171-181, 1979.

[31] K.E. Bow, D.A. Voltz “Cable with Overall Shield for Protection from Lightning and Faults” , *IEEE Transaction on Power delivery*, Vol. 7, pp. 627-663, 1992.

[32] N. Klairuang, T. Khatsaengand, J. Hokierti “Lightning Electric Field in the Soil and Its Effect to Buried Cables”, 7th *International Power Engineering Conference, 2005. IEEE- IPEC,* Vol. 2, pp. 782 - 787, 2005.

[33] Z. Song, M.R. Raghuveer, H. Jingliang, "Complete Assessment of Impact of Lightning Strikes on Buried Cables", *Canadian Conference on Electrical and Computer Engineering, IEEE-CCECE 2002,* vol.1. pp 30 -36.

[34] M. Muhr, H. Haidvogl, "Effects of Lightning Strikes on 20 kV cables", *Proceedings of the CIRED 97*, June 2-5, 1997.

[35] IEEE working group on lightning performance of Electric Power Overhead Line. 2004. *IEEE Guide for improving the Lightning Performance of Electric Power Overhead Lines.* , NY, IEEE Std 1410tm- 2004.

[36] G. M. Hashmi, Partial Discharge Detection for Condition Monitoring of Covered-Conductor Overhead Distribution Network using Rogowski Coil, *Published doctoral thesis dissertation, TKK,* Finland, 2008.

[37] P. Chowdhuri, *Electromagnetic transients in power systems*, Research studies Press Ltd, Somerset, England, 1996

[38] S. Yokohama and A. Asakawa, "Experimental Study of Response of Power Distribution Lines to Direct Lightning Hits" *IEEE Trans. Power Delivery,* Vol. 4 (4), pp. 2248-2254, 1989.

[39] C. A. Nucci and F. Rachidi, "Lightning-induced Overvoltages" , *IEEE Transmission and Distribution conference, Panel session on Distribution Lightning Protection*, New Orleans, April 14, 1999.

[40] M.A. Omidiora and M. Lehtonen "Performance of Surge Arrester to Multiple Lightning Stroke to Distribution Transformer", *Proc. 7th WSEAS Conference on Power Systems, China,* pp. 59-66*,* Sept. 2007.

[41] H. R. Armstrong and E.R. Whitehead "Field and analytical studies of transmission line shielding", *IEEE Trans. on Power Apparatus and Systems,* Vol. PAS-87, pp. 270-281, 1968.

[42] K. Yamamoto, Z. Kawasaki, K. Matsuura and S. Sekioka "Shielding Effect of Reinforced Concrete Building on Direct Stroke to Distribution Line by using Electro-geometric Model", *proc. 11th Intern. Symposium on High Voltage Engineering, London*, Vol. 2. pp. 204-207*,* 1999.

[43] A. M. Mousa and K. D. Srivastava "Effect of Shielding by Trees on the Frequency of Lightning Strokes to Power Lines", *IEEE Trans. on Power Delivery,* Vol. 3, pp 724-732, 1988.

[44] M. A. Omidiora and M. Lehtonen "Simulation Performance of Induced Voltages on Power Distribution Line due to Lightning Discharge to nearby Tree" *EEUG2009 conference*, pp. 70-79, Oct. 2009.

[45] D.W. Deno, J.M. Silva, "Transmission Line Electric Field Shield by Objects" *IEEE Trans. on Power Delivery*, Vol. PWRD-2, pp 269-280, 1987.

[46] S. Rusck "Induced Lightning Overvoltages on Power Transmission Lines with Special Reference to the Overvoltage Protection of Low-Voltage Net Works", Trans*. Roy. Inst. Technol. (KTH)*, No. 120, 1958.

[47] P. P. Barker, T.A. Short, A. Eybert-Berard and J.B. Berlandis "Induced Voltage Measurements on an Experimental Distribution Line during nearby Rocket Triggered Lightning Flashes", *IEEE Trans. Power Delivery*, Vol. 11, pp. 980-995, 1996.

[48] M. Ishii, K. Michishita, Y. Hongo and S. Ogume "Lightning-Induced Voltage on an Overhead Wire Dependent on Ground Conductivity", *IEEE Trans. Power Delivery*, Vol. 9, pp. 109-118, 1994.

[49] A. Piantini and J.M. Janiszewski "An Experimental Study of Lightning Induced Voltages by Means of a Scale Model", *21st Int. Conf. Lightning Protection*, Berlin, Germany, paper 4.08, pp. 195-199, 1992.

[50] C.A. Nucci, V. Bardazzi, R. Iorio, A. Mansoldo and A. Porrino "A code for the Calculation of Lightning-Induced Overvoltages and its Interface with the Electromagnetic Transient Program", *22nd Int. Conf. Lightning Protection*, Budapest, Hungary, Paper R3b-05, 1994.

[51] A. Xemard, P. Baraton and F. Boutet "Modeling with EMTP of Overhead Lines Illuminated by an External Electromagnetic Field", *Proc. Intern. Conf. Power Systems Transients,* Lisbon, Portugal, 1995.

[52] H. K. Høidalen "Calculation of Lightning-Induced Voltages in MODELS Including Lossy Ground Effects", *Intern. Conf. Power Systems Transients (IPST)*, New Orleans, USA, pp. 1-6, 2003.

[53] A. Hochrainer, "Einige Bemerkungen zum Stromnulldurchgang in Wechselstromschaltern", EuM, Vol. 87, No.1, pp. 15-19, 1970.

[54] E. Kuffel "Influence of Humidity on the Breakdown Voltage of Sphere-Gaps and Uniform-Field Gaps", *Proc. of the IEE- Part A: Power Engineering,* pp 295-301, 1961.

[55] A. Piantini and J. M. Janiszewski "Lightning Induced Voltages on Distribution Lines Close to Buildings", *25th Intern. Conf. Lightning Protection*, pp. 558-563, 2000.

[56] C. E. Cinieri, A. Fumi and C. Mazzetti "Short Tail Lightning Impulse Behavior of Medium Voltage Line Insulation", *IEEE Trans. Power Delivery,* Vol.14, pp. 218-226, 1999.

[57] S. Yokoyama, K. Miyake, S. Fukui: "Advanced Observations of Lightning Induced Voltage on Power Distribution Lines", *IEEE Trans. Power Delivery*, Vol. 4, pp. 2196-2203, 1989.

[58] A. Ancajima, I. Baran, M. Costea, A. Carrus, E. Cinieri, G. Dragan and C. Mazzetti "Breakdown Characteristics of MV Distribution and Electric Traction Lines Insulators Stressed by Standard and Short Tail Lightning Impulses", *IEEE Power Tech*, Russia, pp. 1-7, 2005.

[59] E. Cinieri, F. Muzi "Lightning Induced Overvoltages. Improvement in Quality of Service in MV Distribution Lines by Addition of Shield Wire", *IEEE Trans. Power Delivery*, Vol.11, pp. 361-372, 1996

[60] H. W. Dommel, *Electromagnetic Transients Program (EMTP) Reference Manual (EMTP Theory Book),* DE-AC79-81BP31364, August 1986.

[61] S. Meyer, T. Liu*, Alternative Transient Program (ATP) Rule Book,* Canadian/American EMTP User Group, EMTP Center, USA.

[62] J. R. Marti, "Accurate Modelling of Frequency- Dependent Transmission Lines in Electromagnetic Transient Simulations," *IEEE Trans. Power Apparatus and Systems*, Vol. 101, pp. 147-155, 1982.

[63] N. A. Sabiha, Lightning-Induced Overvoltages in Medium Voltage Distribution Systems and Customer Experienced Voltage Spikes, *Published PhD Thesis (TKK Dissertation,),* Aalto University, Finland, 2010.

[64] A. Ametani, K. Matsuoka, H. Omura, Y. Naga "Surge Voltages and Currents into a Customer Due to Nearby Lightning", *Electric Power Systems Research.* Vol. 79, pp. 428–435, 2009.

[65] A. Ametani, T. Kawamura "Method of a Lightning Surge Analysis Recommended in Japan using EMTP", *IEEE Transactions on Power Delivery,* Vol. 20 No. 2, pp. 867-875, 2005.

[66] T. Noda, M. Sakae, S. Yokoyama "Simulation of Lightning Surge Propagation from Distribution Line to Consumer Entrance via Pole-Mounted Transformer", *IEEE Trans on Power Delivery,* Vol. 19, No. 1, pp.

442-444, 2004.

[67] R. Zeng, X. Gong, J. He, B. Zhang and Y. Gao "Lightning Impulse Performances of Grounding Grids for Substations Considering Soil Ionization", *IEEE Transactions on Power Delivery*, Vol. 23, No. 2, pp. 667-675, April 2008.

[68] Y. Tu, J. He, and R. Zeng, "Lightning Impulse Performances of Grounding Devices Covered with Low-Resistivity Materials", *IEEE Trans.on Power Delivery*, Vol. 21, No. 3, pp. 1706-1713, July 2006.

[69] F. E. Menter and L. Grcev, "EMTP-based model for grounding system analysis", *IEEE Transactions on Power Delivery*, Vol. 9, No. 4, pp. 1838-1849, October 1994.

[70] F. A. M. Rizk, "Modeling of Substation Shielding Against Direct Lightning Strikes", *IEEE Transactions on Electromagnetic Compatibility*, Vol. 52, No. 3, August 2010.

[71] H. R. Armstrong and E. R. Whitehead "Field and Analytical Studies of Transmission Line Shielding*", IEEE Trans. Power App. Syst.*, Vol. PAS-87, no. 1, pp. 270–281, Jan. 1968.

[72] A. J. Eriksson "An improved Electrogeometric model for Transmission Lines Shielding Analysis," *IEEE Trans. Power Del.*, Vol. PWRD-2, No. 3, pp. 871–886, Jul. 1987.

[73] F. A. M. Rizk "Modeling of Transmission Line Exposure to Direct Lightning Strokes", *IEEE Trans. Power Del.*, Vol. PWRD-5, No. 4, pp. 1983–1997, Oct. 1990.

[74] G. W. Brown and E. R. Whitehead, "Field and Analytical Studies of Transmission Line Shielding: Part II," *IEEE Transactions On Power Apparatus and Systems*, Vol. PAS-88, No. 5, May 1969.

Appendix- Publications I- VIII

The appendix contains Publications I- VIII belonging to this article dissertation.

This dissertation studies the lightning performance of different Medium Voltage distribution lines, which are overhead lines, underground cables and covered conductors. New protection schemes are subsequently proposed for the lines. The study was based on modeling and simulations using the EMTP and FEM software, and laboratory experiments. Further, a new knowledge is introduced in terms of the contributions of surrounding trees to the lightning performance of distribution lines. By means of experimental studies, a lightning arc phenomenon between a tree and a nearby distribution conductor under artificial raindrops is confirmed and reported in this work. With the aid of the EMTP and its TACS features, the lightning arc characteristics have been modeled by combining the existing static and dynamic arc equations. By employing modeled arc characteristics in the EMTP, this thesis also evaluate the lightning arc performance of the MV/ LV network under the influence of nearby trees and the network characteristics.

ISBN 978-952-60-4243-5 (pdf)
ISBN 978-952-60-4242-8
ISSN-L 1799-4934
ISSN 1799-4942 (pdf)
ISSN 1799-4934

Aalto University
School of Electrical Engineering
Department of Electrical Engineering
www.aalto.fi

BUSINESS + ECONOMY

ART + DESIGN + ARCHITECTURE

SCIENCE + TECHNOLOGY

CROSSOVER

DOCTORAL DISSERTATIONS

Aalto-DD 70/2011